

# Journal Pre-proof

Potential of building integrated and attached/applied photovoltaic (BIPV/BAPV) for adaptive less energy-hungry building's skin: A comprehensive Review

Aritra Ghosh



PII: S0959-6526(20)33388-6

DOI: <https://doi.org/10.1016/j.jclepro.2020.123343>

Reference: JCLP 123343

To appear in: *Journal of Cleaner Production*

Received Date: 12 January 2020

Revised Date: 29 May 2020

Accepted Date: 17 July 2020

Please cite this article as: Ghosh A, Potential of building integrated and attached/applied photovoltaic (BIPV/BAPV) for adaptive less energy-hungry building's skin: A comprehensive Review, *Journal of Cleaner Production*, <https://doi.org/10.1016/j.jclepro.2020.123343>.

This is a PDF file of an article that has undergone enhancements after acceptance, such as the addition of a cover page and metadata, and formatting for readability, but it is not yet the definitive version of record. This version will undergo additional copyediting, typesetting and review before it is published in its final form, but we are providing this version to give early visibility of the article. Please note that, during the production process, errors may be discovered which could affect the content, and all legal disclaimers that apply to the journal pertain.

© 2020 Elsevier Ltd. All rights reserved.

**Potential of building integrated and attached/applied photovoltaic (BIPV/BAPV) for adaptive less energy-hungry building's skin: A comprehensive Review**

Journal Pre-proof

# Potential of building integrated and attached/applied photovoltaic (BIPV/BAPV) for adaptive less energy-hungry building's skin: A comprehensive Review

Aritra Ghosh<sup>1,2</sup>

<sup>1</sup>Environmental and Sustainability Institute, University of Exeter, Penryn, Cornwall, TR10 9FE, UK

<sup>2</sup>College of Engineering, Mathematics and Physical Sciences, Renewable Energy, University of Exeter, Cornwall TR10 9FE, UK

\*Corresponding author: [a.ghosh@exeter.ac.uk](mailto:a.ghosh@exeter.ac.uk); [aritrighosh\\_9@yahoo.co.in](mailto:aritrighosh_9@yahoo.co.in)

## Abstract:

The inclusion of photovoltaic (PV) technologies add extra functionalities in a building by replacing the conventional structural material and harnessing benign electricity aesthetically from PV. Building integration (BI) and building attached / applied (BA) are the two techniques to include PV in a building. Currently, first, and second-generation PV technologies are already included for BIPV and BAPV application in the form of wall, roof, and window whereas third generation PVs are under rigours exploration to find their potential suitability. To alleviate enhanced temperature from both BIPV and BAPV, active and passive cooling can be introduced, however passive techniques are influential in trimming down the temperature for retrofit building. Shading from snow, dust cover and nearby building can be an obstacle for BIPV/BAPV application. The hydrophobic (icephobic) self-cleaning coating is suited for snow covering PV while hydrophobic and hydrophilic are both applicable for anti-soiling. Electric vehicles, autonomous switchable glazing, low heat loss glazing and lightweight BIPV are the different future application for PV in BI and BA integration.

## Highlights:

- A review about building integrated/ attached photovoltaic is presented
- Different possible PV application in building has been discussed
- Issues associated with BIPV/BAPV system has been critically reviewed
- Potential future BIPV application has been introduced.

**Keywords:** BIPV, glazing, energy, temperature, zero energy, dust, snow, shading, PCM, active, passive

## 1. Introduction

### 1.1. Necessity of BIPV/BAPV

It is expected that in 2035 the world energy consumption can be increased up to 50% compared to 1990 due to urbanization and rapid population growth, which will have an impact on the consumption of building energy. Presently buildings consume 40% energy globally due to heating, cooling and artificial lighting loads by the exploitation of fossil fuel (Belussi et al., 2019; Cao et al., 2016; Lu and

36 Lai, 2019; Y. Zhou et al., 2019)(Ng and Mithraratne, 2014a). Thus, the environment is greatly  
37 affected by the emitted pollutant gas during the energy generation process. Energy consumptions and  
38 greenhouse gasses (GHG) emission from building sector in megacities such as New York, San  
39 Francisco, Tokyo, Hongkong are much higher than even their transport sectors (IPCC, 2014)(Yoo,  
40 2019). International roadmaps target to convert all high energy consumed buildings to zero-energy or  
41 net-zero energy building by replacing the energy generation from green sources over fossil fuel  
42 sources (Bauer and Menrad, 2019; Jacobson et al., 2017; Taveres-Cachat et al., 2019). In Europe, to  
43 fulfil these targets, the new building will be built as near-zero energy consumption by the end of 2020.  
44 By 2050, the UK government has set the ambition of reducing national emissions by 80% (García  
45 Kerdan et al., 2016) which was later modified and aimed for a more ambitious zero-emission target  
46 (The Lancet, 2019). In Asia, Japan has set that all new public buildings by 2020 and all new  
47 residential buildings by 2030 should be zero energy. In the USA, new residential construction should  
48 be zero energy by 2020, and by 2030 all-new commercial construction should be zero energy (Hu and  
49 Qiu, 2019). To achieve this, primary energy use in buildings should be reduced by using an energy-  
50 efficient building envelope (Lufkin, 2019).

51 Photovoltaic (PV) technologies are one of the potential candidate which generates benign energy by  
52 harnessing abundant, inexhaustible, clean solar power (van Sark et al., 2010)(Jäger-Waldau et al.,  
53 2020). At the end of 2018, global installed PV capacity exceeded over 500 GW (Haegel et al.,  
54 2019)(Kurtz et al., 2020). The worldwide PV technology market is expected to grow at a 1.7%  
55 compound annual growth rate which shows an increment of 46700 million US\$ in 2024 from 42100  
56 million US\$ in 2019 (Research, 2020). In Europe, 40% electricity demand by 2020 can be achieved  
57 by 1400 TWh electricity production from 1500 GWp installed PV plant which requires 22000 km<sup>2</sup>  
58 ground floor area, 40% of existing building's roof and 15 % of façade buildings (Hachana et al.,  
59 2016). Use of PV device in a building replaces the actual dead load of the building, i.e., walls,  
60 rooftops made with concrete, generates building energy from fossil-fuel free sources which in turn  
61 offers a pollution-free environment (Norton et al., 2011). In addition, this can introduce daylighting  
62 by replacing opaque building façade which can save 50-80% artificial lighting (Bodart and De Herde,  
63 2002), 11% cooling load and 13% electricity consumption for an office building (Lam and Li, 1999).  
64 Addition of PV over a glass, steel and other common cladding material, increase the marginal extra  
65 cost only between 2-5% (Paul et al., 2010). Primarily, the inclusion of PV in a building is possible by  
66 building integration (BI) or building attached or applied (BA) techniques (Cronemberger et al., 2014).

## 67 **1.2. Overview of BIPV/BAPV**

68 Building integrated photovoltaic (BIPV) is an integral part of a building which substitute or replace  
69 the traditional building materials or envelopes such as roof, window, atria and shading elements,  
70 components by PV and concomitantly generates benevolent electricity at the point of use (Peng et al.,  
71 2011). Glass on glass type semi-transparent type BIPV structure is attractive due to its ability to allow  
72 daylighting into indoor space and control over solar gain and offers to view from interior to the  
73 exterior (Reddy et al., 2020). Semi-transparent BIPV is also promising for large glazed façade  
74 architecture. However, damaged BIPVs have direct access to the internal function of the building  
75 (Wang et al., 2006).

76 The building attached/applied photovoltaic (BAPV) does not replace the construction component, can  
77 be rack-mounted or standoff arrays type, opaque in nature and are only employed for power  
78 generation and do not contribute to any heat gain into building interior, rather it alleviates heat gain by  
79 generating shading the roof or wall from direct solar heat (Peng et al., 2011). Thermal regulation of  
80 BAPV systems is straightforward compared to BIPV due to available space between PV systems and  
81 building skin. Comparison between BIPV and BAPV is documented in Table 1.

82 Table 1: Comparison of BIPV and BAPV system (Shukla et al., 2018)

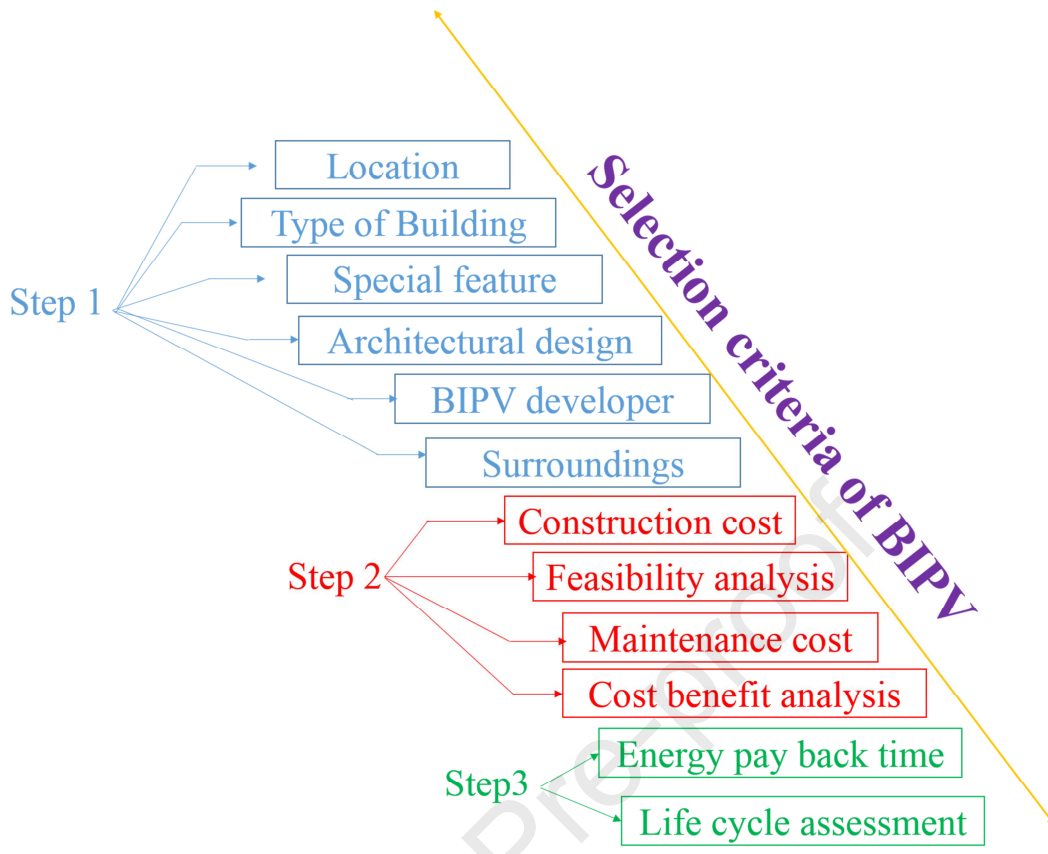
Property	Building integrated photovoltaics	Building applied photovoltaics
Integration	Integrated directly within the building structures like roof or façade	Indirect integration by using mounting hardware and roof perforations
Weight	Lightweight and heavyweight	Heavyweight
Stability	Durable	Breakable
Wind effect	Highly resistance to winds	Lift or drag is possible
Visual impact	Aesthetically pleasing	Clunky looking

83

84 BIPV and BAPV both generate onsite clean energy which reduces the transmission and distribution  
85 losses. Absence of moving part makes it silent, and no hazardous comes out during operation  
86 (Scognamiglio, 2017; Scognamiglio and Rostvik, 2013). BIPV has triple-point effect as it maintains  
87 day-lighting, controls thermal transmittance and generates electricity. Performance of BIPV and  
88 BAPV both depends on the different selection criteria as shown in Figure 1; however, the most  
89 indispensable parameters are local meteorological conditions, the tilt angle and the type of material.  
90 To obtain electricity from BIPV and BAPV systems, a converter is required to alter direct current  
91 (DC) to alternating current (AC) for building and grid both application (Norton et al., 2011). The main  
92 component of a BIPV/BAPV system is PV devices which are made from PV cells. Other necessary  
93 components of BIPV/BAPV systems are referred as a balance of systems (BOS) which includes an  
94 inverter, storage device (battery), switches for control, electrical wiring, and support structure (Shukla  
95 et al., 2016a) (Benemann et al., 2001)(Spiliotis et al., 2019) (Saretta et al., 2020). Application  
96 possibilities of BIPV and BAPV systems are shown in Figure 2.

97

98



99

100 Figure 1: Best selection methods for BIPV. Redrwan from (Alim et al., 2019).

101

102



(a) BIPV daylighting application



(b) BIPV wall application



(c) BIPV window application



(d) BAPV roof application



(e) BIPV roof application



(f) BIPV roof application

103

104 Figure 2: Application of different BIPV and BAPV systems in building (Photo taken from  
105 (Cronemberger et al., 2014)). (Image source: SDEurope)

106

107 Due to the present interest of BIPV/BAPV systems, several researchers made high-quality review  
108 work. Tripathy et.al. reviewed and mentioned the state-of-the-art of the building envelope products  
109 and their properties along with international standards and test conditions, which suggested that the  
110 roof-integrated BIPV is lucrative for experiencing uninterrupted incident solar radiation.  
111 Monocrystalline PV is responsible for generating much higher greenhouse gasses compared to other  
112 PV technologies while life cycle was considered. This work lacks abysmally from providing  
113 information on emerging new BIPV application and also shading from snow and dust accumulation  
114 (Tripathy et al., 2016). BIPV and its thermal regulation using BIPVT applications have been reviewed  
115 in terms of energy generation amount, nominal power, efficiency, type and performance assessment  
116 approaches (Biyik et al., 2017). Advancement of dye-sensitized PV based BIPV application has been  
117 reported in this work. However, emerging new BIPV technologies are missing from this work (Biyik

117 et al., 2017). Another BIPV and BIPVT review documented that BIPVT system is the future for less  
118 energy-hungry building application (Debbarma et al., 2016). Seretta et.al. summarised literature  
119 review for building energy demand in urban area and retrofit rate of BIPV and predicted that these  
120 two disciplines could merge together where multifunctional BIPV element improve building's energy  
121 performance and produce electricity from solar radiation in urban contexts (Saretta et al., 2019).  
122 Shukla et.al. reviewed the properties of BIPV products such as foil, title, module, glazing and BAPV  
123 system were investigated based on PV performance parameters (efficiency, open-circuit voltage, short  
124 circuit current, maximum power, fill factor ), and their life cycle was assessed by considering energy  
125 payback time and GHG emission (A. K. Shukla et al., 2017a).

126 In this review, a detailed application of BIPV and BAPV system, their advantages and challenges  
127 associated with this application and solution for these obstacles are presented. Potential future  
128 application has been documented in this work which transforms this review to a unique study.

## 129 **2. PV technology for BIPV and BAPV**

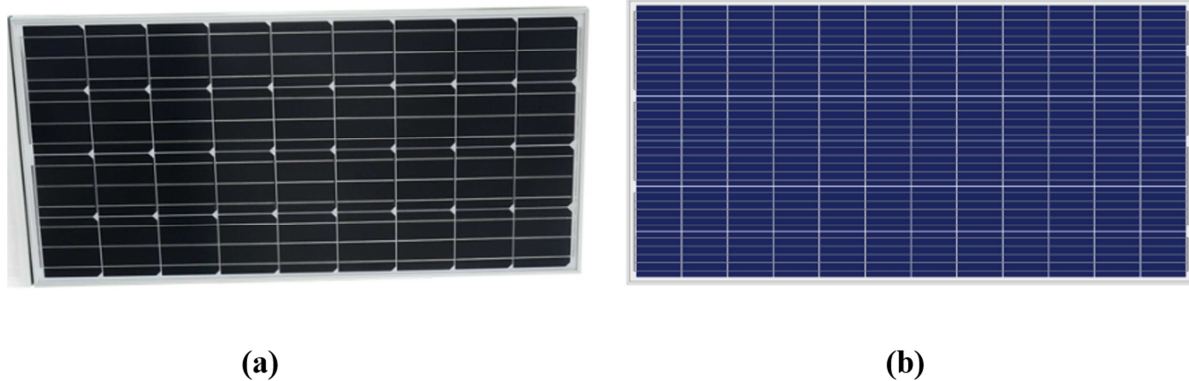
130 PV technologies for three different generations have been included in this section where first and  
131 second generations are already exploited for BIPV, and BAPV application and third generations are  
132 under exploration for their potential integration (Nayak et al., 2019; Sinke, 2019).

### 133 **2.1. First-generation crystalline silicon PV cell**

134 Crystalline silicon (c-Si) (as shown in Figure 3) PV cells are produced from silicon wafers and can be  
135 subcategorized into single /monocrystalline (m-Si) and multi/polycrystalline (p-Si). c-Si PV  
136 technology is mature, non-toxic, abundant and possess long term performance (Battaglia et al., 2016;  
137 Glunz et al., 2012; Zarmai et al., 2015). Monocrystalline cells are produced by the Czochralski  
138 process from single silicon crystals which are expensive manufacturing methods due to precise  
139 processing requirement form large single crystals. The efficiency of the monocrystalline type lies  
140 between 17%-18% (Saga, 2010; Sharma et al., 2015). Polycrystalline type of cells is produced by  
141 molten silicon solidification. The efficiency of this type of cells is between 12%-13%. c-Si PV shows  
142 20-30 years of durability under outdoor exposure (Aste et al., 2016; Rand et al., 2007). High  
143 durability and mature technology make c-Si suitable for BIPV and BAPV systems application. Silicon  
144 prices which rose steeply between 2000 to 2008 with a peak of \$475/kg, also declined rapidly in the  
145 last decade having steady prices of approximately \$25/kg (Fu et al., 2015). It is estimated that globally  
146 c-Si PV market would reach \$163 billion by 2022, which is 11.3% enhancement from the 2016 level.  
147 Energy payback period lies between 3-4 years for this type of technology (Luo et al., 2018; Ogbomo  
148 et al., 2017). Canadian Solar, JA Solar, JinkoSolar, Hanwha Q-CELL, LONGI, Tongwei, Trina Solar  
149 are the present leading vendor for first-generation crystalline silicon PV cells.

150





151

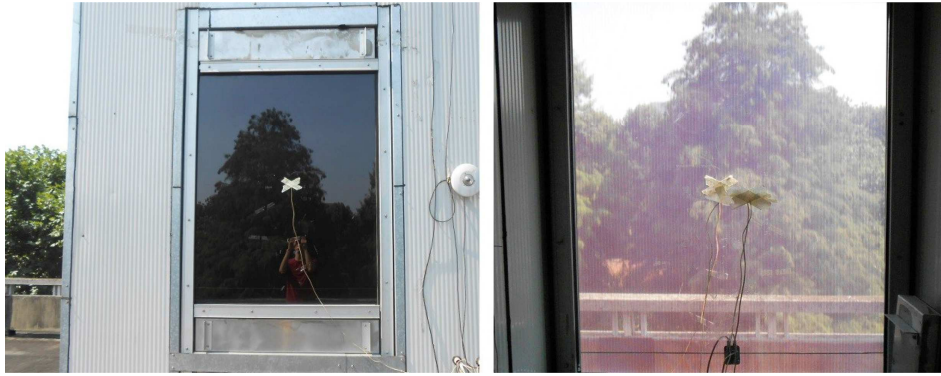
152 Figure 3: Crystalline silicon (a) mono and (b) poly type. (Image courtesy: SHINESOLAR and DH-  
153 SOLAR)

## 154 2.2. Second generation thin film technology

155 Cadmium telluride (CdTe), copper indium gallium selenide sulphide (Cu (In, Ga)Se<sub>2</sub>, CIGS) and  
156 amorphous silicon (a-Si) are the second generations thin film technology which has low  
157 manufacturing cost and low-temperature coefficient compared to crystalline silicon solar cell (Tossa  
158 et al., 2016). However, low solar to electrical conversion efficiency compared to crystalline silicon  
159 PV cell and performance degradation after long-term outdoor exposure (Jordan and Kurtz, 2013;  
160 Muñoz-García et al., 2012) is the significant barrier of using this technology. Irradiance, spectrum,  
161 angle of incidence, ambient temperature and wind speed also affect the performance of thin-film  
162 technologies in a similar way to c-Si technology; however, the temperature dependence is weaker in  
163 comparison to c-Si technologies. These technologies absorb the solar spectrum much more efficiently  
164 than single crystalline or multi-crystalline and use only 1–10  $\mu\text{m}$  of active material (Shukla et al.,  
165 2016b, 2016a)

### 166 2.2.1. Amorphous silicon (a-Si)

167 a-Si PV absorbs a higher amount of solar radiation than c-Si because of the absence of the crystalline  
168 structure (Muñoz-García et al., 2012). Low-temperature coefficients of a-Si cells make it a potential  
169 candidate than c-Si cells in summer and warm climate (Ruther and Livingstone, 1995)(Virtuani and  
170 Strepparava, 2017). Due to the Staebler–Wronski effect, a-Si shows light-induced metastability which  
171 requires time to produce a sufficient amount of power from a-Si PV (Matsui et al., 2018; Staebler and  
172 Wronski, 1977). Spectral changes of terrestrial insolation in summer and winter remarkably  
173 influences the changes of efficiencies for a-Si (Eke et al., 2017; Polo et al., 2017; Ruther and  
174 Livingstone, 1995). Investigation in India showed that a-Si module offered 14% higher energy than p-  
175 Si in summer while 6% less in winter (Sharma et al., 2013). Experiment results from Spain also  
176 supported that argument (Cañete et al., 2014). Spectral variation of external incident solar radiation  
177 has an adverse impact on fill factor (FF) (FF depends on both quality and quantity of solar radiation)  
178 of an a-Si PV cell. Blue spectra have a positive impact, while red spectra reduce the FF (Rüther et al.,  
179 2002). Device flexibility, low-temperature processing, low negative temperature coefficient of a-Si  
180 has created commercial interest significantly for BIPV applications (Stuckelberger et al., 2017). To  
181 rectify a-Si's light-induced degradation, tandem amorphous/microcrystalline silicon thin-film PVs  
182 have also been investigated (Tsai and Tsai, 2019). **Figure 4** shows the a-Si PV module integrated into  
183 a building. The energy payback time and operational lifetime of a-Si PV are 2-3 years and 25 years,  
184 respectively (Peng et al., 2013a; Zhang et al., 2018; Zhou and Carbajales-Dale, 2018). Presently they  
185 have a market share of 5% (Ogbomo et al., 2017).



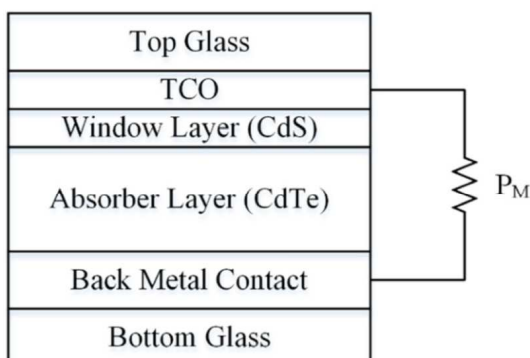
186

187 Figure 4: Photograph of an a-Si integrated to a building and viewing through a-Si PV from building  
 188 interior to exterior. (Liao and Xu, 2015).

### 189 2.2.2. Cadmium telluride (CdTe)

190 In cadmium telluride (CdTe) PV cells, consist cadmium which is a by-product of zinc and telluride.  
 191 Cadmium (Cd) is a heavy metal and has a potential toxic property for human, animals and plants.  
 192 CdTe contains  $\leq 7$  g of elemental Cd in per square metre of PV cell compared to average single-cell  
 193 nickel-cadmium battery (Kuhn et al., 2016; Kuribayashi et al., 1983; Ogbomo et al., 2017; Rodriguez  
 194 et al., 1995; Shukla et al., 2016b, 2016a). The second material, telluride (Te), is scarce and as rare as  
 195 platinum in nature which increases the price of the CdTe PV cell. The limited supply of Cd and its  
 196 potential environmental hazards are the main issues with this technology (Fthenakis, 2004; Raugei et  
 197 al., 2012). Thus recycling and disposal of CdTe cells are expensive (Sethi et al., 2011). Although the  
 198 Cd element is hazardous, however, the compound CdTe used in PV cells is much more  
 199 environmentally benign. CdTe thin-film PV was commercialized in 2001 which had power density  
 200 between  $62.5 \text{ W/m}^2$  to  $76.38 \text{ W/m}^2$  and the efficiency for this 55 Wp module had 8% (Enríquez and  
 201 Mathew, 2003; Lee and Ebong, 2017). CdTe type PV cell has a theoretical efficiency limit of 29%  
 202 (Dobson et al., 2000). Synthesization of CdTe became popular after the development of screen  
 203 printing, vacuum evaporation and electron deposition techniques (Virtuani et al., 2011). It is  
 204 recommended that the CdTe PV module should be kept under direct sunlight for four hours before  
 205 taking the measurements (Muñoz-García et al., 2012). Long term (23 months) outdoor analysis in  
 206 tropical climate (Delhi  $28.70^\circ \text{ N}$ ,  $77.10^\circ \text{ E}$ , India, as shown in Figure 5) showed 2.91% open circuit  
 207 voltage deviation, and no deviation was found for short circuit current (Rawat et al., 2018). The  
 208 energy payback time of CdTe varies between 0.75 to 2 years while operational lifetime is 20 years  
 209 (Peng et al., 2013a; Zhang et al., 2018; Zhou and Carbajales-Dale, 2018; Zidane et al., 2019).  
 210 Presently they have a market share of 5% (Ogbomo et al., 2017).

211

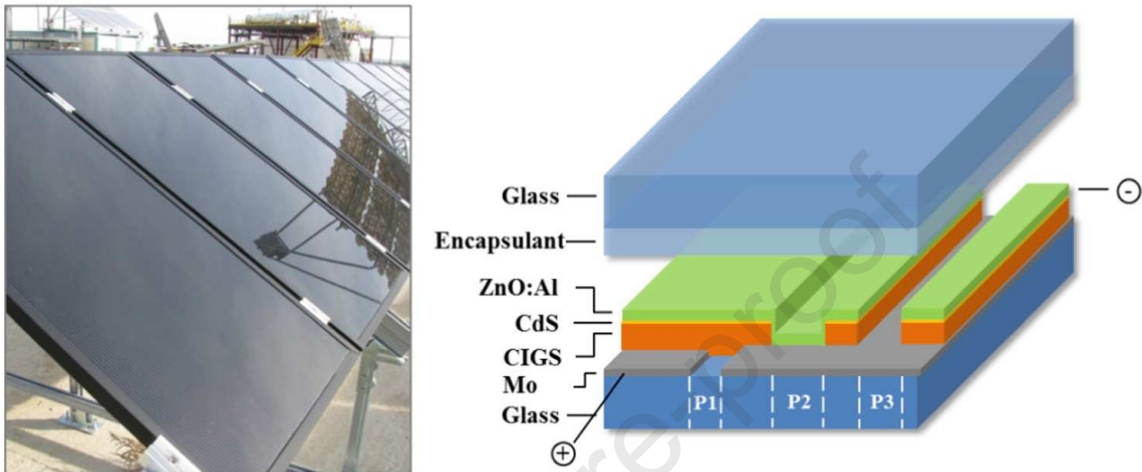


212

213 Figure 5: Layer diagram and experimental test setup of CdTe module (Rawat et al., 2018)

### 214 2.2.3. Copper indium gallium diselenide (CIGS)

215 Copper indium gallium diselenide (CIGS) PV cells as shown in Figure 6 comprises of the four  
 216 elements, namely: Copper, Indium, Gallium and Selenium (Dhere, 2011; Kazmerski et al., 1976).  
 217 Gallium-free variants of the semiconductor material are abbreviated as CIS. The manufacturing cost is  
 218 lower than the crystalline silicon PV cells but more expensive than other single-junction thin-film cell  
 219 like cadmium telluride.



220

221 Figure 6: Large scale CIGS PV module [taken from (Delgado-Sanchez et al., 2017)]

222 CIGS PV technology has average production efficiencies between 12% to 15% for commercial  
 223 modules and achieved a record efficiency of 22.3% in the laboratory. Degradation rates of CIGS are  
 224 the most significant challenge (Theelen et al., 2015). Through the simulation process, it is predicted  
 225 that CIGS modules will still yield 80% of their initial power after 20 years of field exposure.  
 226 However, a real-time experiment is required to prove this (Yalçın and Öztürk, 2013) hypothesis.  
 227 Results from different outdoor experiment offered a significant variation from 0.02% to 4.1%  
 228 degradation (Theelen et al., 2015). The energy payback time of CIGS varies between 1.2 to 2.4 years  
 229 while operational lifetime is 20 years (Peng et al., 2013a; Zhang et al., 2018; Zhou and Carbajales-  
 230 Dale, 2018). Presently they have a market share of 4% (Ogbomo et al., 2017).

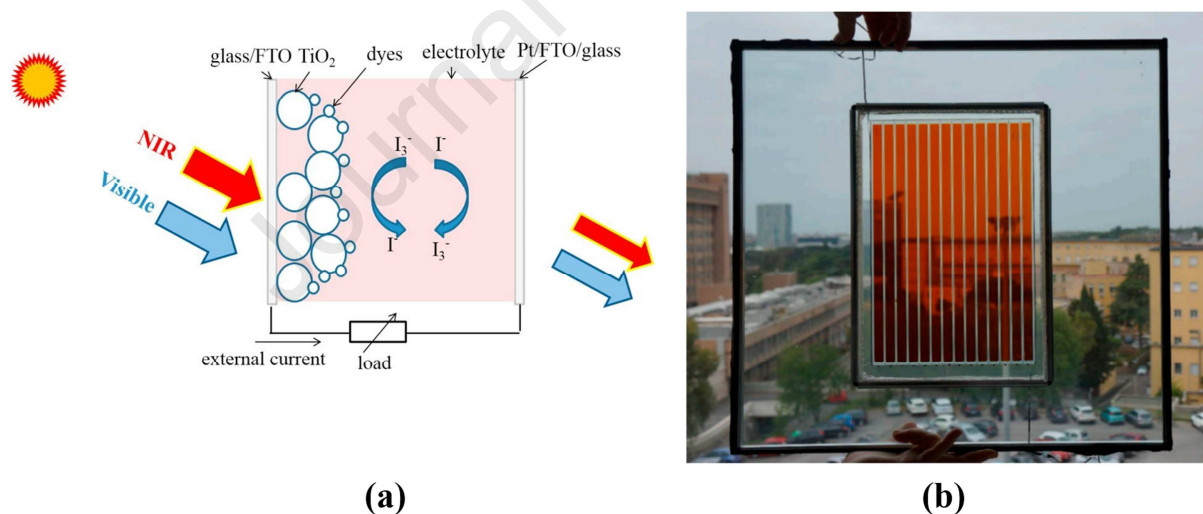
231 The Global thin-film PV cell market is expected to be USD 13,256.13 Million by the end of 2025  
 232 with a compound annual growth rate of 12.87% from USD 5,678.13 Million in 2018. Leading vendors  
 233 for global thin-film PV cell are Ascent Solar Technologies., Asia Ltd., First Solar, Global Solar,  
 234 Miasole Hi-Tech Corp., US, Hankey Kaneka Corporation, Trony Solar, Mitsubishi Electric and  
 235 Xunlight Kunshan Co. Ltd (Report, 2020).

### 236 2.3. Third or new generation PV

237 Sunlight can generate electricity with close to Carnot limit or 95%. However, first and second-  
 238 generation solar cells can only exploit 31% due to Shockley-Queisser limit. Rest of the energy for  
 239 single-junction cells are lost as heat. Third-generation solar cells are free from this Shockley-  
 240 Queisser limit. The aim of using third generations is to generate low-cost electricity using high-  
 241 efficiency conversion (Dupré et al., 2015).

### 242 2.3.1. Dye-sensitized solar cell (DSSC)

243 A dye-sensitized solar cell (DSSC) consists four main components: mesoporous oxide layer ( $\text{TiO}_2$ ),  
 244 dye sensitizer, an electrolyte containing redox couple, counter electrode made of platinum-coated  
 245 glass as shown in Figure 7 (O'Regan and Grätzel, 1991). DSSC fabrications are simpler and low cost,  
 246 environmentally benign than other PV cells as it is processable under ambient temperature. Flexible,  
 247 lightweight, convenient design such as multicolour option and transparency and short energy payback  
 248 time, working in cloudy weather or low-light conditions make it more viable for building integration  
 249 (Gong et al., 2017, 2012) (Mathew et al., 2014). DSSC efficiency currently reached to 11.9% (Green  
 250 et al., 2019). Photochemical degradation of sealants, solvents, dyes and solvent leakage is the hurdle  
 251 for its promulgation. Thermal stress due to day/night cycle can also influence of intrinsic chemical  
 252 degradation. Instability issue of DSSC due to leakage from a liquid electrolyte can be rectified by  
 253 using solid-state hole transport material. Highly conductive and stable polymer electrolytes are better  
 254 candidate for large scale DSSC manufacturing (Xia et al., 2006). Replacement of platinum catalyst  
 255 with graphene can offer higher electrochemical stability which solves the degradation of the platinum  
 256 catalyst (Kavan et al., 2011) and 20 years lifetime of DSSC is possible by solving these issues  
 257 (Grätzel, 2003) (Upadhyaya et al., 2013). Recently the use of uncleaned FTO glasses showed the  
 258 highest efficiency for DSSC than that of cleaned FTO glasses by using water, acetone, isopropanol or  
 259 ethanol. Uncleaned FTO glasses contained stains and residual dirt (Gossen and Ehrmann, 2019).  
 260 Energy payback period of DSSC varies from 1.99 years to 2.63 for varying cell efficiency (Greijer et  
 261 al., 2001; Mustafa et al., 2019; Parisi et al., 2014, 2011). In 2022, the market value of DSSC is  
 262 expected to be USD 59.52 million, while the significant application of DSSC will be in BIPV and  
 263 BAPV. Globally major DSSC companies include 3GSolar Photovoltaics, Dyesol, Exeger Sweden AB,  
 264 Fujikura Ltd., G24 Power., GCell, Merck KGaA (View, 2016).



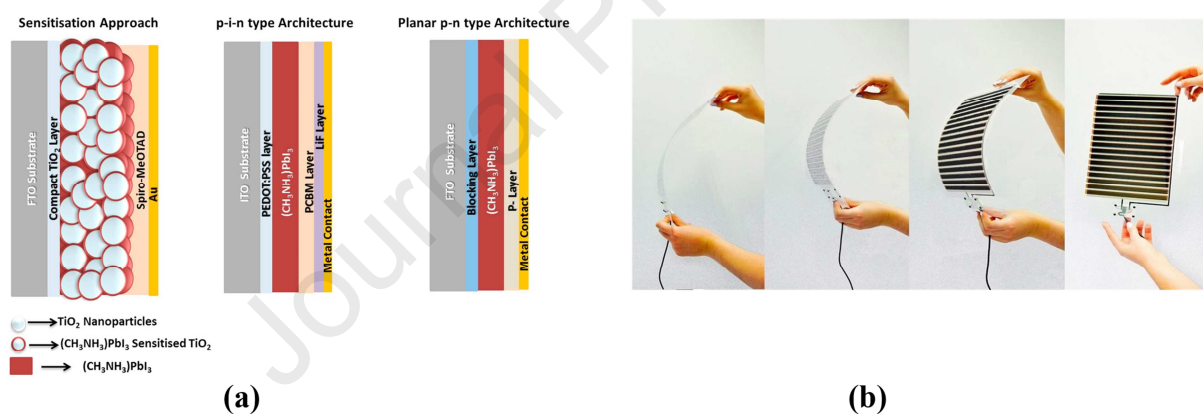
265

266 Figure 7: (a) Schematic diagram of the dye-sensitized solar cell (DSSC), (b) Semi-transparent DSSC  
 267 (Cornaro et al., 2018).

### 268 2.3.2. Perovskite solar cells

269 In a perovskite solar cell (PSC) perovskite structure absorbs light similar way as dye work in a DSSC.  
 270 PSC offered efficiency from 3% to 22% within a very short span of less than 10 years which attracts  
 271 researcher to work on it (Bi et al., 2016; Son et al., 2016). The general formula for perovskite is  
 272  $\text{ABX}_3$ , where A indicates cation and B indicates anion. **Figure 8** shows different perovskite  
 273 architecture. Most popular PSC consists of Methyl-ammonium-lead-iodide ( $\text{MAPbI}_3/\text{CH}_3\text{NH}_3\text{PbI}_3$ )  
 274 (Asghar et al., 2017; Ku et al., 2013; Seo et al., 2014; L. Zhou et al., 2019). This type of PV cells can

275 offer semitransparency which is suitable for BIPV glazing and glazed façade application (Cannavale  
 276 et al., 2017a, 2017b). Stability of perovskite under outdoor environment is a critical issue as exposure  
 277 to moisture and oxygen; perovskite performance degrades significantly which limits its large scale  
 278 production (Asghar et al., 2017). Due to the presence of moisture, the formation of  $\text{CH}_3\text{NH}_3\text{PbX}_3$ 's  
 279 mono- and di-hydrates, convert to  $\text{PbX}$ . Thus airtight conditions are recommended during perovskite  
 280 processing. Efficient PSCs contain toxic lead which can hamper the acceptance of this technology and  
 281 could conflict with legislative barriers (Bush et al., 2016; Howard et al., 2019; Z. Wang et al., 2017).  
 282 Ambient processed perovskite have also been under investigation (Bhandari et al., 2019) (Niu et al.,  
 283 2018; Tai et al., 2016; Wei et al., 2019; Yang et al., 2018). Two-dimensional Ruddlesden–Popper  
 284 (RP) PSCs exhibited a power-conversion efficiency as high as 20.62% and with 2880 hours without  
 285 encapsulation stability (Niu et al., 2018). Recently perovskite stability till 1,800 hrs at 70 to 75°C, and  
 286 8% drop from peak performance after 5,200 hrs was achieved (Bai et al., 2019). Considering its lower  
 287 stability, PSC still in consideration as its transparency can be tuned. Making thinner PSC (Della  
 288 Gaspera et al., 2015) or controlling the morphology of PSC, semitransparency is achievable. In 2017  
 289 alone, over 3000 academic journal regarding perovskite indicates its popularity among the researcher  
 290 (Snaith, 2018). Work on energy payback for perovskite is less explored are however few works  
 291 suggested that it can vary between 0.2 to 5 years depends on the type of material employed (Espinosa  
 292 et al., 2011; Gong et al., 2015; Ludin et al., 2018). In 2017, the global perovskite market was \$3.7  
 293 billion and it is growing with compound annual growth rate (CAGR) of 7.0% hence, in 2022 market  
 294 value should reach \$5.2 billion (B. Research, 2018). Oxford photovoltaics, OIST's Technology,  
 295 Solliance, Toshiba and NEDO are currently the major perovskite PV cell developer (Roy et al., 2020).



296

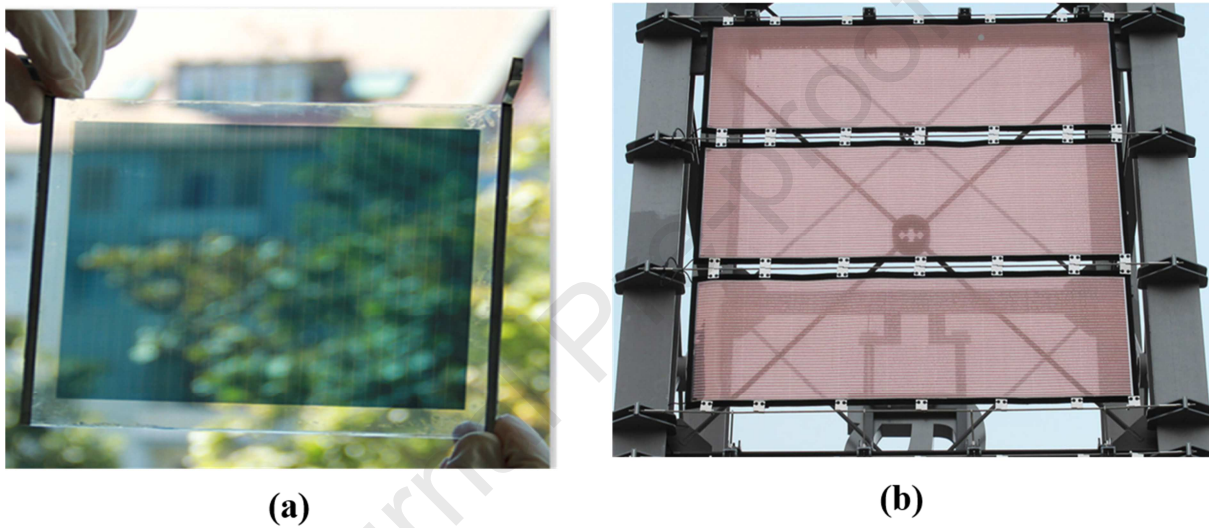
297 Figure 8: (a) Schematic of different perovskite PV cells architectures (Taken from (Senthilarasu et al.,  
 298 2015)) (b) Printed, flexible, perovskite photovoltaics by inkjet printing technique developed by Saule  
 299 Technologies, (image courtesy: Saule Tehcnologies)

### 300 2.3.3. Organic PV

301 Organic materials have the ability to absorb the entire solar spectrum due to the presence of  $\pi$ -bonded  
 302 electrons being able to move along the delocalized  $\pi$ -orbitals arising from  $sp^2$ -hybridization states of  
 303 carbon atoms (Kippelen and Brédas, 2009). Most organic semiconductors are p-type with a relatively  
 304 large optical bandgap (1.5–3 eV), reducing the production costs and the cell mass, because of the very  
 305 thin layers involved. The excitons diffusion length is relatively small for organic PV cells which are a  
 306 drawback compared to inorganic cells. Organic PV (OPV) is not suitable for low light condition as it  
 307 affects with photon having energy level, between 1.7 to 2.1 eV; however, its open-circuit voltage  
 308 rarely crosses 1.0V (Elumalai and Uddin, 2016). Open circuit voltage of OPV may have a logarithmic  
 309 relation with irradiation (Bristow and Kettle, 2016) (Mulligan et al., 2014). Though it has low  
 310 efficiency still possess shorter energy payback time ( $\sim 2.02$ – $0.79$  years) is shorter compared to c-Si

311 (~4.12–2.38 years) CIGS (~2.26–2.2 years) (Darling and You, 2013)(Anctil et al., 2019). Figure 9  
 312 shows a photographic view of OPV module. OPV shows lower thermal coefficient due to lower  
 313 infrared absorption than silicon (Bristow and Kettle, 2018). After three years of outdoor exposure,  
 314 OPV module initially degraded rapidly while secondary degradation rate was gradually, and following  
 315 seasonal variation due to metastability of the solar cells (Sato et al., 2019). In 2012, the world's first  
 316 grid-connected 0.2kW OPV system where nine flexible and transparent OPV modules formed of a sun  
 317 sai was commissioned at Mainova AG in Frankfurt. The global market value of OPV is expected to be  
 318 US\$97.4 million by the end of 2020 which expanded with the phenomenal compound annual growth  
 319 rate of 21.20% between 2014 and 2020. Epishine, Heliatek GmbH, Merck Group, OPVIUS GmbH,  
 320 infinity PV are the major companies which manufacture organic PV cells (Report, 2018). Table 2  
 321 listed comparison of different PV cells.

322



323

324 Figure 9: Rigid organic PV (OPV) module.(Lucera et al., 2017)

325 Table 2 : Comparative analysis of different PV cells.

Type of PV cell	Generaion	Efficiency	Advantages	Disadvantages
Mono-crystalline silicon (m-Si)	1 <sup>st</sup>	26.7% (Green et al., 2019)	Highly standardized, highly efficient, commercially abundant	Expensive manufactruing process and silicon waste is maximum in the production process
Polycrystalline silicon (p-Si)	1 <sup>st</sup>	22.3(Green et al., 2019)	Lesser energy and time needed for production, lower costs, Easily available on the market, Highly standardized	Relatively low efficiency than mono-crystalline silicon
Copper indium diselenide (CIGS)	2 <sup>nd</sup>	22.9(Green et al., 2019)	High temperatures and shading have lower impact on performance,	Higher amount of space is reuiqred for the equal amount of output

			Highest cost-cutting potential	power is needed
Cadmium telluride (CdTe)	2 <sup>nd</sup>	21% (Green et al., 2019)	Higher temperatures and shading have lower impact on performance, Less silicon needed for production	Similar to CIGS degradation, limited supply of Cd and potential environmental hazards.
Amorphous silicon (a-Si)	2 <sup>nd</sup>	10.2% (Green et al., 2019)	Higher temperatures and shading have lower impact on performance, Less silicon needed for production	Similar to CIGS and CdTe
Perovskite	3 <sup>rd</sup>	20.9% (Green et al., 2019)	High efficiency achievable, transparency is possible	Instability issue at outdoor ambient, Large scale device
DSSC	3 <sup>rd</sup>	11.9% (Green et al., 2019)	Low cost and low fabrication process, semitransparency is possible by tuning thickness	Instability issue at outdoor ambient, and large scale fabrication
Organic	3 <sup>rd</sup>	11.2% (Green et al., 2019)	Presence of $\pi$ -bonded electrons absorb huge range of solar spectrum, Temperature has lower impact on the efficiency degradation	Degradation varies from weeks to about 2 years, Positive and negative both type temperature coefficients are possible depends on the employed material

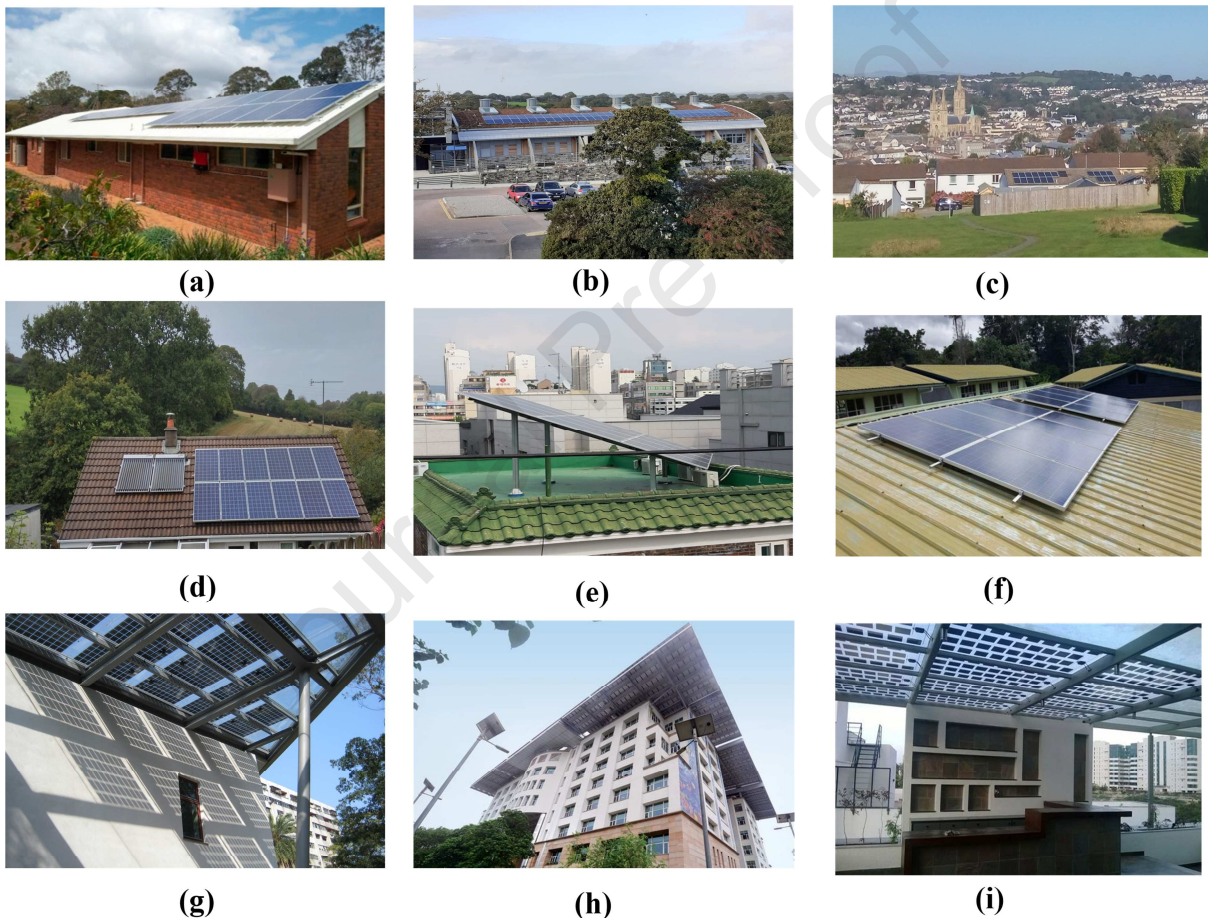
326

### 327 3. PV for BI/BA application

#### 328 3.1. roof integration

329 Inclusion of PV on the roof of a building utilizes the not productively used roof area and PV system  
 330 act as a power generating roof. Roof integration includes both BIPV and BAPV (Alnaser, 2018) types.  
 331 Commercially available mature silicon and thin-film technologies are the presently employed for  
 332 roof-integrated BIPV and BAPV (Aaditya et al., 2013; Aste et al., 2016; Sorgato et al., 2018; Zomer  
 333 et al., 2013). For BAPV system naturally ventilated are preferred for simpler installation while for  
 334 BIPV technology, semitransparency is a precondition. BAPV generates higher power while BIPV  
 335 enhances the overall performance of the building as semi-transparent BIPV roof renders daylight into  
 336 an interior and also controls the heat gain and loss (Jelle et al., 2012; Zomer et al., 2013). For roof  
 337 integration, the area available on the roof is essential parameters which can be evaluated from the  
 338 ground floor (Yadav and Panda, 2020). In general, it was found that the ratio between potential PV-  
 339 suitable rooftop area vs. ground floor area is 0.4 (Peng and Lu, 2013). For pitched roof commercially

340 available standard BIPV, BAPV or solar tiles are applicable (A. K. Shukla et al., 2017a). BIPV and  
 341 BAPV Roof integration with traditional PV systems are shown in Figure 10. Figure 10 (a) 3. 6 kWp  
 342 BAPV roof in Australia, (b) BAPV roof integration, University of Exeter, Penryn Campus, (c,  
 343 d) Typical house construction with BAPV in Southwest of England (Truro and Falmouth), (e) Typical  
 344 house BAPV in South Korea (f) Rooftop BAPV application at a school in Suriname (Raghoebarsing  
 345 and Reinders, 2018) (g) Typical roof-integrated semi-transparent BIPV installed in Taipei Public  
 346 Library Solar LEO House BIPV, (h) shows India's first zero energy building using BAPV,  
 347 constructed in 2014 where PV panels occupy 4,600 m<sup>2</sup> area and annual energy generation: 14 lakh  
 348 (\$19k) Unit kWh while the cost of installation was Rs 18 crore (\$2533k), (i) Semi-transparent spaced  
 349 type crystalline silicon-based glass-glass BIPV for roof application having installed capacity of  
 350 168kWp (Image courtesy: HHV Solar Bangalore, India. Roof integration of PV is beneficial if they  
 351 are not shaded by nearby trees, tall buildings.



352

353 Figure 10: (a) 3. 6 kWp BAPV on equatorial facing roof in Australia (taken from (Miller et al.,  
 354 2018)), (b) BAPV roof integration, University of Exeter, Penryn Campus, Figure (c, d) Typical house  
 355 construction with BAPV in Southwest of England (Truro and Falmouth), (e) Typical house BAPV in  
 356 South Korea, (f) Rooftop BAPV application at a school in Suriname (Raghoebarsing and Reinders,  
 357 2018), (g) Taipei Public Library Solar LEO House BIPV (no copyright was required), (h) Indira  
 358 Paryavaran Bhawan India (Jaymin, 2018), (i) semi-transparent spaced type crystalline-silicon based  
 359 glass-glass BIPV for roof application (Image courtesy : HHV Solar Bangalore , India

360 Solar tiles replace the conventional 'roof tiles' with solar PV tiles which are elegance in looking,  
 361 aesthetics for roof and also eliminate existing utility costs, easy for installation and highly durable



362 (Huang et al., 2014). Presently Dow Chemical, CertainTeed (Apollo line), SunTegra, Atlantis Energy  
 363 (SunSlates), and Tesla are the provider of solar shingles. CertainTeed product contains 14 high-  
 364 efficiency monocrystalline silicon solar cells in a single solar shingle which produce 60W. For Luma  
 365 Solar product, airflows are allowed underneath the shingle, which shows 21% solar-to-electricity  
 366 conversion efficiency, even higher than rack-mounted panels. SunTegra's solar shingles are  
 367 lightweight and use 50% less wiring than rack-mounted solar panels. Powerhouse 60-Watt shingles  
 368 will have an energy conversion efficiency factor of 17.1. Figure 11 shows the presently available  
 369 different solar shingles. In 2016, the global BIPV roofing market value was US\$ 2.4 billion, which is  
 370 expected to grow with a compound annual growth rate of 14.65 % over the between 2019 - 2027. In  
 371 2027, BIPV roof market values are expected to be US\$ 37.26 billion (Analysis, 2020).



372

373 Figure 11 : Different Solar Shingles (image courtesy : CertainTeed, Suntegra, LumaSolar,  
 374 Powerhouse, Sunflare)(Guess, 2018)

### 375 3.2. Wall integration

376 PV systems for wall application includes (Peng et al., 2013b) (1) mounting of PV module on the  
 377 existing wall as BAPV systems and (2) direct integration of PV module on the building wall to  
 378 replace the external wall or glass as BIPV system and. PV cladding is the common BAPV wall  
 379 application where between building envelope and PV, gaps are maintained to enhance the PV  
 380 performance (Yang et al., 2000) (Peng et al., 2013b). The external wall of a black-painted Trombe  
 381 wall can be replaced by a bluish PV system to transform it aesthetically in nature (Sun et al., 2011).  
 382 Performance of the PV Trombe wall depends on the PV coverage as opaque PV cells restrict the  
 383 incident solar radiation to reach the Trombe wall and the wall thickness can vary between 0.3-0.4 m to  
 384 minimize the thermal swing inside the room and zero thermal heating (Taffesse et al., 2016) (Sun et  
 385 al., 2011).

386 Investigation on retrofit building in Italy using c-Si, a-Si and CIGS based BIPV exhibited 45% and  
 387 20% less power generation from a-Si and CIGS respectively than c-Si. This was due to a higher  
 388 operating temperature of a-Si and CIGS as they had lower NOCT than c-Si. Semi-transparent a-Si  
 389 thin-film based BIPV wall is shown in **Figure 12a**. The performance showed that PV power  
 390 generation was almost half of that in the rated values. The possible reason was predicted that the

391 building was tilted to 50° to the southwest and also was affected due to the self-shading created from  
 392 its own building mass (Yoon et al., 2011). (Evola and Margani, 2016). Ventilated a-Si based BIPV  
 393 wall at Zhuhai, China ( Latitude 22.37 N, 113.54 E) showed 0.5~1.5°C lower operating temperature  
 394 and 0.2%~0.4% higher power generation compared to non-ventilated counterpart. Annual energy  
 395 output difference between both the system was 0.41% (shown in Figure 12b) (Zhang et al., 2014).



396

397 Figure 12: (a) Photograph of wall integrated completed building of R&D Institute, Kolon Engineering  
 398 and Construction, Yongin city, Gyeonggi, the central region of Korea (latitude 37°17' N, longitude of  
 399 127°12' E)(Yoon et al., 2011), (b) The two amorphous silicon PV walls under experiment Zhuhai,  
 400 China ( Latitude 22.37 N, longitude 113.54 E) (Zhang et al., 2014), (c) BIPV wall made of dye-  
 401 sensitized cell (DSSC) technology; System provider: Konarka Technology\* (Heinstein et al., 2013).  
 402 Konarka Technology was spin out company from University of Massachusetts, Lowell, USA, presently out of operation (d) Ekoviikki Sustainable  
 403 City Projects, Finland (image courtesy: SOLPROS), (e) External elevator glass was integrated with  
 404 OPV. (Image courtesy: OPVIUS GmbH), (f) energy-efficient ETFE façade installed using printed

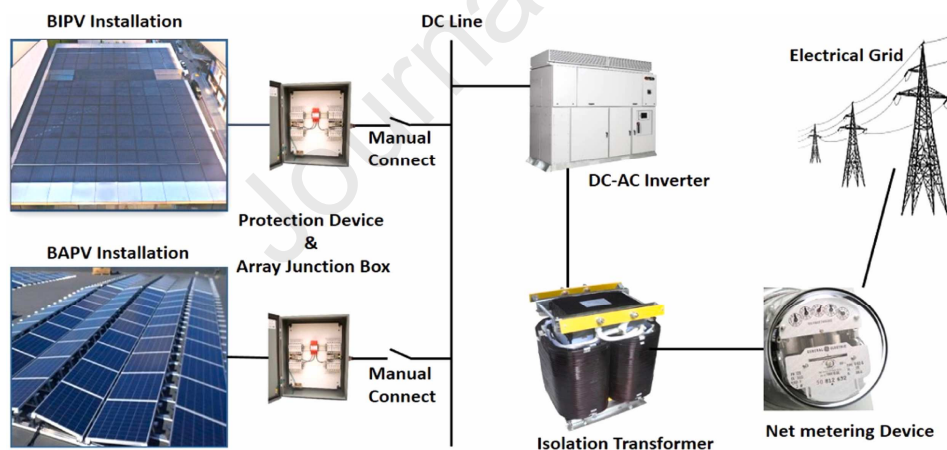
405 Organic Photovoltaic implemented it as part of the rebuilding work on the premises of Merck KGaA  
 406 in Darmstadt (Image courtesy: OPVIUS GmbH).

407 First and second-generation PVs are predominant for wall application whilst third-generation PV cell-  
 408 based BIPV/BAPV wall is rare. Figure 12c shows DSSC based wall, which was developed by  
 409 Konarka Technology (Heinstein et al., 2013). OPV based BIPV for cladding application was  
 410 investigated using indoor experimental data which was scaled for simulation of commercial size OPV  
 411 BIPV cladding. The system simulations compare typical energy demand profiles of small commercial  
 412 buildings and illustrate that OPV arrays show strong potential to be used with excess energy  
 413 generation for 8 months of the year based upon a 4.22 kWp OPV system and can adequately meet the  
 414 energy demand in spring, summer and autumn for a small commercial building in Northern Europe  
 415 (Stoichkov et al., 2019). Installing PV in balcony also another approach where obstacle for viewing is  
 416 negligible. Total 240 m<sup>2</sup> of photovoltaic modules were installed for balcony glazing on the south and  
 417 west sides of the house in a residential building in Finland, as shown in Figure 12d. Figure 12 e and  
 418 Figure 12f show external elevator glass were integrated with OPV and first energy-efficient ETFE  
 419 façade installed using printed OPV which was implemented as part of the rebuilding work on the  
 420 premises of Merck KGaA in Darmstadt.

### 421 3.3. Grid integration

422 Grid-connected BI/BAPV reduces the necessity of storage device and generated electricity to supply  
 423 both building and grid or grid only (Benemann et al., 2001; Eltawil and Zhao, 2010; Gorgolis and  
 424 Karamanis, 2016; Hagemann, 1996; Leon and Vinnikov, 2015). Figure 13 shows the schematic of the  
 425 grid-connected BIPV and BAPV system.

426



427

428 Figure 13: Schematic view of grid-connected BIPV and BAPV system (Taken from(N. M. Kumar et  
 429 al., 2019))

430 Energy from grid-connected BAPV and BIPV both depends on rated characteristics of a PV system,  
 431 the geographical location of the systems while the reliability of control systems also play an essential  
 432 role. For grid connection, employed different types of inverters are central, string, multi-string, AC-  
 433 module and microinverter (Kjaer et al., 2005) (Allouhi et al., 2016; Aristizábal and Gordillo, 2008;  
 434 Kazem and Khatib, 2013; Liu et al., 2012; Yang et al., 2004)(Elavarasan et al., 2019). To use string  
 435 inverter, BA/BIPV modules are connected in series, and the string is connected to one inverter which  
 436 can lead to a lower PV energy yield during partial shading conditions, thereby degrading the overall  
 437 system performance. Especially when different sizes and types of PV are used, stringing becomes

438 extremely challenging (Ravyts et al., 2019). Microinverters are attached to the back of each PV  
439 module and beneficial for partial shading condition and different types and sizes of PV systems (R.  
440 Hasan et al., 2017). To obtain maximum power from PV-inverter combination, the power rating of  
441 inverter should match the power rating of the PV system (Mondol et al., 2006). Except inverter to  
442 convert the generated DC power output from PV to AC, filters are required between PV and grid to  
443 reduce the inverter's harmonics and minimize or neutralize the spikes from the grid (Liserre et al.,  
444 2004; Milan Pradanovic and Timothy Green, 2003). Voltage level fluctuation, voltage flicker and  
445 unintentional islanding is the major issue occur for PV and grid connection (Shivashankar et al.,  
446 2016). Intermittent nature of PV changes the voltage level, which creates trouble for grid connection.  
447 The magnitude of cloud cover is independent of the voltage fluctuation (Woyte et al., 2006). Voltage  
448 harmonics in grid mainly the effect of generated current harmonics due to PV inverters. Harmonics  
449 are the biggest reason for losses in the distribution system. PV power output changes also create  
450 frequency fluctuations which can not be nullified by the PV system due to its lack of inertia. Voltage  
451 flicker and fluctuation of the PV system can be reduced if the size of the PV arrays is big enough.  
452 Larger the size of the PV array lowers the fluctuations (Marcos et al., 2011). Inverter selection and  
453 design of new inverter are required for grid-tie PV as inverter converts DC power to AC, controls  
454 power factor, regulates reactive power (Tsengenes and Adamidis, 2011)(Yan et al., 2019).

455

456

### 457 **3.4. Window application**

458 BIPV window plays a vital role in the overall building energy performance of retrofitted or new  
459 buildings. A window of a building is responsible for viewing while it allows daylight and higher heat  
460 to flow from interior to exterior and admits solar heat gain (Ghosh and Norton, 2018). BIPV window  
461 controls the entering daylight and solar energy transmission while can also reduce the heat flow from  
462 building interior to the exterior (Ng and Mithraratne, 2014a; Yoon et al., 2013). BIPV for window  
463 application should be transparent or semi-transparent in nature (Alrashidi et al., 2020a, 2020b). For  
464 BIPV glazed window the most indispensable fact is to maintain a balance between the visible light  
465 transmission and power conversion efficiency, in addition, considering colour comfort and thermal  
466 comfort (Wheeler and Wheeler, 2019). To achieve BIPV window, spaced type structure by  
467 maintaining gaps between PV cells (Sánchez-palencia et al., 2019) (Park et al., 2010) or by tuning the  
468 PV material thickness, transparency is achievable. Spaced type structure is popular for first-generation  
469 opaque crystalline silicon which has higher absorption and low transmittance (Riverola et al., 2018;  
470 Santbergen and van Zolingen, 2008). The percentage of PV area coverage offers the semi-  
471 transparency of this type window as depicted in **Figure 14a**. Thus, solar heat gain, indoor  
472 illuminance, daylight factor for spaced BIPV window depends on the glazing area covered by PV  
473 whereas efficiency and thickness of PV have less impact on those parameters (Chau et al., 2010; Fung  
474 and Yang, 2008; Karthick et al., 2018; Park et al., 2010; Peng et al., 2019). This spaced type semi-  
475 transparent BIPV window offers similar quality of daylight as the light passes through only the glass  
476 materials (Ghosh et al., 2019b).

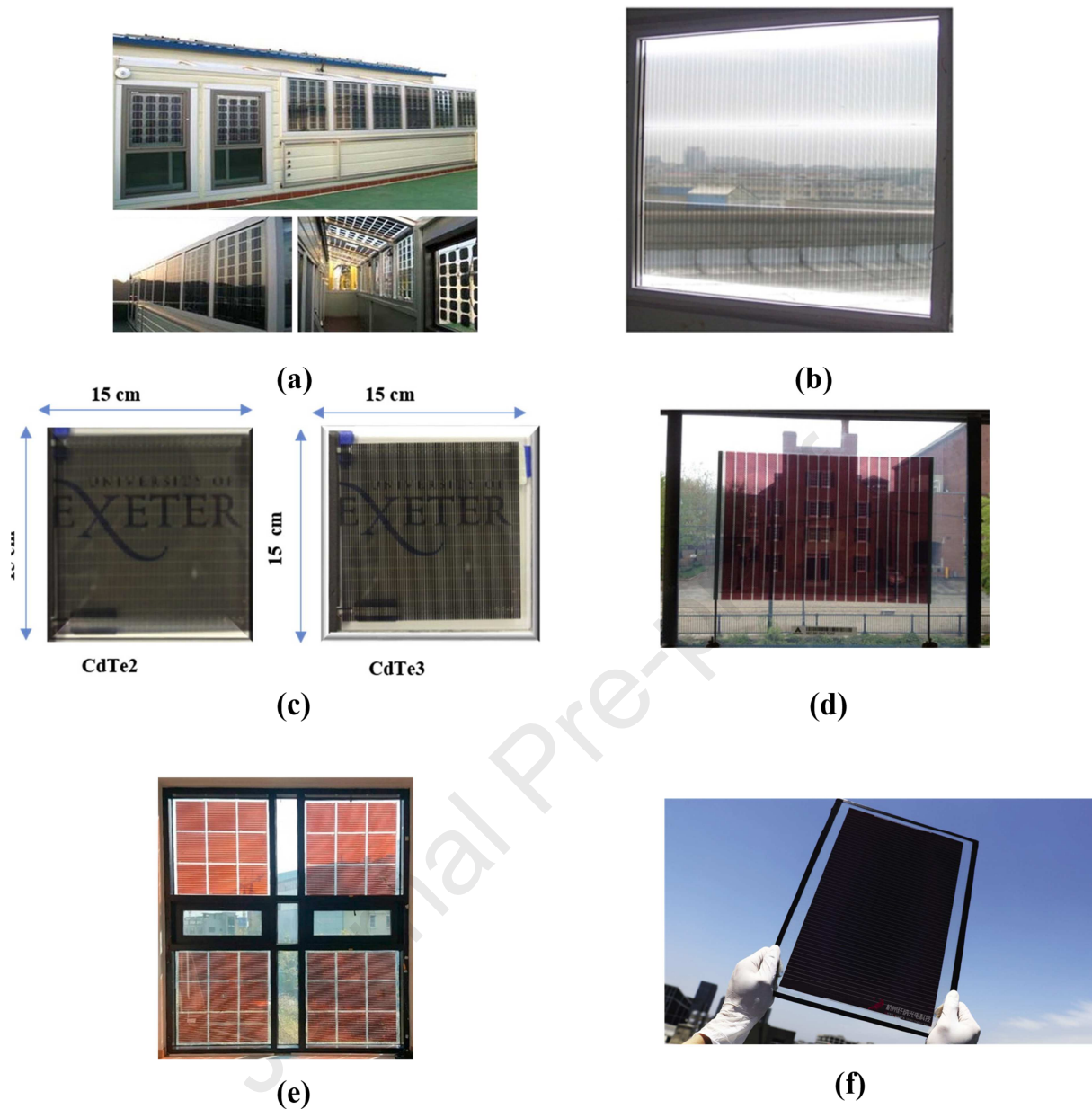
477 Tuning the material thickness, semi-transparency is achievable from second-generation thin film and  
478 third-generation emerging PV technologies. For this type of BIPV window, transmittance or material  
479 thickness is directly related to PV power generation where thinner material possesses higher  
480 transmittance and generates low power (Chow et al., 2007; Miyazaki et al., 2005; Takeoka et al.,  
481 1993). The solar factor is directly related to transmittance, while  $U$ -value has no impact on the  
482 window transmittance (Alrashidi et al., 2019; Barman et al., 2018). a-Si type has temperature

483 enhancement issue which can be reduced by creating airflow in a double pane window while tilted  
484 always showed higher operating temperature than horizontal or vertical orientation (Han et al., 2009)  
485 (Yoon et al., 2013)(Chatzipanagi et al., 2016). Recently, highly insulated a- si based BIPV window  
486 was fabricated which showed 79% absorption, 7% visible transmittance, 100% UV blockage, 95%  
487 restriction of undesired thermal radiation, 24.9% better daylighting performance compared to ordinary  
488 glazing while  $U$ -value was  $1.10 \text{ W/m}^2\text{K}$  (Cuce et al., 2015a, 2015b). The energetic performance of  
489 CdTe and Perovskite-based window was evaluated which recommended that for higher transmission  
490 window to wall ratio needs to be high to generate higher power than low transmission material (Sun et  
491 al., 2018) (Cannavale et al., 2017b, 2017a). Organic PV (OPV) based BIPV window (OBIPV) also  
492 currently under investigation (shown in Figure 17 b). The efficiency of this OPV system varies  
493 between 4%-10% (Chemisana et al., 2019; Chen et al., 2012; Duan et al., 2019; Yan et al., 2012). In  
494 another work one 20% transmittance, 15% reflectance and 65% absorptance OPV glazing overall heat  
495 transfer coefficient was about  $6.0 \text{ Wm}^{-2} \text{ K}^{-1}$ (Friman Peretz et al., 2019)

496 Visual comfort gets higher priority for BIPV window. DSSC based BIPV window (Figure 14 d)  
497 where dye colour can be anything, colour property analysis is essential before installing them (Kang  
498 et al., 2003)(Aritra Ghosh et al., 2018c). Material degradation often enhances the transmissivity which  
499 may enhance the visual perception and colour render (Roy et al., 2019; Selvaraj et al., 2019). Carbon  
500 counter electrode based mesoscopic Perovskite was investigated for BIPV window where this PV  
501 device had 20% visible transmission, 0.33 solar heat gain coefficient and  $5.6 \text{ W/m}^2\text{K}$  overall heat  
502 transfer coefficient (Ghosh et al., 2020). 25% visible transmittance and CRI close to 100 (Chen et al.,  
503 2012) while in another work CRI close to 90.7 was possible for and visual transmittance 16.3%,  
504 suitable for semi-transparent BIPV window integration (Duan and Yi, 2019).

505 Currently, BIPV glass providers are Asahi Glass Co., Ltd., Ascent Solar, Canadian Solar, Centrosolar  
506 Group AG, DuPont, EMMVEE Solar Systems Private Limited, First Solar, Hanergy, Hanwha Solar  
507 One, Onyx Solar, Power Film, Inc Sun Power, GE, Pythagoras Solar, Suntech Power Co., Ltd , Solar  
508 Frontier Pilkington (Z. M. Research, 2018).

509



510  
511

512 Figure 14: (a) Overview of crystalline silicon based semi-transparent BIPV installation in a sunroom,  
513 Republic of Korea (Park et al., 2010) (b) amorphous-silicon BIPV single window (He et al., 2011) (c)  
514 Photographs of three different CdTe glazing (Alrashidi et al., 2019) (d) Viewing through Organic  
515 BIPV window (Yan et al., 2012), (e) DSSC glazing for outdoor experiment (Lee and Yoon, 2018) (f)  
516 14.24% conversion efficiency record for a large-area (200×800 cm<sup>2</sup>) perovskite solar module (image  
517 source: microquanta)

### 518 3.5. Low concentrating façade

519 Use of concentrator in the PV system reduces the expensive PV material cost by reducing the use of  
520 expensive and toxic product involved in the production of PV material, better use of space, ease of  
521 recycling of constituent materials (Baig et al., 2015, 2014, 2013, 2012). The concentrator includes low  
522 (<10), medium and high (>100) type based on the concentration ratio (Chemisana, 2011)(G. Li et al.,  
523 2020)(Chong et al., 2013). Low concentration is suitable for BIPV application, as no coolant is  
524 required to cool down an enhanced PV system temperature (Amanlou et al., 2016). Low concentrator

525 for BIPV application includes compound parabolic concentrator (CPC) (Tian et al., 2018)(Jaz et al.,  
 526 2017), luminescent solar concentrator (LSC) (Meinardi et al., 2017; Rafiee et al., 2019) and  
 527 holographic solar concentrator (HSC) (Collados et al., 2016).

528 Mirror-based or dielectric-filled compound symmetric (Muhammad-Sukki et al., 2014) and  
 529 asymmetric (Sarmah et al., 2014) parabolic concentrators have a prospect for BIPV application. Due  
 530 to non-imaging nature, this type of concentrator can collect both direct and diffuse solar radiation.  
 531 Asymmetric two dimensional (2d) compound parabolic concentrator (CPC) can improve the  
 532 maximum power point by 62% compared to its non-concentrating counterpart (Mallick et al., 2004).  
 533 In another work, asymmetrical dielectric-filled 2dCPC based PV generated 2.27 times higher  
 534 electrical power than a system without concentrator which could bring the solar panel cost down by  
 535 20% per kWp (Sarmah et al., 2014). The circular entry and exit apertures in 2d CPC create hindrance  
 536 for placing with the most available square and rectangular PV cells in the market. Thus, three  
 537 dimensional (3d) CPCs were proposed which is formed by the rotation of 2d CPC. 3d CPC geometry  
 538 can be improved by intersecting two symmetrical 2d CPCs orthogonally and this new shape is called  
 539 crossed compound parabolic concentrator (CCPC) (Sellami and Mallick, 2013a). Reflective type  
 540 3dCCPC achieved three times higher power output than similar non-concentrating PV panel.  
 541 Dielectric material filled CPC (dCPC) is an alternative to the mirror CPC. Refraction on air–dielectric  
 542 interface allows it to collect solar radiation from a wider angle. Using 2d dCPC 40% cost reduction  
 543 possibilities have been reported earlier (Mallick and Eames, 2007). Square elliptical hyperboloid  
 544 shape dielectric-filled 3d CPC was investigated for static window application. The geometrical  
 545 concentration ratio of this system was  $6\times$  while optical efficiency was 55% (Sellami and Mallick,  
 546 2013b). It was found that the CCPC with a concentration ratio of  $3.6\times$  represents an improved  
 547 geometry compared to a 3-D CPC for the use as a static solar concentrator. In another work,  
 548 mimicking of V-shaped posture of basking white butterflies as V-trough concentrator to a solar cell  
 549 increased its output power by 42.3% (Shanks et al., 2015). However, the experimental work is still  
 550 requiring to validate this hypothesis. Recently CPC-perovskite combination offered 10.73 times  
 551 higher short circuit current than non-concentrating counterpart (Baig et al., 2020). In northern latitude  
 552 due to cloud cover, solar irradiance is mostly the diffuse type whose spectral characteristics are  
 553 different and lower in intensity than direct irradiance. Thus, the inclusion of low concentrating CPC  
 554 window, as shown in **Figure 15** is potential which collects both direct and diffuse solar radiation.

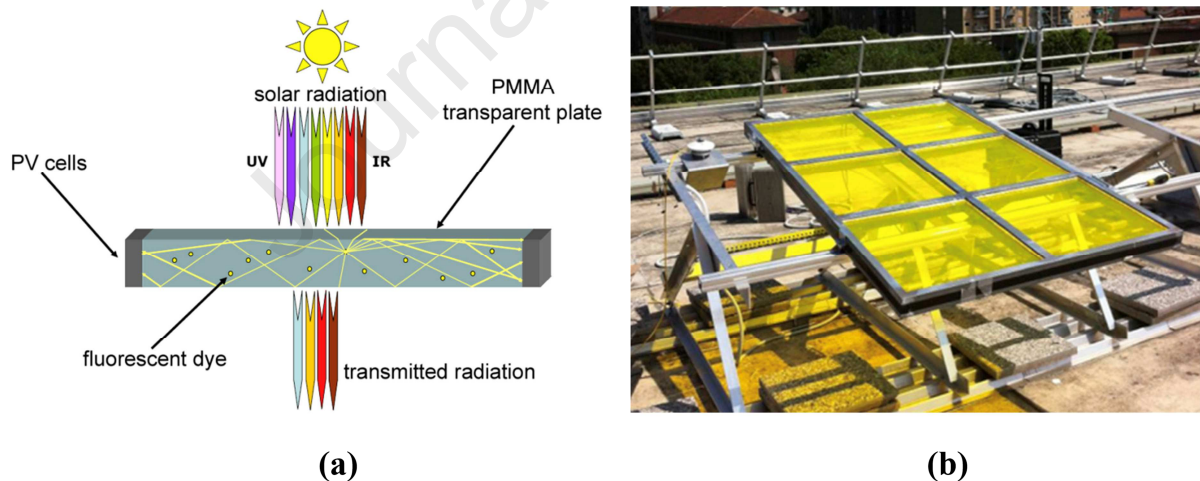
555



556

557 Figure 15: Semi transparency effect of the square elliptical hyperboloid concentrator for BIPV  
 558 window application (taken from Sellami and Mallick 2013).

559 Luminescent solar concentrator (LSC) is another suitable low concentrator and promising for  
 560 transparent solar BIPV window application, as shown in Figure 16. LSC harvest both diffuse and  
 561 direct sunlight was proposed in late 1970 for PV applications (Hermann, 1982; van Sark, 2013). An  
 562 LSC consists of a transparent polymer sheet, doped with a low concentration luminescent particles  
 563 (Luminophore) which can be organic dyes (Reisfeld et al., 1994), quantum dot (Chandra et al., 2015,  
 564 2012) (AbouElhamd et al., 2019) or rare-earth material (Day et al., 2019). These particles absorb a  
 565 fraction of the incident sunlight and emit photons with a near-unity quantum yield. If the refractive  
 566 index of the carrier material is higher than that of the surrounding medium (in this context, air), a  
 567 large proportion of the emitted photons will reach the edges following total internal reflection. LSCs  
 568 are less sensitive to their orientation angle compared to silicon PV modules; however, LSCs are  
 569 unaffected by efficiency losses and electrical stresses due to shadow effects, often occur in bulk and  
 570 thin-film PVs. The prime advantages of LSC-BIPV window are they can be the shaped to any size  
 571 and its, transparency, colour and flexibility is fully controlled depends on occupant needs (Meinardi et  
 572 al., 2017). Using double-glazed LSC may offer lower electrical performance than an LSC plate  
 573 without glass due to higher reflection losses (Aste et al., 2015a). They can also behave as a spectrally  
 574 selective window where UV spectrum can be shifted to the visible spectrum and directed to the edge  
 575 of the window where PV cells are mounted. Thus building interior can be protected from the adverse  
 576 effect of UV and will generate benign electricity from them concomitantly (Fathi et al., 2017). High  
 577 power generation from an LSC window depends on the higher percentage of coloration of the film or  
 578 glass, however, for visual performance a lower percentage of colored glass is required (Vossen et al.,  
 579 2016). At the Netherlands location, 25% window covered by an LSC was found soothing than that of  
 580 a traditional clear glass window (Vossen et al., 2016). It is expected that concentrating PV market will  
 581 reach USD 2,710.6 Million by 2023 (Future, 2018). However, this includes low, medium and high all  
 582 three types of the concentrator.



583

584 Figure 16: (a) Diagram of the incident photons and of the photons emitted by a dye molecules inside  
 585 the LSC (b) LSC window (Aste et al., 2015b)

586 Holographic solar concentrator technology employs holographic optical elements (HOE) to enable the  
 587 solar spectrum incident on the PV cell (Collados et al., 2016). Dichromated gelatin, photoresists,  
 588 photopolymers, photochromic, silver halide photographic emulsions are the different types of HOE  
 589 recording material (Abhijit Ghosh et al., 2018, 2015; Naydenova et al., 2013). Due to the spectral  
 590 selectivity, HOE allows only those solar spectra similar to PV cell to incident on it and rejects above  
 591 and lower spectrum band of solar radiation. Hence overheating of PV cells can be avoided (Brooks et  
 592 al., 2012; Hull et al., 1987; Müller, 1994; Zhang, 2011). Holographic solar concentrator (HSC) are



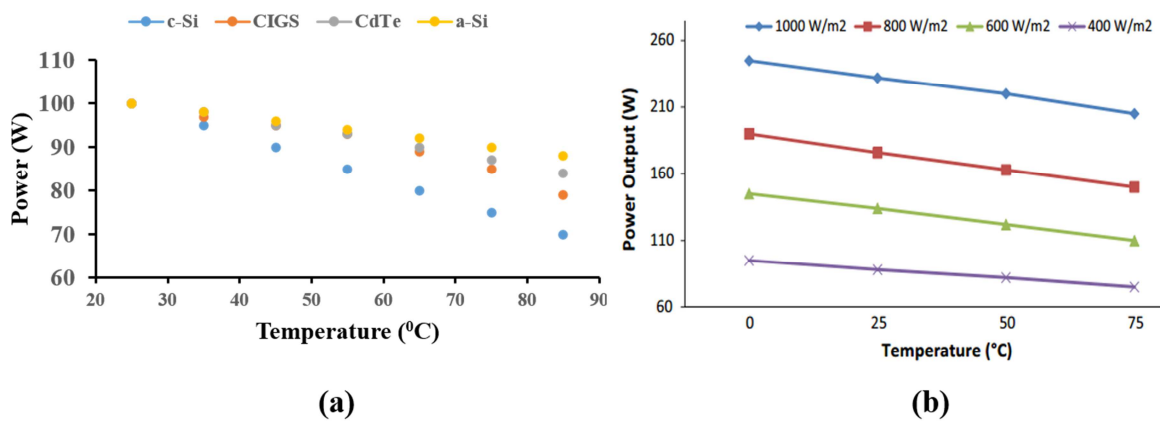
593 diffractive structures that are constructed holographically by the interference of two beams of light.  
 594 HOE diffracts light due to the ability of angular selectivity which makes it a see-through building  
 595 envelop suitable for window and transparent facade application. HOEs are classified based on  
 596 recording geometry, thickness, and method of modulation of optical properties. Based on recording  
 597 geometry hologram can be transmission or reflection types. The thickness of hologram can be thick  
 598 and thin. Modulation during recoding of hologram can be amplitude and phase type. Because of the  
 599 low efficiency thin amplitude and phase, both holograms are not, are not suitable for solar  
 600 applications. Ludman in 1982 for the first time proposed the use of holographic solar concentrator for  
 601 PV power generation. HOE with a concentration ratio of 1.23 (holographic cylindrical lens and c-Si  
 602 PV) (Chemisana et al., 2013), 1.27 (holographic spherical lens and a p-Si PV) (Aswathy et al.,  
 603 2018), 1.80 ( holographic spherical lens, an array of two holographic cylindrical lenses and an array of  
 604 two holographic spherical lenses with c-Si PV ) (Akbari et al., 2017), 1.90 (two holographic gratings  
 605 and a dye-sensitized PV cell) (Sreebha et al., 2018), 3.48 (cylindrical holographic lenses and c-Si  
 606 PV)(Marín-Sáez et al., 2019) were investigated and found to be an excellent result.

#### 607 4. Technical challenges associate with BI/BAPV

608

##### 609 4.1. PV performance degradation at elevated temperature

610 PV cells convert a certain wavelength of the incoming irradiation that contributes to the direct  
 611 conversion of light into electricity, while the rest is dissipated as heat. Only 15–20% of incident solar  
 612 energy is converted into electricity. The remaining part of the solar energy is converted into heat,  
 613 which causes heating of the solar cells in PV panels (Agathokleous and Kalogirou, 2016). **Figure 17**  
 614 shows the linear power drops of c-Si, a-Si, CdTe, CIGS PV for enhanced temperature. Maximum  
 615 power drop occurred for c-Si and minimum was for a-Si. Minimum drop for a-Si was found because  
 616 of annealing of a-Si cells, which promotes regenerative effect (Stabler-Wronsky effect) and an  
 617 intrinsic drop of the cell's conversion efficiency at a higher temperature. With elevated temperature,  
 618 reverse saturation current and open-circuit voltage of c-Si, a-Si, CdTe and CIGS PV increase and  
 619 decrease respectively which in turn decrease the fill factor and thus the overall PV cell efficiency  
 620 becomes lower than its standard test condition (STC) value (Singh and Ravindra, 2012). c-Si PV cell  
 621 has temperature coefficients around 0.4%/K, whereas for a-Si, this value is approximately  $-0.1\%$  K  
 622 (Bücher, 1997). PV temperature for first and second-generation can reach as high as 80 °C,  
 623 particularly in hot arid regions (Reddy et al., 2015). Long term thermal stress on PV cells also can  
 624 damage the PV module (Chow, 2010) (B. J. Huang et al., 2011).



625

626 Figure 17: (a) Effect of temperature on different PV materials,(Özkul et al., 2018) (b) The maximum  
627 power output of the mono-crystalline Si-PV modules (Jiang et al., 2012)

628 Temperature impact on third-generation PV cells is not similar to the first- or second-generation type.  
629 DSSC PVs show temperature coefficient of 0.1% between the temperatures from 30° to 50°. After  
630 that temperature, the generated vapour pressure from the liquid electrolyte may crack the cells (Tian  
631 et al., 2012). Increased FF was also found for DSSC PV at a higher temperature (Selvaraj et al.,  
632 2018). Also DSSC temperature coefficient shows positive and negative such as oscillatory behaviour  
633 which can be from the different velocities of the redox processes occurring at the electrolyte/counter  
634 electrode TiO<sub>2</sub>/dye, dye/electrolyte interfaces of a DSSC stack (Sebastián et al., 2004; Selvaraj et al.,  
635 2018). Ruthenium based DSSC showed that efficiency decreased at a rate of 0.05%/°C (Parisi et al.,  
636 2017). Another work reported that DSSC efficiency first increased from -7°C to 40°C and after 40°C  
637 it's started decreasing due to accelerated recombination (Raga and Fabregat-Santiago, 2013).

638 Under the real operating condition, perovskite solar cells temperature can easily reach up to 45 °C.  
639 Effect of temperature on the performance of Perovskite was explored by exposing the PV cells in a  
640 range of temperatures between -5 °C and 80 °C. The performance perovskite cells at -5°C displayed  
641 approximately 5 % less power conversion efficiency than at 22 °C. At 80 °C, a significant decrease  
642 occurred for open-circuit voltage and short circuit current which leads to a decrease of 36.0±5.5 %  
643 (Mesquita et al., 2019). Table 3 listed the temperature coefficients of different PV devices.

644

645 Table 3: Details of temperature coefficient of different PV technologies.

PV types	Temperature coefficient (K <sup>-1</sup> )
c-Si	-(0.2-0.3)
CdTe	-0.25 (Lee and Ebong, 2017)
CIGS	-0.33 to -0.50
a-Si	-0.10 to -0.30
Perovskite	Not available
<b>DSSC</b>	
Organic	+0.7

646

#### 647 **4.2. Thermal regulation of BI/BAPV using active and passive approach**

648

649 Dissipation of heat from BIPV/BAPV systems is possible by active or passive heat removal methods  
650 to improve PV performance similar or better than STC. The passive systems depend on convection,  
651 conduction and radiation while active methods utilize pumps or fans to maintain a flow of air or water  
652 over the front or at the back of the PV panel for cooling purposes (Baljit et al., 2016) as shown in  
653 Figure 18a. Thus, the inclusion of thermally regulated PV system produces electricity and thermal  
654 energy simultaneously which enhances 15–30% higher annual exergy output than that of the similar  
655 non-thermally regulated PV system (Agrawal and Tiwari, 2010a, 2010b; Chow, 2010; Hasanuzzaman  
656 et al., 2016; Lamnatou and Chemisana, 2017; Prakash, 1994). Temperature regulation of crystalline  
657 PV is the most economical compared to organic or thin film due to the detrimental effect on the  
658 efficiency of the silicon PV (Browne et al., 2015).

659 The gap between PV and building façade element should be between 10 to 15 cm to allow the  
660 ventilation (natural air flow) that can reduce the PV device temperature and enhance the electrical

661 power output producibility. No gap between PV and building skin creates a thermal bridge and  
662 conductive heat flow allow unwanted solar heat gain into the building space and degrades the PV  
663 efficiency(Agathokleous and Kalogirou, 2016; Fossa et al., 2008; Wang et al., 2006). No  
664 maintenance, low initial cost, no noise, no electricity consumption, simpler integration are the  
665 advantages of natural air flow for reduction of elevated temperature of PV panels (A. Shukla et al.,  
666 2017). However, natural airflow offers limited gain on PV performance due to low thermal  
667 conductivity, low density, low volumetric heat capacity and low mass flow rate of air. As wind speed  
668 is influential for this system, higher wind speed can reduce PV temperature significantly whereas  
669 lower wind speed restricts to lose heat (A. Shukla et al., 2017).

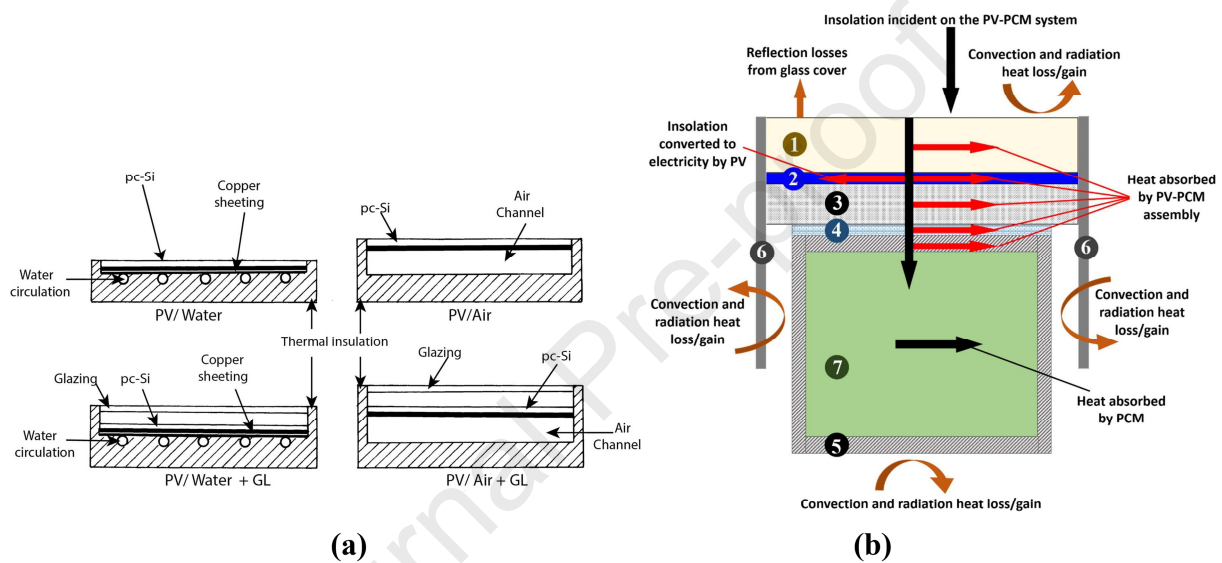
670 To regulate the PV temperature using active forced airflow circulation requires an auxiliary pump and  
671 the warm air can be used for end-users to supply space heating demand, agriculture/herb drying,  
672 increased ventilation, as well as the electricity generation (Kamthania et al., 2011). Using  
673 duct/collector behind the PV panel dissipates heat due to airflow buoyancy created from warm air at  
674 the rear of the panel (Brinkworth et al., 1997)(Phiraphat et al., 2017). Increase the rate of uniform  
675 airflow, collector diameter and collector length enhance the thermal and electrical efficiency for a PV  
676 system (Garg and Adhikari, 1999; Ghani et al., 2012; Hegazy, 2000; Solanki et al., 2009; Vats and  
677 Tiwari, 2012; Yang and Athienitis, 2014). For BIPV system air cooling are most investigated than  
678 water cooling (Joshi and Dhoble, 2018) while they offer energy payback period around 1 to 14 years  
679 (Lamnatou and Chemisana, 2017).

680 Using water flow on the top or rear of the PV device can maintain a PV device's STC temperature and  
681 water has higher heat capacity than air (Gil-Lopez and Gimenez-Molina, 2013a, 2013b). This water  
682 can be employed for the building hot water application (Krauter et al., 1999; Shyam et al., 2015;  
683 Tomar et al., 2017; Tripanagnostopoulos et al., 2002; Wilson, 2009). Depends on location water flow  
684 rate varies to offer best results such as 0.003 kg/s water flow was suitable to obtain the optimum based  
685 result for polycrystalline silicon solar cell based BIPV in Hong Kong (Chow et al., 2009) whereas 0.2  
686 kg/s in Älvkarleö, in the central part of Sweden (Davidsson et al., 2012). Natural circulation water  
687 type PVT systems are more economical as compared to forced circulation systems (Joshi and Dhoble,  
688 2018). Investigation of BAPVT using water is higher than BIPVT system (Lamnatou and Chemisana,  
689 2017). Depends on the technology this BPAVT water system energy payback time varies between 1  
690 to 4 years (Lamnatou and Chemisana, 2017). Addition of water and air both can serve the seasonal  
691 energy demand of the building where air mode will provide hot air in winter to reduce space heating  
692 load and water will work for the rest of the year (Xu et al., 2020).

693 To enhance further PV performance by dissipating elevated heat, fluids with less than 100 nm size  
694 metallic nanoparticles of copper (Agarwal et al., 2016), aluminium (Rejeb et al., 2016), zinc (K.S. et  
695 al., 2016), silicon (Singh et al., 2009), iron (Ghadiri et al., 2015), titanium (Sardarabadi and  
696 Passandideh-Fard, 2016), gold (Wang et al., 2019), silver (Stephen et al., 2019) and non-metallic  
697 nanoparticles of aluminium oxide ( $Al_2O_3$ ), copper oxide (CuO), silicon carbide (SiC), carbon  
698 nanotubes (SWCNT, DWCNT and MWCNT)(Mizuno et al., 2009; Said et al., 2014; Shende and  
699 Ramaprabhu, 2016) can be used while ethylene glycols, engine oil, distilled water, glycerol can be the  
700 base fluid (Farhana et al., 2019). The mass fraction of nanoparticles influence the thermal  
701 performance of the combined PV thermal system significantly and slightly on electrical performance.

702 The phase change material (PCM) has the ability to reduce the elevated PV temperature by absorbing  
703 a large amount of heat at a constant temperature (Alagar Karthick et al., 2020) (Kant et al., 2019; A.  
704 Karthick et al., 2020) Thus, it behaves isothermally during charging and discharging process (Browne  
705 et al., 2016, 2015; Huang et al., 2006, 2004; M. J. Huang et al., 2011). The energy flow of a typical

706 BIPV-PCM system is shown in **Figure 18b**. The paraffin waxes, salt hydrates, fatty acids and eutectic  
 707 organic/non-organic compounds are different types of PCM used for thermal regulation from PV  
 708 (Baetens et al., 2010; Kalnæs and Jelle, 2015; Pielichowska and Pielichowski, 2014). BAPV-PCM is  
 709 able to improve 2-6% electrical efficiency compared to without PCM-PV(A. Hasan et al., 2017; Park  
 710 et al., 2014; Smith et al., 2014). PCM can reduce the c-Si PV cell temperature up to 10 °C in  
 711 temperate climate while can reduce up to 16-21°C at a hot and humid climate (Hasan et al., 2015,  
 712 2014) and 10°C for CIGS PV in a temperate climate (Curpek et al., 2019; Čurpek and Čekon, 2020).  
 713 BIPV cooling using PCM for high ambient temperatures are effective, however, for low ambient  
 714 temperature PCM may reduce heating effect if the stored heat is not dissipated by introducing another  
 715 facility (metal matrix, conductive particle) (Chandrasekar et al., 2015). PCM based BI/BAPV system  
 716 shows a payback time of 14.5 years (Panayiotou et al., 2016). Table 4 summarises the comparison of  
 717 different thermal regulation techniques.



718  
 719 Figure 18: (a) Cross section of PV/Water, PV/Water+Glazing, PV/Air, and PV/Air+Glazing  
 720 experimental models (Tripanagnostopoulos et al., 2002) (b) Schematics of the energy flow in the  
 721 BIPV-PCM system (taken from (A. Hasan et al., 2017) )

722 Table 4: Comparison of different thermal regulation techniques.(Chandrasekar et al., 2015)(Hasan et  
 723 al., 2010)

Thermal regulation	Types	Advantages	Disadvantages
Natural Air	Passive	<ul style="list-style-type: none"> <li>low initial cost,</li> <li>no maintenance,</li> <li>no noise,</li> <li>no electricity consumption,</li> <li>longer life</li> </ul>	Low -thermal conductivity -heat capacity, -heat transfer rates, -mass flow rates Depends on – wind direction and speed, dusty air reduces heat transfer, Not useful for low latitude location where ambient temperature is higher than 20 °C
Forced air	Active	<ul style="list-style-type: none"> <li>higher heat transfer rates compared to natural circulation of</li> </ul>	high initial cost for fans and ducts to handle large mass flow rates, high electrical consumption, maintenance

		air <ul style="list-style-type: none"> <li>• independent of wind direction and speed,</li> <li>• higher mass flow rates than natural air circulation achieving high heat transfer rates,</li> <li>• higher temperature reduction compared to natural air circulation</li> </ul>	cost noisy system, difficult integration compared to natural air circulation system
Forced Water	Active	<ul style="list-style-type: none"> <li>• Similar to forces air in addition higher thermal conductivity than air.</li> </ul>	<ul style="list-style-type: none"> <li>• Tank is required to store water and also needs pump and pipes.</li> <li>• Electricity requires to operate pumps. in case of roof integration overall system increase the weight of the installation</li> <li>• Pumping power requirement is higher than forced air</li> </ul>
Nano fluid	Active	<ul style="list-style-type: none"> <li>• high thermal conductive metal nano particle enhances the heat transfer</li> </ul>	<ul style="list-style-type: none"> <li>• Long term stability of nano particles in nano fluid is a complex work</li> </ul>
PCM	passive	<ul style="list-style-type: none"> <li>• higher heat transfer rate compared to both forced air and water circulation,</li> <li>• higher heat absorption due to latent heating,</li> <li>• no electricity consumption/ noise/ maintenance cost, on demand heat deliver</li> </ul>	<ul style="list-style-type: none"> <li>• Choice of suitable melting temperature is essential.</li> <li>• If PCM is not able to release heat to ambient, combined system will be heat up further, PCM will behave as insulator.</li> <li>• higher cost, toxic nature, fire safety issues, strongly corrosive, disposal problem after completion of life cycle</li> </ul>

724

725 It should be noteworthy that major thermal regulation work of BIPV/BAPV system was based on c-Si  
 726 (Jia et al., 2019; Joshi and Dhoble, 2018; A. Shukla et al., 2017) while 2<sup>nd</sup> generation system is  
 727 significantly less (Kalogirou and Tripanagnostopoulos, 2006; Ren et al., 2019), and third-generation is  
 728 rare or no work has been performed. Large scale development using third-generation PV for  
 729 BIPV/BAPV is the biggest challenge which limits the exploration of thermal regulation work. Also,  
 730 thermal performance knowledge of third-generation PV is not well established.

### 731 **4.3. Shading on BIPV and BAPV**

732 Depending on the local climate BIPV and BAPV both can suffer from wind-driven dust, snow and  
 733 shading from other building or construction or trees (Ilse et al., 2019). Deposited dust particle sizes  
 734 vary between 1 to 50  $\mu\text{m}$  which causes shielding effect on PV and thus decrease solar transmission  
 735 through the PV surface glass which in turn decreases the power output (Appels et al., 2013; Toth et  
 736 al., 2018; Weber et al., 2014). Curtailment of transmission also varies with dust deposition density,  
 737 wind speed and humidity, particle diameter and PV tilt angle (Smestad et al., 2020). Dust particles  
 738 include chemical, biological, electrostatic types, whereas its size shape and density are indispensable  
 739 (Micheli et al., 2019, 2018b, 2018a; Micheli and Muller, 2017). A rough surface accumulates a higher  
 740 amount of dust than a smoother one (Yusuf N Chanchangi et al., 2020). Electrostatically attracted

741 inorganic materials are common in the desert location and salts and rain-driven dirt are common in a  
 742 coastal area. Industrial and cooler location is subject to windblown organic dirt, deposits from  
 743 evaporated rain and atmospheric pollutants from fossil fuels (Yusuf N. Chanchangi et al.,  
 744 2020)(Ghosh, 2020a). The Middle East and North Africa have the worst dust accumulation zones in  
 745 the world (Ghazi et al., 2014). Even in the cleanest region of the world UK, dust effect reduces the  
 746 solar intensity by 5–6% after one- month continuous exposure (Ghazi et al., 2013). For a fixed period  
 747 of exposure, the rise of tilt angle reduces the dust deposition density. For a constant tilt angle, dust  
 748 deposition density increase with the number of exposure days (Hegazy, 2001; Xu et al., 2017). Wind  
 749 directions and orientation of collector have an influential impact on dust deposition (Goossens et al.,  
 750 1993). In Greece, the effect of 0.4 mg/cm<sup>2</sup> ash deposition reduced 30% of power output than a similar  
 751 clear PV panel. Relatively small ash deposition (i.e. 0.06 mg/cm<sup>2</sup>) reduced 2.5% of the generated  
 752 power output (Kaldellis and Fragos, 2011). In another work, PV module efficiency drops by 33% for  
 753 each 1 g/m<sup>2</sup> of dust accumulation (Al-hasan and Ghoneim, 2005). Heavy rainfall in any location  
 754 reduces the soiling effect (Lopez-Garcia et al., 2016). Exposed PV on the third floor in the Politeknik  
 755 Elektronika Negeri building in Surabaya, Indonesia (longitude of 112.533° and latitude of 7.2361°)  
 756 during the dry season and the beginning of the rainy season in 2014, showed 2.05% power output  
 757 reduction which increased to 87.29% compared to a clean module after a short period of drizzle  
 758 (Ramli et al., 2016). **Figure 19a** shows the uneven soiling on PV array in Doha, and Figure 19b shows  
 759 the heavily soiled modules on the Gran Canaria Island. Accumulated dust on PV enhances the  
 760 electricity cost (Tanesab et al., 2018).

761



762

763 Figure 19: (a) Uneven soiling on a PV array following a sandstorm in Doha, Qatar (Figgis et al.,  
 764 2017), (b) Heavily soiled modules on the Gran Canaria Island (Schill et al., 2015).

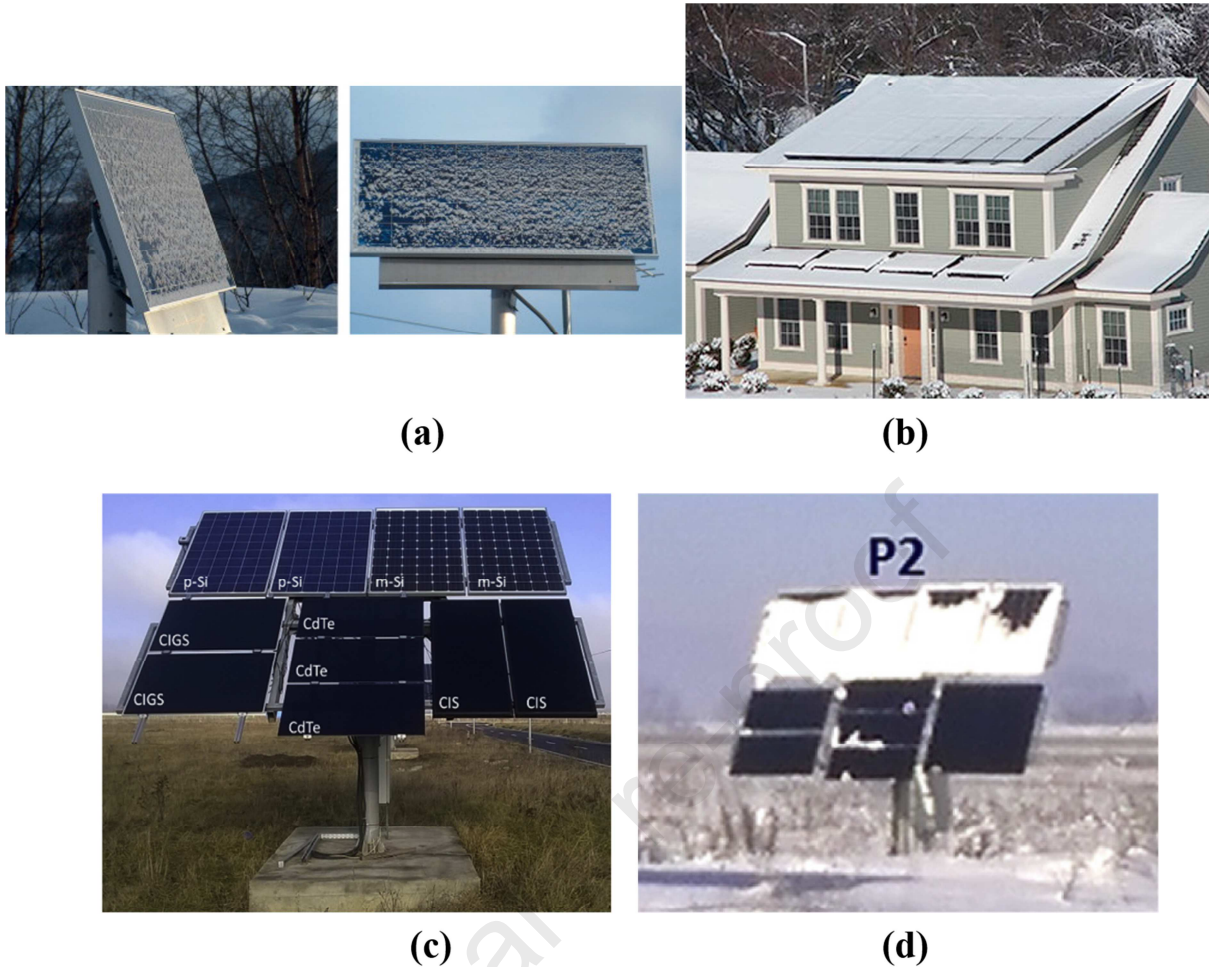
765 Snow accumulation on the top of the PV modules (as shown in **Figure 20**) reduces the power  
 766 generation due to a low transmission of incident solar radiation on the PV (Gullbrekken et al.,  
 767 2015)(Borrebaek et al., 2020). When snow covering is light, and it melts easily, the generation losses  
 768 are less; however, the impact is adverse when snow is heavy and does not quickly melt or shed  
 769 (Brench, 1979). Snow is highly scattering optical medium at the visible range, which makes it white.  
 770 Even a thin layer of snow is a bright and white colour, reflect the entire solar spectrum at the visible  
 771 wavelength and transmit little (Perovich, 2007). Little 2 cm thick snow can reduce 90% of visible  
 772 transmission whereas 95% reduction of visible and 99% reduction infrared transmission is possible  
 773 from 10 cm thick layer (Perovich, 2007). However, some light still can penetrate through the  
 774 snowpack. 2 cm snow can allow 20% of incident solar radiation whereas 10 cm thick allow 3-4%.  
 775 Annual production losses from a snow-covered PVs are directly proportional to the amount of snow

776 received and proportional to the squared cosine of the tilt angle of the panels (Powers et al., 2010).  
777 Annual losses from a snow-covered photovoltaic array in Ontario, Canada, varied from 1 to 3.5%  
778 (Andrews et al., 2013). Snow-covered BIPV can be considered as PV under low light condition.  
779 Mapped PV efficiency for irradiance levels as low as  $2.9 \text{ W/m}^2$ , were investigated which indicated a  
780 logarithmic correlation between incident solar radiation and efficiency for crystalline silicon cells,  
781 whereas the efficiency of amorphous silicon and gallium arsenide cells are less affected by this weak  
782 irradiance (Reich et al., 2005). However, snow-covered ground, in reality, enhance the reflection of  
783 solar radiation which in turn increase the total incident solar radiation on PV and thus yield of PV  
784 panels when tilt angles are optimal. Snow can increase local yield by 10% at snowy Switzerland  
785 location (Kahl et al., 2019). Mono-, poly-crystalline silicon, CdTe, CIS and CIGS modules (shown in  
786 **Figure 20 c, d**) were mounted on a platform at temperate mountain climate in Brasov, Romania  
787 ( $45.65^\circ\text{N}$ ,  $25.65^\circ\text{E}$ , 600 m above the sea level) where winters are snowy, and summers are warm. The  
788 best performing modules were of poly-crystalline silicon, whereas CIGS was the best thin-film  
789 modules having the highest output power and CdTe had the steadiest efficiency (Visa et al., 2016).

790 Trees, tall buildings, bird droppings and passing clouds are the other most common shading on BIPV  
791 and BAPV systems. Tilted PV panels in a parallel row also limit solar radiation due to self-shading.  
792 Das et al classified shading as static and dynamic and soft and hard. Slow change soft solar angles are  
793 static shading while fast change due to moving clouds are dynamic shading. Shading due to flying  
794 birds or nearby trees is soft shading, whereas PV modules are blocked completely due to hard shading  
795 (Das et al., 2017).

796

797



798

799

800 Figure 20: (a) Snow covering a solar cell panel at an inclination angle of  $70^\circ$  (Jelle, 2013) (b) Snow on  
 801 photovoltaic modules mounted on pitched roofs (Andenæs et al., 2018), Mono, poly-crystalline  
 802 silicon, CdTe, CIS and CIGS modules on platform (c) without snow covered, (d) with snow covered  
 803 at Brasov, in Romania ( $45.65^\circ\text{N}$ ,  $25.65^\circ\text{E}$ , 600 m above the sea level) (Visa et al., 2016).

804 Cleaning off the dust from BIPV/BAPV module surfaces is possible by natural rainfall, wind or  
 805 gravity, mechanical, electromechanical, electrostatic and self-cleaning methods (Said et al., 2018).  
 806 **Table 5** listed the cleaning cycle and mitigation method based on different climate conditions and  
 807 characteristics. Rainfalls are free of charge but seasonally volatile, thus highly unreliable when soiling  
 808 is intensive, and rainfall is not enough either in quantity or in intensity to clean off the soil. Brushing,  
 809 blowing, vibrating and ultrasonic driving are the mechanical methods to remove dust from PV. Broom  
 810 or brush is generally used for brushing method which is driven by some machine. For small size and  
 811 the strong adhesivity of the dust, this method is not very efficient. In a blowing method, wind from the  
 812 blower is employed which needs high energy to operate. Electromechanical methods encompass  
 813 shakes or vibrates the PV module array and use subsonic or ultrasonic waves to break the dust  
 814 particle. The electrostatic approach has been proposed by NASA to mitigate the negative effects of  
 815 dust on lunar-solar panels. Attached parallel or spiral transparent UV- radiation resistant plastic sheets  
 816 repel the dust particle when a single- or multiple-phase AC voltage supply produces an  
 817 electromagnetic field on the surface (Calle et al., 2009; Sharma et al., 2009; Sun et al., 2012).



818 Table 5 :Cleaning cycle and mitigation method based on different climate conditions and  
 819 characteristics (Ghazi et al., 2014)

Climate condition	Cleaning cycle	Mitigation
Humid cold temperature	Every six months	Wet type cleaning methods by using soap and warm water
Humid hot temperature	Every three months	Surface coating, self-cleaning hydrophobic
Humid equator	Monthly	Automatic cleaning systems for wiping snow and dust Use a plastic mesh over PV panels to reduce the problem of bird droppings
Dry	Weekly	Dry type cleaning methods such as rotary brush, automated robotic device

820

821 Self-cleaning methods can be categorized into hydrophobic and the photocatalytic hydrophilic (Ahuja  
 822 et al., 2017) (Mehmood et al., 2016). Hydrophobic and hydrophilic are understood by water contact  
 823 angle experiment where contact angle greater than  $90^{\circ}$  possess hydrophobic and higher than  $150^{\circ}$   
 824 possess superhydrophobic. On the other hand, the water contact angle less than  $90^{\circ}$  are known as  
 825 hydrophilic and less than  $5^{\circ}$  superhydrophilic (Jang et al., 2019). Presence of hydrophobic coating, the  
 826 water drops roll off the surface quickly due to the water repellent which also removes the  
 827 contaminants from the surface. In the case of superhydrophobic which is also known as the lotus  
 828 effect, ball-shaped water droplet, runs down the surface and collects the dirt with small sliding angle  
 829 (Zhang and Lv, 2015). It is worth mentioning that superhydrophobic and hydrophobic are applicable  
 830 for snow (A. Kim et al., 2015) and superhydrophilic and hydrophilic are suitable to clean dust covered  
 831 BIPV/BAPV (Nundy et al., 2020). Superhydrophobic coatings include fluorocarbons, silicones,  
 832 carbon nanotubes (Hanaei et al., 2016), polymeric materials such as polystyrene, polyurethane urea  
 833 copolymer, poly (methyl methacrylate), polycarbonate, poly (vinyl chloride), organic materials and  
 834 inorganic materials zinc oxide (ZnO) and titanium dioxide (TiO<sub>2</sub>). Using UV treatment super  
 835 hydrophobic and hydrophobic can be made as hydrophilic or super hydrophilic. TiO<sub>2</sub> is the most  
 836 common super hydrophilic self-coating layer. Superhydrophobic fluorinated ethylene propylene  
 837 (FEP) into a silicon PV enhanced the short circuit current density by 1.1% and 93.6% recovery ratio  
 838 of short circuit current (Roslizar et al., 2019) (Vüllers et al., 2018). Superhydrophobic coating can  
 839 improve 10% maximum power of c-Si-based PV module (Z. Huang et al., 2018). Addition of TiO<sub>2</sub>  
 840 and KH550 superhydrophilic coated PV provided maximum 4.3% efficiency improvement (Zhong et  
 841 al., 2017). Superhydrophobic nanostructure glass surface allowed only 1.39 efficiency drop while bare  
 842 glass reduced 7.7% efficiency (Son et al., 2012). Potential of self-cleaning coating for PV surface  
 843 cleaning is well documented elsewhere and shows its supreme applicability (Gullbrekken et al., 2015;  
 844 Liu et al., 2019; Loh et al., 2013).

845 Further improvement from snow and ice challenges can be addressed by using icephobic surface  
 846 coatings (Fillion et al., 2014; Hejazi et al., 2013). Icephobicity is related to superhydrophobicity, but  
 847 superhydrophobic surfaces are not necessarily icephobic (Kulinich et al., 2011; Nosonovsky and  
 848 Hejazi, 2012). Specific materials and coatings have achieved degrees of icephobicity, however,  
 849 opaque nature makes them ineligible for BI/BAPV applications. **Table 6** summarised the advantages  
 850 and disadvantages of different cleaning methods.

851 Table 6: Advantages and disadvantages of different cleaning methods

Cleaning methods	Advantages	Disadvantages
Manual	Restoration of standard PV performance is possible.	Needs constant manpower, as frequent cleaning cycles require. Depends on location and dust intensity, intense cleaning needs weekly or monthly.
Mechanical	Less productive compared to manual cleaning	Requires electrical power, due to initial and maintenance cost suitable for large systems,
Electrodynamic screens (Bock and Robinson, 2008)	Removes 90% of soiling Less power consumption; as low as 0.003% of generated power	Doesn't work properly under rainy condition and requires dry conditions for effective work.
Stowing of PV arrays	Protects from soiling when not in use (nighttime; dust storms)	Ineffective during daytime if sudden dust storm approaches (insufficient stowage time)
Self-cleaning	Passive self-cleaning, no manpower, electrical supplies are required.	Depends on rainfall and long-term stability

852

853 **4.4. Scale up issues and lack of standard**

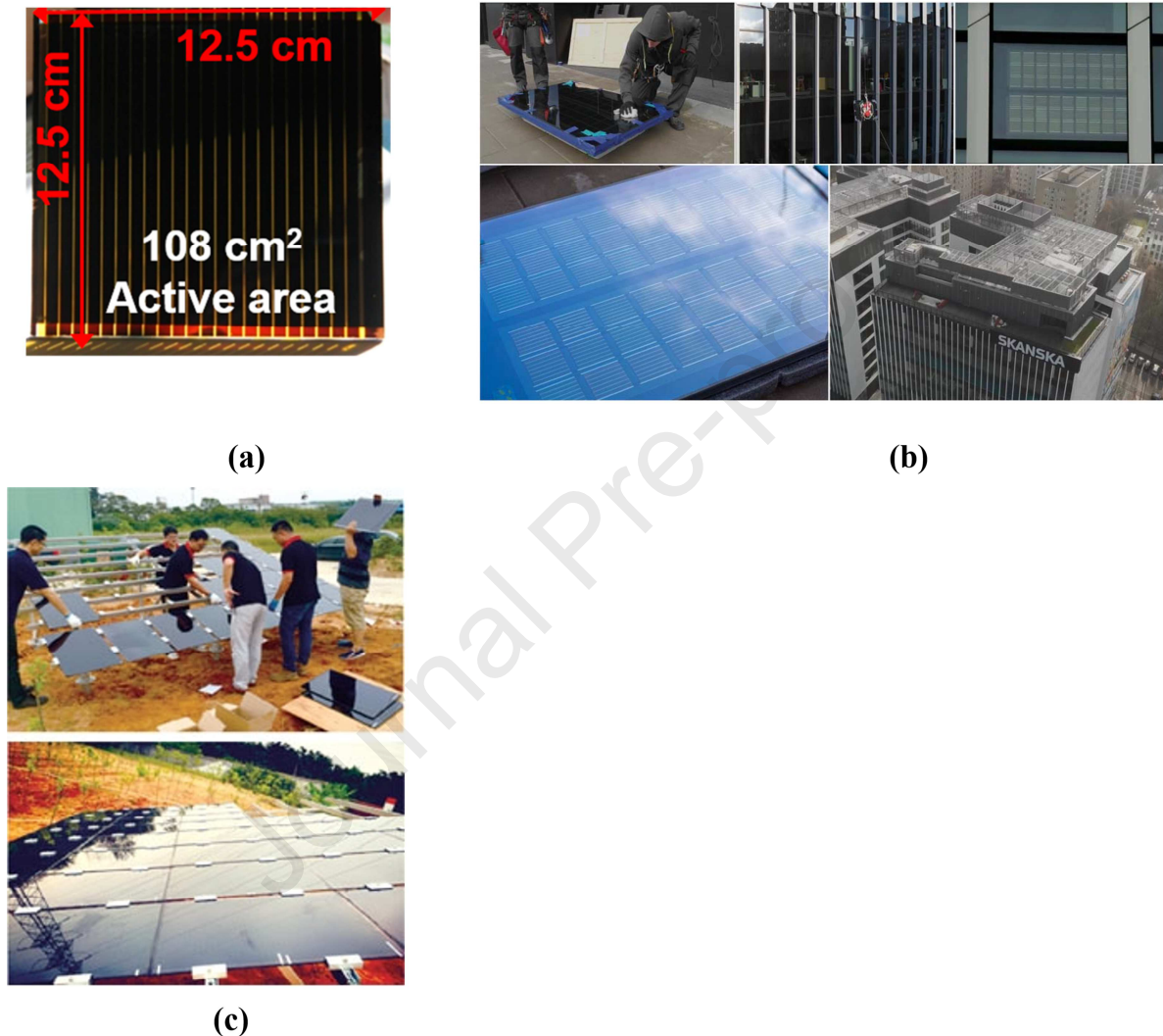
854 Large-scale development for three different generations PV has its own issue. First-generation silicon-  
855 based crystalline-silicon-wafer PV modules have more than 90% of market share. First generation-  
856 commercial PV panels consume 100 mg/cell silver (ITRPV, 2015). Reduction in silver use for the rear  
857 contact of silicon PV cells with partial substitution by using aluminium is already standard practice  
858 but not for the frontal part yet. The rate of decrease in silver paste use in PV cells contacts  
859 metallization and the rate of increase in first-generation PV installed capacity can possess 70% of the  
860 variance of the yearly silver demand in the year 2050 (Lo Piano et al., 2019). Thus, the reduction in  
861 silver paste use for contact metallization needs meaningful pace, to ensure smooth deployment of PV  
862 power generation at a sustained pace.

863 Large scale deployment of CdTe PV technology requires two key elements which are cadmium and  
864 tellurium, by products of zinc and copper, respectively. CdTe is the fifth most expensive  
865 semiconductor material based on future extraction costs among 23 semiconductor materials (Wadia et  
866 al., 2009). Available tellurium reserves can support CdTe-based solar power production of 1438 GWp  
867 in 2020, 19149 GWp in 2050, and 20211 GWp in 2075 (Fthenakis, 2009).

868 Third generation type PV cells are particularly gaining interest in BIPV application due to their ability  
869 to tune the transparency. However, presently they are facing issue to fabricate in large scale primarily  
870 due to the material degradation under ambient exposure and drop of efficiency. Dyesol is working on  
871 large-scale DSSC installations in collaboration with Tata Steel in North Wales, UK. Exeger received a  
872 USD 20 million investment to build a 20 MW DSSC production line in Stockholm, Sweden (View,  
873 2016).

874 Serially interconnecting different numbers (five, eight, or ten) of Perovskite PV cells (each cell made  
875 by a triple layer of mesoporous TiO<sub>2</sub>, ZrO<sub>2</sub> and carbon as a scaffold for mixed cation lead halide)  
876 fabricated a large-area 100 cm<sup>2</sup> module (active area of 49 cm<sup>2</sup>) that exhibited a PCE of 10.4% and  
877 stability till 1000 h. Later printable perovskite PV panel having 7 m<sup>2</sup> active area was fabricated for  
878 BIPV application (Hu et al., 2017). Recently scaled up perovskite (shown in Figure 8c) was achieved  
879 which had 108 cm<sup>2</sup> active area and 13.4% power conversion efficiency, stability till 1000hrs at 65°C

880 (Agresti et al., 2019) as shown in Figure 21a. Based on the techniques applied on the  $5 \times 5 \text{ cm}^2$   
 881 Perovskite cells 10.6% efficiency were used to increase the module size to  $45 \times 65 \text{ cm}^2$ . A  
 882 demonstration power station was made of 32 perovskite panels. No significant degradation was found  
 883 after 140 days of outdoors testing as shown in Figure 21c (Cai et al., 2017). Presently perovskite  
 884 based BIPV which was manufactured by Saule Technologies and installed in Skanska's Spark  
 885 building in Warsaw (Wojciechowski et al., 2019), is shown in Figure 21b. The system consists of 52  
 886 perovskite modules, and its performance is monitored by a maximum power point tracker.



887

888 Figure 21 : (a) Photograph of a representative large-area Perovskite ( $108 \text{ cm}^2$  active area,  $156.25 \text{ cm}^2$   
 889 substrate area (“Reprinted (adapted) with permission from, (Agresti et al., 2019) Copyright (2019)  
 890 American Chemical Society”) (b) Flexible perovskite solar modules laminated into a glass facade  
 891 element and integrated into the Skanska's Spark building in Warsaw, Poland. Reproduced with  
 892 permission. Copyright 2019, Skanska and Saule Technologies (c) Large area perovskite solar cell  
 893 module Longhua (Cai et al., 2017) © 2017 Chinese Institute of Electronics

894 Standards, codes or guidelines for inclusion of PV in buildings are not available. Integration of the  
 895 BIPV system into the building requires a large number of cable connections which may penetrate  
 896 through the roof or under the layer of the roof (Agathokleous and Kalogirou, 2019). Thus, installation  
 897 barriers, such as the cabling and connections, failure of fixings, islanding can create an issue after  
 898 integration of PV into the building. Particularly replacement of BIPV system is more critical than

899 BAPV. Improper silicone waterproofing, can possess water penetration which is a serious drawback  
900 for a building. Thus, health and safety which can cover the cases of fire, electricity shortcut, wires  
901 failures play a major role while codes will be prepared. Noise control should be under examination as  
902 well. Standards for noise protection by integrating PV in buildings are not clear in the building codes.  
903 Lack of allowance of extra loads on BIPV from snow, ice, wind can cause BIPV system bending and  
904 this will lead to various failures requiring repairs or replacement (Yang, 2015; Yang and Zou, 2016).  
905 Thus standard test method is essential which can explain all details of the requirement for the  
906 combined building structure and BIPV cable connection (Gullbrekken et al., 2015). Ubiquitous  
907 standards are available for PV system but not for BIPV/BAPV systems (A. K. Shukla et al., 2017a).  
908 However, recently, for BIPV, only one standard EN 50583 is initiated (Ferrara et al., 2017).

909

#### 910 **4.5. Colour comfort evaluation**

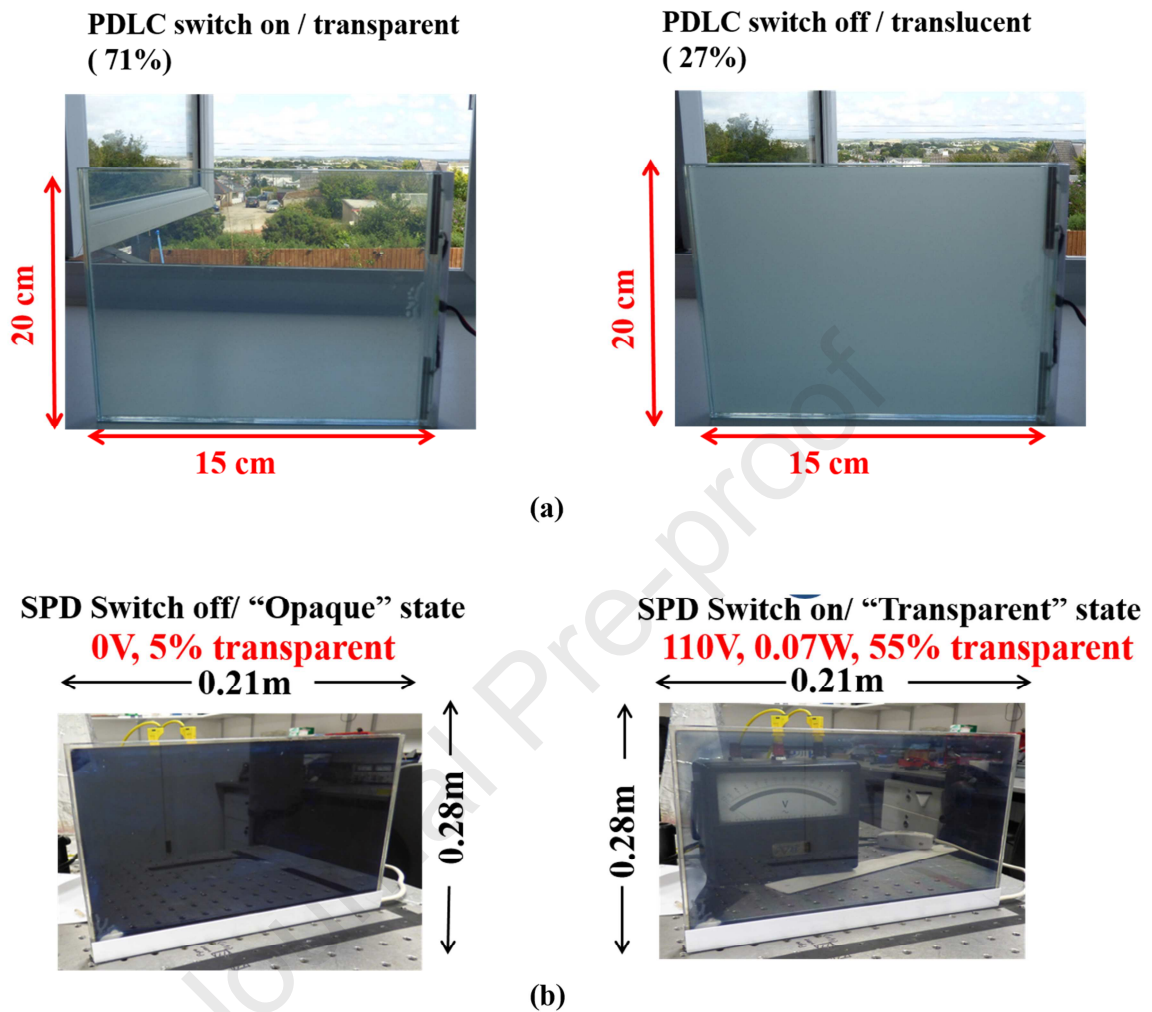
911 Presence of BIPV in a retrofit or new building has a significant impact on the behaviour of occupants.  
912 However, occupant comfort analysis for BIPV is the most underestimated area. In a building,  
913 occupant behaviour is complex and stochastic nature and primarily depends on comfort level at indoor  
914 space (Andargie et al., 2019). Occupant comfort hugely influences the cognitive activity of occupant,  
915 mental health, controls physiological reactions by maintaining melatonin production, core body  
916 temperature, heart rate, and cortisol production (Biswas et al., 2016). Occupant comfort includes  
917 visual and thermal both. For visual comfort glare and daylight analysis and for thermal indoor  
918 temperature and PPD-PVD methods are considered. However, for visual comfort, quality and quantity  
919 of light both are equally important (Smolders and de Kort, 2014). Daylight and glare analysis quantify  
920 the quantity of light where colour properties indicates the quality of light. Thus, for BIPV glazed  
921 façade application evaluation of colour properties which includes colour rendering index (CRI) and  
922 correlated colour temperature (CCT) are essential to understand the visual comfort of building  
923 occupants. CCT and CRI provide the details of the quality and quantity of daylight (Hernández-  
924 Andrés et al., 1999; Prathap et al., 2016; Valencia et al., 2013). CCT near 6500 K and CRI above 95  
925 indicates the comfortable daylight into space (Ghosh and Norton, 2017a) (Ghosh and Mallick, 2018).  
926 Variations of these may generate different CCT and CRI values that may not be suitable for indoor  
927 comfort. PV materials filter external ambient daylight while it is passing through it. Thus, penetrated  
928 daylight through a window in an indoor space has different wavelength dependent spectrum than the  
929 original daylight available outside. CCT and CRI both depend on full spectral than one single  
930 transmittance value (Ghosh and Norton, 2017a; Gunde et al., 2005). Similar average transmittance c-  
931 Si, a-Si, CdTe, CIGS, DSSC and perovskite PV will generate different CCT and CRI. Thus, before  
932 applying PV material for glazing or glazed façade, evaluation of CCT and CRI are equally essential.

### 933 **5. Potential future application of BIPV and BAPV**

#### 934 **5.1. Source for switchable window**

935 Traditional static/ constant transparent windows are not thermally insulated and need shading device  
936 to control the daylight. Semi-transparent BIPV windows can replace those traditional ones but  
937 transparency cannot be modulated. Thus, rather integrating BIPV window, a switchable window can  
938 be introduced where BIPV can power those switchable windows (Gorgolis and Karamanis, 2016;  
939 Rezaei et al., 2017; Saifullah et al., 2016). Switchable windows include electrically and non-  
940 electrically actuated (Ghosh and Norton, 2018) types. However, electrically actuated switchable  
941 glazings are preferred for building application due to its controllable transmission (Ghosh et al.,  
942 2016a). Electrically actuated glazing includes AC powered suspended particle device (SPD) (Aritra

943 Ghosh et al., 2015)(Ghosh et al., 2017a) (Barrios et al., 2015) (As shown in **Figure 22a**) and liquid  
 944 crystal (LC) (shown in **Figure 22b**)(Aritra Ghosh et al., 2018a) (S. Kumar et al., 2019)(Ghosh and  
 945 Mallick, 2017) and DC powered electrochromic (EC) (Granqvist et al., 2017; Xiong et al., 2017).



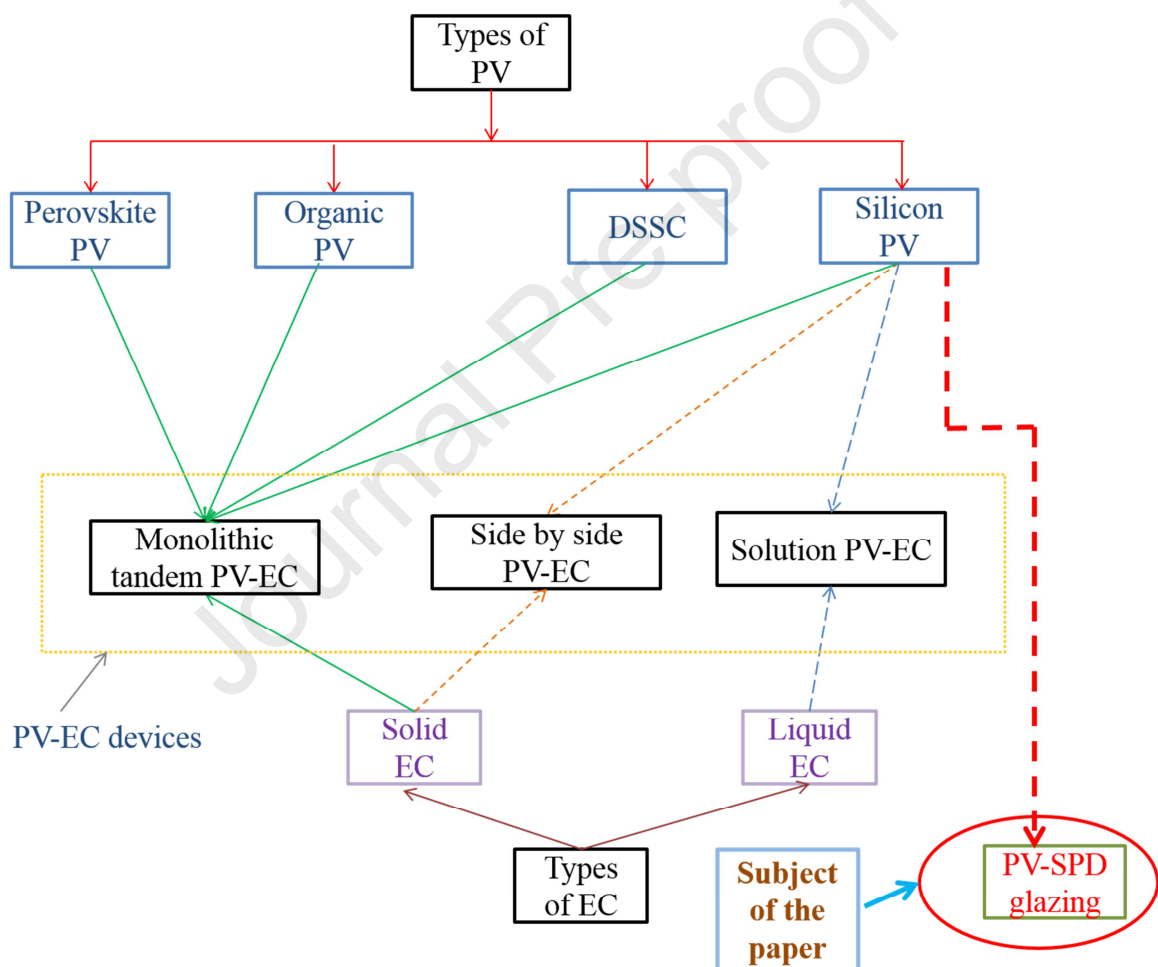
946

947 Figure 22: (a) Electrically actuated switchable glazing (PDLC type) (Taken from (Aritra Ghosh et al.,  
 948 2018b) (b) Electrically actuated switchable glazing (SPD type) (Taken from (Ghosh et al., 2016b) )

949 Mitigation of external power requirement of those electrically activated glazings is possible by using  
 950 PV devices which are shown in **Figure 23**. This novel system can be termed as self-powered glazing,  
 951 switchable BIPV (Wheeler et al., n.d.), autonomous switchable glazing, photoelectrochromic  
 952 (Cannavale et al., 2016) or photo-voltachromic which are suitable for less energy-hungry building.  
 953 These combinations find solutions for seemingly impossible building problems. Powering from PV  
 954 for AC powered SPD (Ghosh and Norton, 2017b) and LC (Hemaida et al., 2020) window needs an  
 955 inverter for conversion as shown in **Figure 24a** (Ghosh et al., 2016b). An inverter increases the power  
 956 losses which increase the required PV compared to EC powered glazing (Ghosh and Norton, 2019).  
 957 However instant switching speed and no power requirement to control the solar heat gain can  
 958 encourage using this type of combination (Ghosh et al., 2016b). Thus, building for hot arid climate  
 959 SPD or LC type glazing is advantageous where power generation from BIPV or BAPV can be stored  
 960 for night-time use (Ghosh et al., 2016c). PV powered EC glazing system has two-fold advantages.  
 961 Firstly, EC glazing works with direct current (DC) power supply and PV produces DC power, thus  
 962 direct coupling between EC and PV is possible where no need for power electronic conversion (Deb

963 et al., 2001; Gao et al., 2000; Ma and Chen, 2012). Secondly, EC at high surface temperature requires  
 964 less power to switch and PV at high ambient temperature generates less power than its standard rating  
 965 (Bell and Matthews, 2001; Matthews et al., 2001). These two advantages make BIPV/BAPV power  
 966 EC switchable glazing a potential candidate for future building integration. Dye-sensitized solar cell  
 967 and silicon-based PV-EC device had already been investigated and found to be promising (Ahn et al.,  
 968 2007; Santa-Nokki et al., 2007). Investigation showed that one 3.7% efficient perovskite PV powered  
 969 an EC device which had an average visible transmittance of 26% (Cannavale et al., 2017a, 2017b).  
 970 Solution type PV-EC material has been reported (Huang et al., 2012b, 2012a) where the  
 971 electrochromic solution is located between the transparent non-conductive substrate and the silicon  
 972 thin-film solar cell (Si-TFSC) substrate. The planarly distributed electrodes create a uniform electric  
 973 field and due to solution type EC, the transparency of the overall device increase.

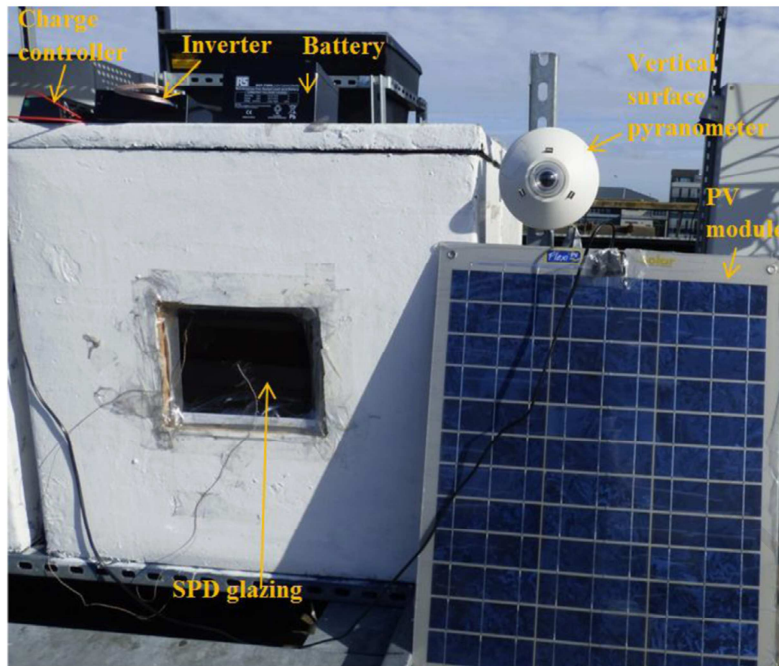
974



975

976 Figure 23: Types of PV powered switchable glazing. (Taken from (Ghosh et al., 2016b))

977



(a)



(b)

978

979 Figure 24: (a) Photographic view of PV powered SPD switchable glazing (Taken from (Ghosh et al.,  
 980 2016b)) (b) 200 mm × 200 mm PDLC was powered by concentrator-type solar window used four  
 981 parallel-connected edge-mounted CuInSe<sub>2</sub> modules of size 198 mm × 25 mm (Vasiliev et al., 2019)

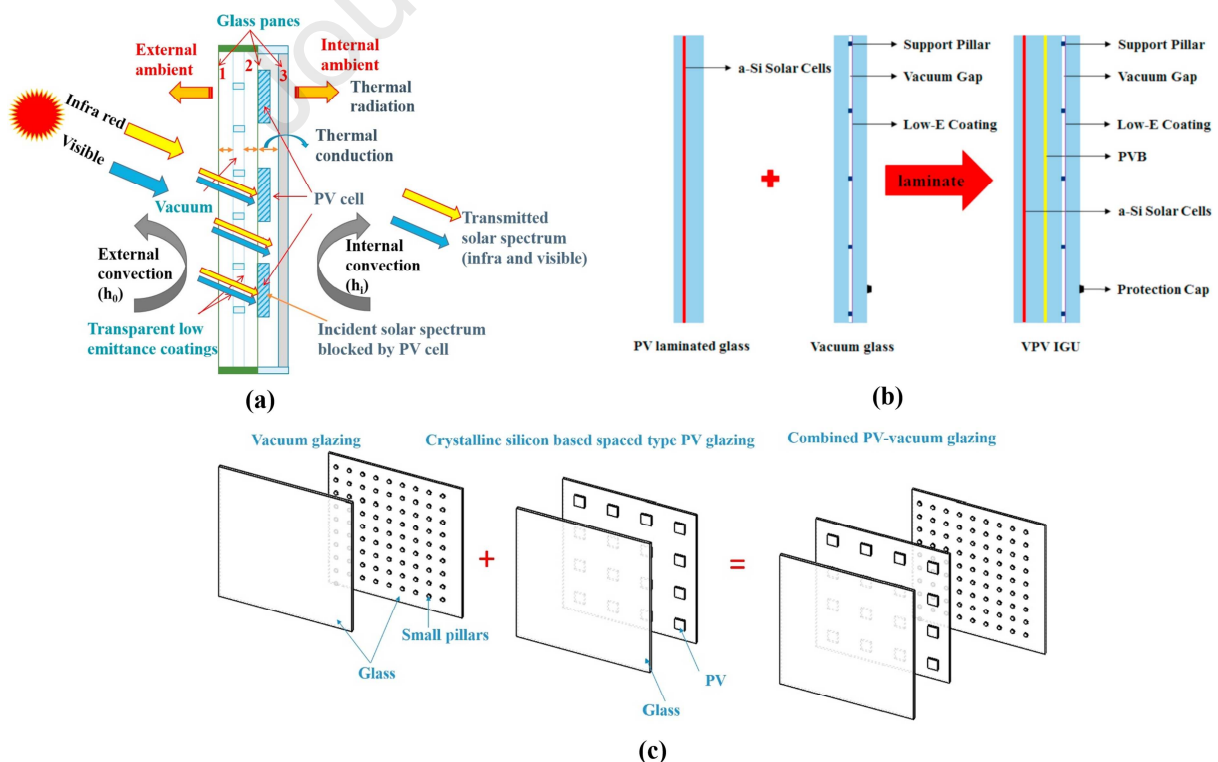
982 Currently, LC-based glazing was also powered by DSSC based PV. However, the investigation was  
 983 performed for a small scale, but the promising result confirms that PV integrated switchable glazing is  
 984 future building architecture material (Kwon et al., 2015). Powering of PDLC glazing by a 13 nm thick  
 985 a-Si PV cells was investigated for low (<0.8 mW/cm<sup>2</sup>) intensity (Murray et al., 2017). Recently  
 986 perovskite PV and a liquid crystal-based window were investigated where LC window switched from  
 987 3% to 79% transparent in the presence of 55V supply. Performance of perovskite was dependent on  
 988 the thickness of the material. Higher thickness reduced the overall system transparency while reduced  
 989 thickness enhanced the power conversion ratio (Xia et al., 2019). A PDLC size of a 200 mm × 200  
 990 mm was electrically driven using by concentrator-type solar window used four parallel-connected

991 edge-mounted CuInSe<sub>2</sub> modules of size 198 mm × 25 mm in Edith Cowan University (ECU), October  
 992 2014 shown in Figure 24b. This is a patent work and not yet fully published academically (Vasiliev et  
 993 al., 2019).

994

## 995 5.2. BIPV for highly insulating glazing

996 Available BIPV glazings are two glass sheets where PV materials are sandwiched between them.  
 997 However, this double glazing has an overall heat transfer coefficient ( $U$ -value) which is near 2  
 998 W/m<sup>2</sup>K. For less energy-hungry building, heat loss from window needs to be reduced and this is not  
 999 achievable using double pane BIPV for cold climate. Highly insulating vacuum glazing has the  
 1000 potential to reduce the indoor heat by reducing the heat flow from indoor space to outdoor ambient  
 1001 (Fang et al., 2014)(Ghosh et al., 2016d). Vacuum glazing is two glass sheets where inside the space,  
 1002 the vacuum is created by using high-pressure air extraction (Ghosh et al., 2016e). To counteract the  
 1003 pressure from external ambient, small pillars are placed in regular order in the internal space (Figure  
 1004 25a and b). Presence of vacuum reduces the conductive and convective heat flow and radiative heat  
 1005 flow is reduced by using low emission coating (Ghosh et al., 2017b). Low-e coatings are metals or  
 1006 metallic oxide based, transmit visible light in the solar spectrum and reflect the infrared (2000 nm -  
 1007 50,000 nm)(Ghosh et al., 2017c). For double glazing, presence of a low-e coating on the internal  
 1008 surface of the inside glass pane reduces the heat loss from the interior room to an exterior  
 1009 environment (Jelle et al., 2015). Integration of vacuum glazing with BIPV (shown in **Figure 25 c**) can  
 1010 thus offer electricity generation, reduction of heat loss and control over admitting heat gain. Spaced  
 1011 type crystalline silicon attached with highly insulated vacuum glazing was also investigated for the  
 1012 temperate and cold climate which showed  $U$ -value of 0.8 W/m<sup>2</sup>K (Aritra Ghosh et al., 2018d). Also,  
 1013 the light penetrated through space between cells allowed to maintain the external daylight at indoor  
 1014 space (Ghosh et al., 2019b). a-Si based BIPV-vacuum system (**Figure 25 b**) having  $U$ -value of 0.5  
 1015 W/m<sup>2</sup>K reduced up to 31.94% heat loss which saves net energy savings of 37.79% in cooling  
 1016 dominated Hong Kong (J. Huang et al., 2018).



1017



1018 Figure 25: (a) Schematic of crystalline spaced type BIPV vacuum glazing (taken from (Ghosh et al.,  
1019 2019b)), (b) a-Si based BIPV -vacuum glazing (taken from (Zhang et al., 2017)), (c) details of BIPV-  
1020 vacuum glazing (taken from (Ghosh and Norton, 2018)).

1021 In another work, BIPV-vacuum glazing's  $U$ -value was found to be  $1.5 \text{ W/m}^2\text{K}$  and SHGC 0.14 from  
1022 an indoor experiment. Combined these effects were employed in Energy Plus and WINDOW software  
1023 and observed that cooling electricity reduction up to 25.4% and 16.5% was possible compared to  
1024 single and double glazing (Qiu et al., 2019). Currently insulated BIPV was designed by using spaced  
1025 c-Si and low  $e$  coated glass, as shown in Figure 19. The SHGC of the highly insulated BIPV was 0.25  
1026 and  $U$ -value was  $3.5 \text{ W/ m}^2 \text{ K}$ . Low  $e$  coating was present in the third surface from exterior to  
1027 interior, could not reflect longwave radiation into indoor space. Presence of low  $-e$  coating in the  
1028 fourth surface could improve the result (Peng et al., 2019). Indoor thermal comfort using BIPV-  
1029 vacuum system showed 39% enhancement than that of BIPV double glazing (Ghosh et al., 2019a).

1030

### 1031 **5.3. Powering electric vehicle (EV)**

1032 One of the major applications of BIPV/BAPV can be in the field of transport which consumes 40% of  
1033 fossil fuel energy worldwide and 90% transport sector is powered by oil-derived fuel (Chandra Mouli  
1034 et al., 2019; Nunes et al., 2015). Consumption of expensive petrol and diesel for vehicles produces  
1035 GHG, volatile organic air pollutant, PM10 and NO<sub>x</sub> (Van Vliet et al., 2011). The transport sector  
1036 accounts for around 25% of EU greenhouse gas emissions. In Ireland, CO<sub>2</sub> emissions increased by  
1037 181% between 1990 to 2007 (Smith, 2010). In Switzerland, transport accounts for 31% GHG yearly  
1038 (Smith, 2010). Deployment of electric vehicles (EV) over oil-powered vehicles can improve the  
1039 situation. Electrically powered EV contains an electric battery that supplies the required energy to  
1040 drive the car engine. Plug-in hybrid electric vehicles (PHEV), and battery-powered electric vehicles  
1041 (BEV) are presently most investigated EV (Van Vliet et al., 2011) (Das et al., 2020; Tie and Tan,  
1042 2013; Yong et al., 2015). The conventional car uses gasoline or diesel fuel that create mechanical  
1043 energy to move forward a vehicle. In a hybrid electric vehicle (HEV), small electric battery supply  
1044 electricity to the drive train to optimize combustion engine's operating efficiency (Yong et al., 2015).  
1045 HEVs are more fuel-efficient than conventional internal combustion engine (ICE) vehicle, but  
1046 ultimately the vehicle is fully powered by liquid fuels. PHEV type works with the same principle to  
1047 HEV, but they have large area high capacity battery that can be charged with a direct connection to  
1048 the grid (Shamshirband et al., 2018). The high capacity battery also allows a car to drive the longer  
1049 distance. Car model named PHEV 20 or 40 indicates car can travel with only the fully charged battery  
1050 to 20 or 40 miles (Richardson, 2013). A battery electric vehicle (BEV) is fully powered by grid  
1051 electricity stored in a large on-board battery. A lithium battery is the most used EV battery as they  
1052 offer power density, energy efficiency and light and compact weight (Mahmoudzadeh Andwari et al.,  
1053 2017; Zhou et al., 2020). The lead-acid battery is not preferable due to poor thermal performance, low  
1054 specific energy and chemical leakage. BEV and HEV face a huge challenge as 45.3% of the EV cost  
1055 is the battery's cost (Petersen, 2011).

1056 EV can increase a household electricity consumption of an industrialised country by 50% (Van Vliet  
1057 et al., 2011) which can be neutralized by powering EVs from PVs. Netherlands sets its targets to  
1058 penetrate 200,000 EV in 2020 (Chandra Mouli et al., 2016). Nordic countries of Denmark, Finland,  
1059 Norway and Sweden have planned to 100% penetration of passenger cars by 2050 (Graabak et al.,  
1060 2016). Thus, the EV charging station can be powered from PV (Ghotge et al., 2020; Ma et al., 2014).  
1061 Considering the potential of PV powered EV, currently, feasibility study using local solar radiation  
1062 has been conducted in New Jersey (Birnie, 2009), Canada (Li et al., 2009), Brazil (Sorgato et al.,

1063 2018), Dublin (Esfandyari et al., 2019) and Australia (Islam and Mithulanathan, 2018). PV-grid and  
 1064 PV-standalone are the two most popular charging station. PV grid charging station gets supply during  
 1065 the insufficient sunshine while PV- standalone rely on PV only (Ghosh, 2020b). However, they are  
 1066 suitable for the remote area where utility supply is not convenient or costly or not available. A 6.5 kW  
 1067 PV standalone charging infrastructure, accommodated four EVs (Nissan Leaf), travelling 50 km  
 1068 throughout the day in Galway in Ireland. The control strategy was adopted to maximize the PV energy  
 1069 usage while meeting the demand of the EV batteries (Kineavy and Duffy, 2014). The parking area of  
 1070 any residential or commercial building can be covered with PV to form PV powered EV charging  
 1071 station, which will charge the battery of EV directly for the car during daytime as shown in **Figure**  
 1072 **26a** (Fattori et al., 2014). These overhead canopies are built by PV and commonly referred to as solar  
 1073 carport. Due to variation of solar intensity in the summer and winter season, battery storage and  
 1074 provision for grid supply when requires are also suggested (Birnie, 2009; Codani et al., 2016;  
 1075 Esfandyari et al., 2019; Igualada et al., 2014; Li et al., 2009). **Figure 26b** shows India's largest carport  
 1076 in India, solarized by Tata Power Solar having 2.67 MW spread across 20289.9 m<sup>2</sup> area which Offsets  
 1077 1868 tonnes of CO<sub>2</sub> annually (Power, 2019). Figure 26c shows solar carport for 22-vehicles at the  
 1078 parking lot located in Fort Lauderdale, Florida. This solar carport solution can produce up to 88, 357  
 1079 kWh of clean energy with an average energy saving of \$10,000 per year respectively. This charging  
 1080 while parking is a potential future option (Van Roy et al., 2014). Charging the EV directly from BIPV  
 1081 is possible for a commercial building where cars are parked during the peak office time and it matches  
 1082 with the sunshine period (Richardson, 2013).

1083



(a)



(b)



(c)



(d)

1084

1085 Figure 26: (a) Design of solar powered EV charging station (Taken from (Birnie, 2009)); (b) Solar  
 1086 Car port In Cochin International airport (9.93606° N, 76.26145° E) India. Image Source ((Power,  
 1087 2019) (c) 22-vehicles at their headquarters parking lot located in Fort Lauderdale, Florida. (Source &

1088 image courtesy: solar carport installation at MOSS Construction by Advanced Green Technologies)  
1089 (d) RV EV car roof-mounted PV module, (image courtesy: Giantour Corp Ltd)

1090 Vehicle integrated PV (VIPV) is another elegant approach to power EV from PV (Bhatti et al., 2016;  
1091 Richardson, 2013). Thin films or traditional c-Si based PVs (shown in Figure 26d) are attractive for  
1092 VIPV to mount on the roof of the EV and converter fitted battery will be there for back up. VIPV  
1093 using brushless permanent magnetic DC motor was also proposed (Rattankumar and Gopinath, 2012).  
1094 This integrated can also be used for the air conditioning or heating purpose inside the car. Thus, VIPV  
1095 systems can be suitable to run an auxiliary device such as fan, audio players, and switchable window  
1096 or for racing cars. A mixture of silicon crystal with fixed quantum points can be painted on the car  
1097 body for VIPV application (Kadar and Varga, 2013). Despite the low efficiency (less than 2%), the  
1098 future of this technology is exciting.

#### 1099 **5.4. Emerging future BIPV/BAPV technology**

1100 **Light weight BIPV**-BIPV and BAPV both are often installed or integrate on an existing building  
1101 which can affect the building structure as the weight of glass-blacken sheet PV modules vary from 12  
1102 to 16 kg/m<sup>2</sup> and glass-glass modules vary from 16 to 20 kg/m<sup>2</sup>. This extra load was not taken into  
1103 account during the building design phase which crates obstacle. Therefore, for BIPV application,  
1104 specific power (power/weight =W/kg) gets higher priority than conversion efficiency. Flexible  
1105 amorphous silicon and c-Si have a specific power of 16 Wp/kg and 12-17 Wp/kg respectively  
1106 (Ransome, 2009). Flexible and lightweight, emerging PV technologies enable novel building  
1107 applications over traditional type PV modules (Ramanujam et al., 2020). Flexible type PV modules do  
1108 not need any ballast which makes easy integration. PV module with a weight of 5 kg/m<sup>2</sup> substitutes  
1109 the typical front glass with a thin polymer sheet and the standard back sheet by a composite sandwich  
1110 structure using stiff ionomer (Martins et al., 2018a) adhesive and polyolefin (Martins et al., 2018b).  
1111 Varying substrates for CIGS PV, specific power can be achieved between 0.2-0.4 kW/kg (steel,  
1112 titanium and polyimide foil) for light weight BIPV integration (Feurer et al., 2017). First 250 m<sup>2</sup>  
1113 flexible OPV fabricated by a roll to roll process had 4.3% average efficiency was installed in the solar  
1114 trees at German pavilion in 2015 Universal Expo in Milan for investigation of future BIPV (Berny et  
1115 al., 2015). **Figure 27** shows that higher specific power is possible from emerging technologies which  
1116 broke the myth that the highest efficiencies are necessary for BIPV application (Reese et al., 2018).  
1117 Third-generation PV technology offers further lightweight high power generation because of their  
1118 low-temperature solution-processable fabrication (Xie et al., 2019).

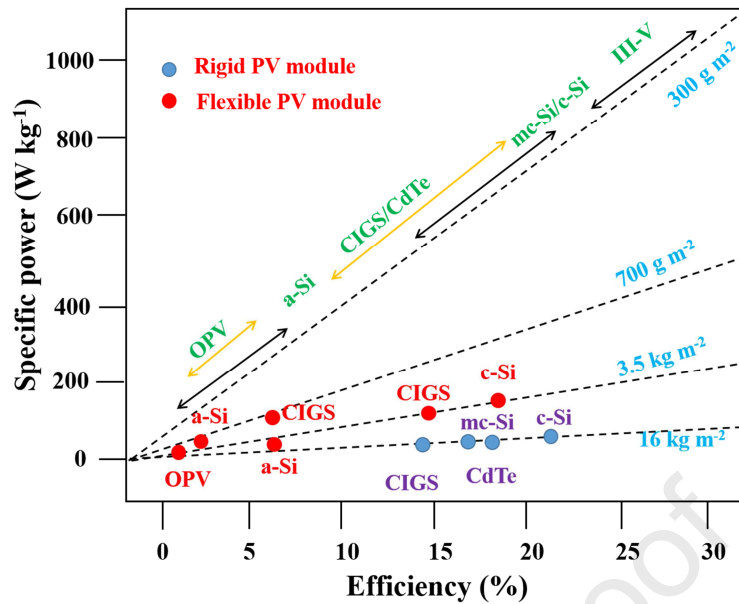
1119

1120

1121

1122

1123



1124

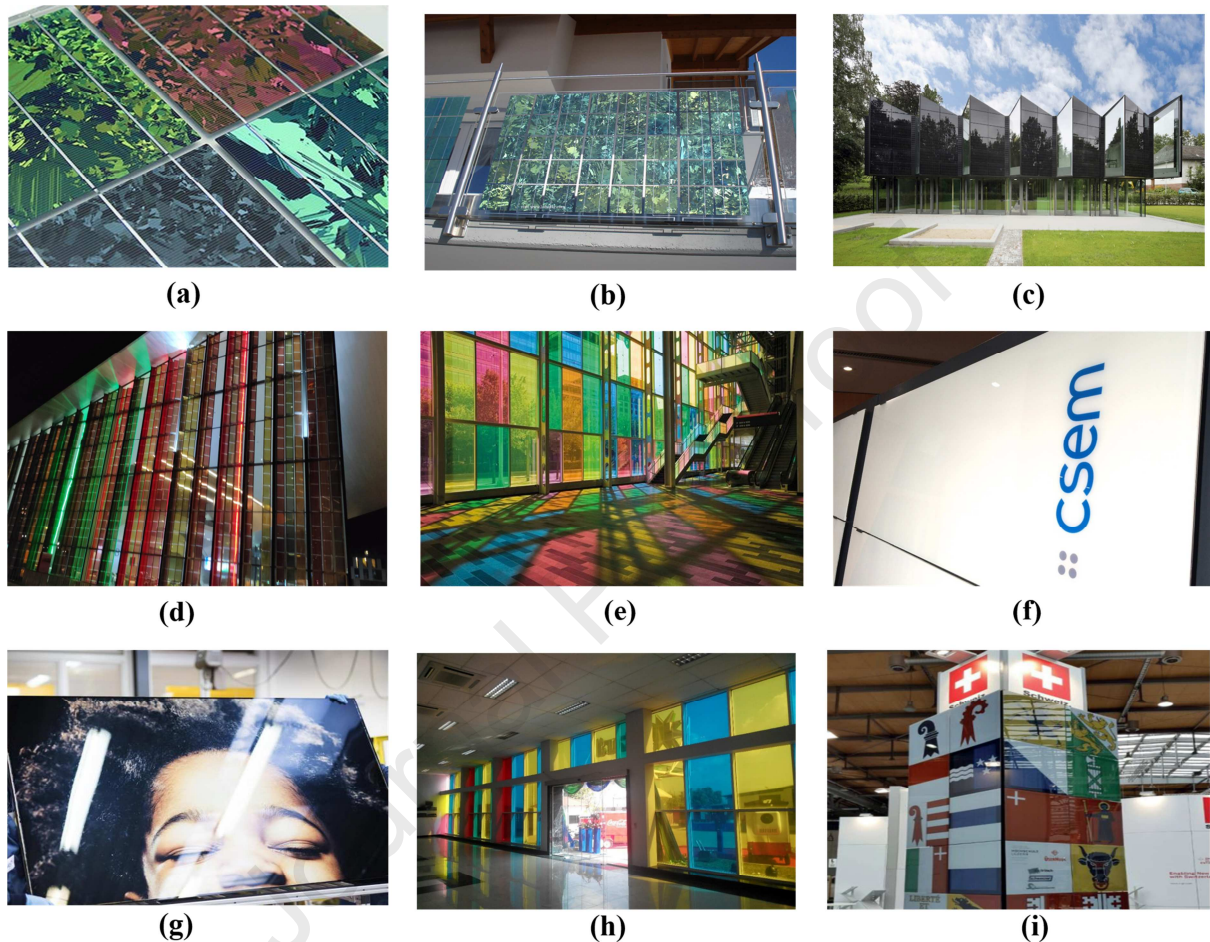
1125 Figure 27: Specific power as a function of AM1.5G module efficiency (Redrawn from (Reese et al.,  
1126 2018))

### 1127 Coloured or invisible BIPV

1128 Coloured BIPV is a new technological solution for the inclusion of coloured PV in modern and  
1129 heritage type building. Coloured PV technology includes traditional and new all new type of PV e.g.  
1130 blueish silicon, DSSC, Organic type while they can be installed as façade, roofing shading or balcony  
1131 glazing (Eder et al., 2019). The prime target is to hide the PV functionality from and treat them as  
1132 invisible PV. Bare c-Si (both monocrystalline and multi-crystalline) offers reflectance around 30 %,  
1133 which can be reduced by introducing antireflective (AR) coatings on their surfaces (Soman and  
1134 Antony, 2019). Varying AR coating thickness gives blue or other colour to the PV cells which also  
1135 influence the PV cell efficiency. AR coated modified colour-based PV cells can be purchased directly  
1136 from the cell manufacturer. Presently few developers are in the market with coloured BIPV. Kameron  
1137 Solar produce Sparkling Gold, Disco Pink, Emerald Green, Stone Elegance, Diamond Blue type  
1138 coloured PV (as shown in Figure 28a). LOF solar built a residence with balcony glazing in Black  
1139 forest Germany where this colour blends seamlessly with surrounding forest and trees as shown in  
1140 Figure 28b. In addition, coloured BIPV is possible to achieve from any semi-transparent type a-Si,  
1141 CdTe, CIGS and third generation DSSC (as shown in Figure 28d), perovskite, organic PV and LSC  
1142 (as shown in Figure 28e) technology.

1143 A certain colour/pattern-based interlayer can be sandwiched as an encapsulant layer between upper  
1144 glass and module or can be introduced at the back also produce coloured BIPV. Such system is  
1145 commercialized by the Centre Suisse d'Electronique et de Microtechnique commercialized (CSEM)  
1146 by Solaxess SA where an elective filter on the front of the glass cover reflects and diffuses solar  
1147 radiation within the visible spectrum, offering a white appearance (Figure 31f), whilst the transmitted  
1148 infrared part is converted into benign electricity. Kaleo-Solar developed (Figure 31g) an integrating  
1149 coloured BIPV system where high-resolution photo printed on a film with special inks is laminated  
1150 between cells and the cover glass. After the module lamination, only the printed photo is visible while  
1151 PV cells are no longer visible. Amorphous silicon technology can be combined with coloured  
1152 polyvinyl butyral as the back encapsulant is shown in Figure 33h for coloured a-Si technology.  
1153 Lucerne University of Applied Sciences developed multi-coloured ceramic digital printing on BIPV

1154 glass (shown in Figure 28i) where ceramic paste can be introduced to the glass prior to the tempering  
 1155 of the glass which bonds strongly to the glass. The printed dotted pattern allows sufficient light to  
 1156 reach the PV cells; offers inhomogeneous shading and losses up to 20% (Mertin et al., 2014, 2011).  
 1157 Use of coloured BIPV requires optimization of colour perception, as mentioned in section 4.4. Also, it  
 1158 must be kept in mind that reduced PV efficiency is achievable from coloured BIPV since there is a  
 1159 reduction of the incident light on the PV cells.



1160

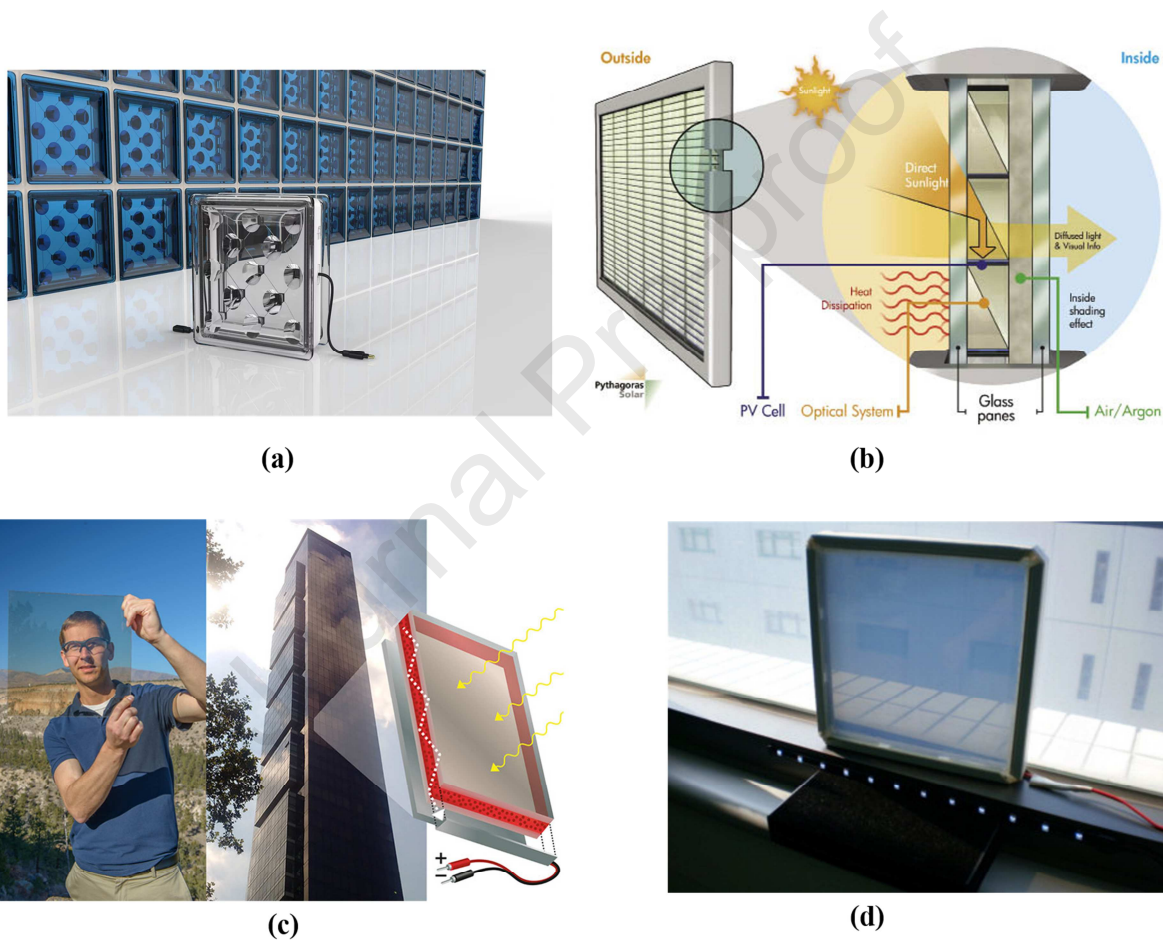
1161 Figure 28: (a) Coloured PV (Image courtesy: KameleonSolar), (b) Balcony glazing by LOFT solar, (c)  
 1162 Black BIPV façade on a children's day-care centre in Marburg; project realized by ertex-solar (d)  
 1163 SwissTech convention centre at EPFL campus, Lausanne Switzerland (Image courtesy: EPFL), (e)  
 1164 Striking facade of the Palais des Congrès in Montreal, Canada,(Debije, 2015) (f) Elective filter based  
 1165 white BIPV (image courtesy: CSEM) (g) High resolution photo integrated coloured BIPV (Image  
 1166 courtesy: Kaleo-Solar (h) Amorphous silicon with coloured polyvinyl butyral (Image courtesy:  
 1167 AppleSun) (i) Multi coloured BIPV modules developed by the University of Lucerne (Image  
 1168 courtesy: Envelopes and Solar Energy Competence Centre within the Hochschule Luzern)

1169 **Sensor application-**BIPV can act as a sensor for an intelligent building energy management system.  
 1170 Voltage is proportional to the temperature and current directly depends on the solar intensity.  
 1171 Mapping the response of a specific PV power- generating BIPV is attractive as over a variety of  
 1172 illumination and temperature condition, output parameters from it can be engaged as input data for  
 1173 intelligent building energy management system. Most often PV arrays incorporate a large number of  
 1174 PV module which can replace the engagement of a large number of sensors. Installed BIPV for a  
 1175 smaller area can also work as sensor and can offset a smaller amount of building energy needs by

1176 producing modest power. BIPV window sensor can inform how to operate the HVAC system which is  
 1177 necessary to operate electrically actuated shading or electrically actuated chromic window(Abe et al.,  
 1178 2020) (John and Conklin, 2017).

### 1179 Emerging product-

1180 Solar squared is a product from BuildSolar, spin-out company from the solar lab, University of  
 1181 Exeter. In this product, the spaced typed structure is present. Low concentrator CPC on crystalline  
 1182 silicon generates power while they are sandwiched between transparent glass blocks. One block is  
 1183 able to produce 1 W DC power while  $U$ -value is  $1 \text{ W/m}^2\text{K}$  (Baig and Mallick, 2018). This product  
 1184 (shown in Figure 29a) has prodigious potential for building integration specially for less-energy  
 1185 hungry, zero energy, sustainable, green, and aesthetic building integration.



1186

1187 Figure 29: Solar squared (Image courtesy Build Solar (taken with permission)) (b) Pythagoras Solar  
 1188 (Image courtesy: Pythagoras Solar) (c) CuInS<sub>2</sub> Quantum dot LSC BIPV Window (taken with  
 1189 permission (Bergren et al., 2018) (d) Transparent PV- window module ( $17 \text{ cm}^2$ ) for LED lightning  
 1190 application (Chau et al., 2010).

1191 Pythagoras Solar as shown in Figure 29 b was conceived in Petach Tikva, Israel, with offices in  
 1192 Taipei, Taiwan and San Mateo, California, specializes energy efficient building by harnessing energy  
 1193 from the sun, generate power directly from it. This aesthetically pleasing BIPV product was employed  
 1194 in Chicago's Willis Tower, formerly known as the Sears Tower. It was founded in 2007, however  
 1195 currently not in operation (Closed from Apr 2013). Figure 29c shows LSC-BIPV window which has

1196 high quantum yield (>90%), NIR-emitting CuInS<sub>2</sub>/ZnS quantum dots into the polymer interlayer  
1197 between two sheets of low iron float glass, a record optical efficiency of 8.1%. A 10 cm × 10 cm  
1198 device is ~44% transparent in the visible spectrum and with silicon solar cells this device converts  
1199 2.2% and 2.9% solar to electrical power conversion while substrates are a black background and  
1200 reflective type respectively (Bergren et al., 2018). Presently it is commercialized and ready for sale in  
1201 the brand name of UbiQD. Figure 29d shows a 17 cm<sup>2</sup> transparent PV based window for LED lighting  
1202 application which was fabricated by integrating traditional silicon PV cells and organic–inorganic  
1203 nanocomposite material. A window having 8 cm<sup>2</sup> active area had an efficiency of 3.4% while  
1204 measured under AM1.5 conditions (Chau et al., 2010).

### 1205 **5.5. BIM embedded BIPV/BAPV performance**

1206 Optimized building design, construction and operation are required to obtain an energy-efficient less-  
1207 energy hungry building. For a new building, this task can be performed before the construction phase  
1208 (during the design phase), and for retrofit building, this is possible using the historical data of the  
1209 building. Building energy modelling is currently gaining high importance which can compare the  
1210 different building components and prescribe the efficient and suitable components for a particular  
1211 location complying with the energy standards. Incorporating of PV particularly BIPV/BAPV is now  
1212 common practice for analysing the self-sufficiency of less-energy hungry/low energy/ zero energy/  
1213 adaptive building (Gao et al., 2019; J. Li et al., 2020).

1214 Successful integration of PV into a building (BIPV/BAPV) requires architectural building design, and  
1215 engineering knowledge to integrate the photovoltaic suitably. Both architecture and engineer need  
1216 software tools to perform the design and analysis of the overall results. Building information model  
1217 (BIM) gives a platform where architecture, engineer and construction people gets benefitted by  
1218 solving the multiphase complex building scenario. BIM contains parametric computable data, such as  
1219 building geometric descriptions, construction typology, and thermal properties which are required for  
1220 building project and particularly applicable for rapid design, generation, planning, and decision-  
1221 making, document creation, cost estimation, and vital project data in a digital format through the  
1222 course of a building life cycle (Sanhudo et al., 2018). For the architectural design, required software  
1223 tools are AutoCAD, MyArchiCAD, Auto Desk Revit and Sketchup while for PV design PVSYST.  
1224 However, for building energy model (BEM), a complete package is required where this drawing  
1225 software will provide the 3d building geometry, PV design will provide the PV parameters for  
1226 particular location and properties of building envelopes e.g. window, roof, wall, door. Currently  
1227 building energy software includes DOE-2, eQuest, DesignBuilder, Ecotect, Energy-10, Green  
1228 Building Studio, IESVE, HEED, and EnergyPlus (J. B. Kim et al., 2015). For EnergyPlus graphical  
1229 user interfaces (GUI) are AECOSim, CYPE-Building Services, DesignBuilder, Demand Response  
1230 Quick Assessment Tool, Easy EnergyPlus, EFEN, Hevacomp, OpenStudio, Simergy, and SMART  
1231 ENERGY. OpenStudio uses SketchUp plug-in to create building geometry editor; an OpenStudio  
1232 application as a main energy modelling interface; RunManager as a simulation interface; and the  
1233 ResultsViewer. BIM based building energy model (BEM) is a potential tool for less energy hungry  
1234 building simulation. Information data stored in BIM need a seamless translation from BIM to BEM.  
1235 However, BIM information does not always need to be translated into BEM or all the required  
1236 parameter always come from BIM. For example, a room in an architectural model does not always  
1237 indicate a zone in an energy simulation model and neither boundary conditions nor thermal zone  
1238 information is stored in BIM.

1239 Input parameters of BIM-BEM for BAPV are different from BIPV. For BAPV, the required input  
1240 parameters include location, PV specification (efficiency, rated power), tilt angle and inverter details.  
1241 For BIPV technology, including the previously mentioned parameters, the additional requirements are

1242 the transmission of PV, daylight transmission, solar heat gain factor or solar energy transmission,  
 1243 thermal transmission, or overall heat transfer coefficient. EnergyPlus (Buildings energy simulation  
 1244 tool) requires input parameters of PV module area, efficiency, open circuit voltage, short circuit  
 1245 current, voltage at the maximum power point, current at the maximum power point, power  
 1246 temperature coefficient, thermal conductivity, infrared emittance,  $U$ -value, solar heat gain coefficient,  
 1247 and visible light transmission, daylight illuminance inside a room due to BIPV, (Ng et al., 2013) (M.  
 1248 Wang et al., 2017)(Peng et al., 2016)(Jakica, 2018). BIM for optimizing BIPV tilt angle (Xuan, 2011)  
 1249 and BIM API program in Autodesk Revit (Dixit and Yan, 2012) (Kuo et al., 2016) was previously  
 1250 employed to simulate production of PV electricity (Gupta et al., 2014).

## 1251 **6. Discussion and perspective**

### 1252 **6.1. Environmental, economic and societal viability of BIPV/BAPV**

1253 Environmental benefits from BIPV/BAPV is the essential study as during the processing, purification  
 1254 and production of raw PV materials, PV system and other BOS fabrication, operation and  
 1255 maintenance, and also during the dismantle of BIPV system there is a provision of power  
 1256 consumption which come from traditional fuel sources (Parida et al., 2011). Life cycle analysis (LCA)  
 1257 of PV system reveals the benefits of using a PV system. LCA analysis indicates for 1kWh energy  
 1258 generation, PV emits only 35 gCO<sub>2</sub>eq while 1138.8 gCO<sub>2</sub>eq for coal. This data clearly indicates the  
 1259 positive environmental impact of PV (Sierra et al., 2020). PV system's energy payback time (EPBT)  
 1260 indicates the electricity balance or net zero gain from PV over its lifetime. Adaptive BIPV window  
 1261 system has ability to enhance the environmental impact up to 50% higher than traditional window  
 1262 (Jayathissa et al., 2016). EPBT of c-Si based BIPV window for Singapore climate was 1.98 years (Ng  
 1263 and Mithraratne, 2014b) while 2.1 kWp domestic BIPV in Southern England showed EPBT of 4.5  
 1264 years (Hammond et al., 2012). In Hongkong climate, roof top BAPV system's EPBT was 7.3 years  
 1265 however variation of azimuthal and inclinational angle this time changes. However, greenhouse  
 1266 payback time was only 5.2 when PV faced south direction and kept an optimal angle (Lu and Yang,  
 1267 2010). Low concentrating BIPV system showed 13% improvement of an environmental impact  
 1268 compared to without concentrating BIPV system (Menoufi et al., 2013). In another work, asymmetric  
 1269 lens-walled compound parabolic concentrator based BIPV showed EPBT which varied between 2.82–  
 1270 4.74 years depends on the different location in China (Li et al., 2018). For BIPVT system EPBT  
 1271 varies between 7.3 to 16.9 years. Cost of energy production for BIPVT varies from 1.61 to 3.61  
 1272 US\$/kWh (Tripathy et al., 2017). For Taiwan climate, EPBT took 10 years (Wu et al., 2018). Hence it  
 1273 is clear that EPBT within 10 years is possible for BIPV/BAPV integration in less energy-hungry  
 1274 building.

1275 Building's construction cost reduction potential using BIPV/BAPV system is one of the most  
 1276 engrossing topics of discussion. It is evident from reported work that cost of BIPV building envelop is  
 1277 higher than the cost of the traditional building envelope. BIPV tiles can increase 2% cost than  
 1278 conventional tiles (Hammond et al., 2012), BIPV window can add \$350–500 per m<sup>2</sup> (Benemann et al.,  
 1279 2001), while in a commercial building, BIPV can add 2-5% of overall construction cost (Eiffert,  
 1280 2003). Also, in some cases, it was found that BIPV façade can reduce 20% cost than polished stone  
 1281 facades (Koinegg et al., 2013). For BIPV tiles, standing seam products and shingles, require  
 1282 additional adhesives and framing and flashing material while for BAPV roof, PV is attached on the  
 1283 existing construction materials. Thus, BIPV actually offset the construction cost of a building. Hence,  
 1284 the higher cost can be expected for BAPV compared to BIPV (Verberne et al., 2014). Other costs for  
 1285 BIPV/BAPV systems arise from BOS and transportation and installation. Most often, this BOS counts  
 1286 only 10-16% from the overall project cost, where inverter and storage systems are the leading cause of



1287 this cost during installation and operation time. Transportation cost is very dynamic, and few reports  
1288 are available for information. In Italy, transport and installation cost was 19% (Cucchiella et al.,  
1289 2012) while in Greece mounting cost was only 2.5% and 3% transportation cost (Bakos et al., 2003).  
1290 However, for BIPV, cost should include building envelope cost and additional benefits from  
1291 electricity generation (Oliver and Jackson, 2000)(Pagliaro et al., 2010; Sozer and Elimeiri, 2007).  
1292 BIPV/BAPV has potential to satisfy the building energy demand by generating the green electricity  
1293 and reducing the electricity consumption by lowering heating, cooling, and lighting load, and excess  
1294 energy can be exported to the grid. Thus BIPV/BAPV shows a positive cost-effective over traditional  
1295 construction cost.

1296 Deployment of BIPV/BAPV has high societal impact and benefits to wider society. Currently,  
1297 because of the rapid urbanization, 55% of the world population lives in urban areas and it is projected  
1298 that in 2050 this will be 68% (Sampson et al., 2020). This urbanization consumes a considerable  
1299 amount of electricity while most of the country depends on the imported fossil fuel energy sources to  
1300 generate that electricity (Foster et al., 2020; Luo et al., 2020; Su, 2019; Xie et al., 2020). Also, the  
1301 economic growth of a nation increases with urbanization (Gasimli et al., 2019). Hence, to maintain  
1302 economic growth and urbanization, and to become an energy secured country, BIPV is the key  
1303 solution. Traditional coal based power plant emits particulate matter (PM) which has a dimension  
1304 between 2.5 micrometre ( $PM_{2.5}$ ) to 10 micrometre ( $PM_{10}$ ) and also  $SO_2$  and  $NO_x$ ,  $CO_2$  and CO (Clark  
1305 et al., 2020; Karplus et al., 2018; Song et al., 2020). While these gasses create a greenhouse effect,  
1306 PM also has a direct adverse impact on human health as  $PM_{2.5}$  influences asthma. In 2015, 24.6  
1307 million people had asthma represented nearly 8% of the population in the USA. In the USA, between  
1308 2008 and 2013, per head asthma treatment cost was \$3266 annually (Williams et al., 2019).  
1309 Replacement of the coal plant with BIPV can displace this  $PM_{2.5}$  and save the medical cost, which  
1310 can be employed for countries development and also help the growth of the energy economy without  
1311 polluting the environment. Also, transmission and distribution losses reduction gives an opportunity  
1312 to the energy provider to reduce electricity tariff (Byrnes et al., 2013) (Yang and Zou, 2016).

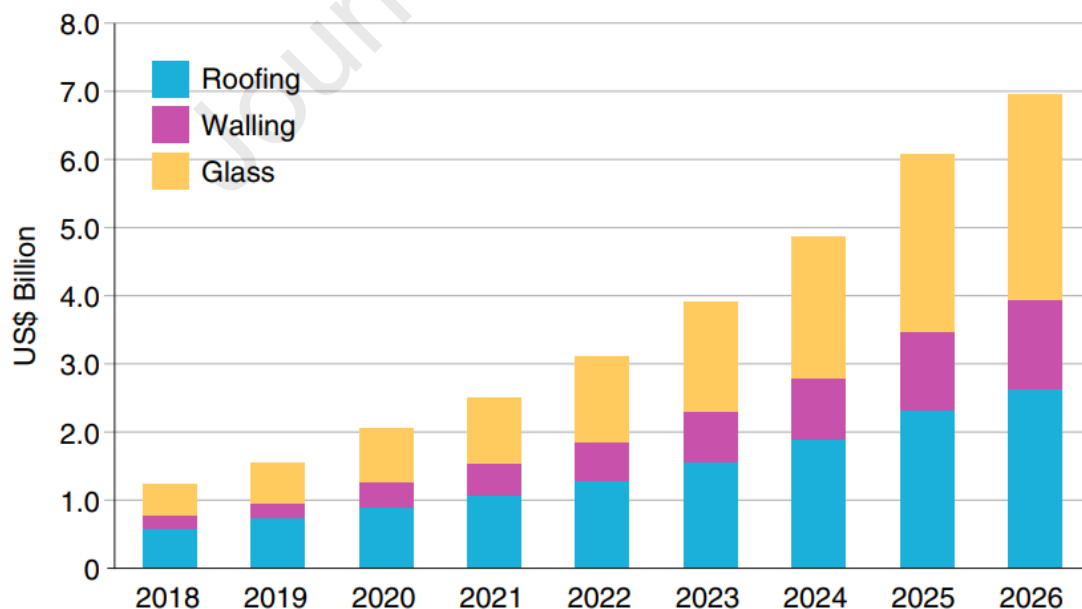
## 1313 **6.2. Limitation and progress towards BIPV/BAPV**

1314 Inclusion of PV in building still is not excitingly triggered due to several factors such as lack of public  
1315 awareness, missing professional knowledge, low communication between designers and engineers, no  
1316 proper knowledge of maintenance. End-users of BIPV technologies are still in the dark about the  
1317 capital and installation cost, ongoing repairing and maintenance cost for BIPV/BAPV systems  
1318 throughout the lifetime of buildings. They have knowledge about the cost of the system but have no  
1319 knowledge about the long-term benefits. Hence, a clear cost-benefit analysis should be there to make  
1320 helpful for users. Although since 1980, 10 fold price dropped for PV modules but concrete data of  
1321 energy payback time is rare (Yang and Zou, 2016). In addition, long payback period, high upfront  
1322 capital cost, low efficiency of BIPV may possess high electricity tariff. BIPV policies are not well  
1323 documents and government supports particularly for small industries are not available in the same  
1324 order (Biyik et al., 2017; Jelle, 2016; Osseweijer et al., 2018; A. K. Shukla et al., 2017b; Shukla et al.,  
1325 2016b, 2016a). Low PV cell efficiency is also another barrier for widespread BIPV/BAPV adoption.  
1326 Low efficiency decreases the power conversion which increases the capital cost and delays the EPBT.  
1327 Lower electricity price from fossil fuel energy sources also creates a barrier for BIPV technology  
1328 (Alnaser and Flanagan, 2007). Hence to promote BIPV technology, an incentive for PV and increase  
1329 the traditional electricity should be implemented. At the end of 2017, global installed PV capacity was  
1330 400 GW which is expected to reach 4500 GW by 2050. If the average PV panel lifetime is considered  
1331 to be 25 years, the worldwide solar PV waste is anticipated at around 78 million tonnes by 2050.

1332 Therefore, the disposal of PV panels, by using environmentally benign waste recycling, recycling  
 1333 technology, recycling policies are also pertinent (Bogacka et al., 2017)(Chowdhury et al., 2020).

1334 Though the presence of so many barriers, many countries including UK, USA, Asia and EU's zero-  
 1335 carbon or decarbonisation in 2050 has escalated the BIPV penetration in the building sector. This is  
 1336 envisaged because of the attractive aesthetic and flexible nature of BIPV (Osseweijer et al., 2018; A.  
 1337 K. Shukla et al., 2017b). Specific region wise BIPV growth is listed in Table 7. Present global BIPV  
 1338 market size is about 2.3 GW where Europe constitute the largest market size (42% of global market ),  
 1339 particularly because of attractive incentive in Germany, Italy, and France. Globally, Europe and the  
 1340 USA dominate the BIPV market than that of Asia. The continuous growth of global BIPV market is  
 1341 happening while compounded annual growth rate (CAGR) is higher for ASIA pacific (Osseweijer et  
 1342 al., 2018). Incentive plan has already been taken by different countries. In Germany, "The thousand  
 1343 Solar Roofs Program" was initiated in 1995 to promote BIPV/BAPV, while in the USA, "Ten Million  
 1344 Solar Roofs Program" was started in 2010 and in China, "enforcement advice for promoting solar  
 1345 energy applications in buildings" and "interim procedures" was started to promote the BIPV/BAPV  
 1346 technologies (Zhang et al., 2018). Indian government has also set target to achieve 40 GW rooftop  
 1347 solar PV integration by 2022 (Reddy et al., 2020). Because of these initiatives, present market growth  
 1348 of BIPV is very promising which shows close to 40% per year in the next decade, from US\$1.1  
 1349 billion in 2017 to over US\$2.7 billion in 2021 shown in Figure 30 (Ballif et al., 2018). Later on, the  
 1350 BIPV market average annual growth rate for 2023 is expected to reach 11200 million \$. Positive  
 1351 media coverage regarding environmental and economic benefits from BIPV/BAPV can increase  
 1352 public awareness as without public support, the whole concept and project will be in jeopardy  
 1353 (Azadian and Radzi, 2013).

1354



1355

1356 Figure 30: Worldwide annual revenue from BIPV (Reprinted with permission from (Ballif et al.,  
 1357 2018) Copyright © 2018, Springer Nature).

1358 Table 7: Global BIPV market development and forecast for 2020 in MW and compounded annual  
 1359 growth rate

Region/Country	2014	2015	2016	2017	2018	2019	2020	Compound annual growth rate (CAGR %)
Asia/Pacific*	300	492	772	1159	1672	2329	<b>3134</b>	47.8
Europe	650	967	1441	2103	2929	3807	<b>4838</b>	39.7
Rest of world	81	125	184	263	355	451	<b>561</b>	37.9
USA	319	476	675	917	1200	1491	<b>1766</b>	33.0
Canada	42	61	86	119	157	190	<b>228</b>	32.6
Japan	143	201	268	349	434	520	<b>612</b>	27.5
<b>Total (GW)</b>	<b>1.5</b>	<b>2.3</b>	<b>3.4</b>	<b>4.9</b>	<b>6.7</b>	<b>8.8</b>	<b>11.1</b>	

1360 \*Asia/Pacific excluding Japan

1361

1362 Hence a smooth entry of BIPV in energy market of any country needs a support from all BIPV  
 1363 stakeholder which includes government (central/national government, energy Review Committees),  
 1364 BIPV industry (BIPV manufacturers/suppliers/wholesale), construction industry (contractors; material  
 1365 suppliers; PV-module installation; architects); academia (Universities; Research institutes), end users  
 1366 (Housing associations and their tenants; Business Rental (office spaces); private homeowners  
 1367 (Osseweijer et al., 2018).

## 1368 7. Conclusions:

1369 The work reviews the available and future application potential of PV systems in a building being part  
 1370 of building-integrated (BI) PV (BIPV) or building attached (BA) PV (BAPV) while they are separated  
 1371 by their integration and purpose of uses. Building wall, roof and window application using semi-  
 1372 transparent PV types are gaining interest because of their multifunctional behaviour such as replacing  
 1373 structural material, provides high insulation, allows daylight, and generates power. To enable BIPV in  
 1374 a colder climate, vacuum integrated BIPV is suitable. BIPV and BAPV both can also be a source for  
 1375 autonomous switchable glazing to change its state based on occupant's requirement. BIPV/BAPV has  
 1376 the ability to be a source of power supply for an electric vehicle (EV). Along with this advantageous,  
 1377 BIPV/BAPV both suffer from temperature issues, dust, and snow accumulation on the devices.  
 1378 Elevated temperature effect can be minimised by using active or passive thermal regulation while  
 1379 shading effect requires a cleaning mechanism. Gaining the interest of photovoltaic technology  
 1380 integration in the building, forced to impose an international standard or country wise standard for  
 1381 installation. In future BIPV and BAPV has a possible application in mainly three application,  
 1382 autonomous switchable glazing, low heat loss glazing and BIPV as a source of EV.

## 1383 Acknowledgement

1384 Author declares no conflict of interest. This research did not receive any specific grant from funding  
 1385 agencies in the public, commercial, or not-for-profit sectors.

## 1386 Reference

1387 Aaditya, G., Pillai, R., Mani, M., 2013. An insight into real-time performance assessment of a  
 1388 building integrated photovoltaic (BIPV) installation in Bangalore (India). Energy Sustain. Dev.

- 1389 17, 431–437. doi:10.1016/j.esd.2013.04.007
- 1390 Abe, C.F., Dias, J.B., Notton, G., Faggianelli, G.A., 2020. Experimental Application of Methods to  
1391 Compute Solar Irradiance and Cell Temperature of Photovoltaic Modules. *Sensors* 1–17.  
1392 doi:10.3390/s20092490
- 1393 AbouElhamd, A.R., Al-Sallal, K.A., Hassan, A., 2019. Review of core/shell quantum dots technology  
1394 integrated into building's glazing. *Energies* 12. doi:10.3390/en12061058
- 1395 Agarwal, R., Verma, K., Agrawal, N.K., Duchaniya, R.K., Singh, R., 2016. Synthesis,  
1396 characterization, thermal conductivity and sensitivity of CuO nanofluids. *Appl. Therm. Eng.*  
1397 102, 1024–1036. doi:10.1016/j.applthermaleng.2016.04.051
- 1398 Agathokleous, R.A., Kalogirou, S.A., 2019. Status , barriers and perspectives of building integrated  
1399 photovoltaic systems. *Energy* 191, 116471. doi:10.1016/j.energy.2019.116471
- 1400 Agathokleous, R.A., Kalogirou, S.A., 2016. Double skin facades (DSF) and building integrated  
1401 photovoltaics (BIPV): A review of configurations and heat transfer characteristics. *Renew.*  
1402 *Energy* 89, 743–756. doi:10.1016/j.renene.2015.12.043
- 1403 Agrawal, B., Tiwari, G.N., 2010a. Life cycle cost assessment of building integrated photovoltaic  
1404 thermal (BIPVT) systems. *Energy Build.* 42, 1472–1481. doi:10.1016/j.enbuild.2010.03.017
- 1405 Agrawal, B., Tiwari, G.N., 2010b. Optimizing the energy and exergy of building integrated  
1406 photovoltaic thermal (BIPVT) systems under cold climatic conditions. *Appl. Energy* 87, 417–  
1407 426. doi:10.1016/j.apenergy.2009.06.011
- 1408 Agresti, A., Pescetelli, S., Palma, A.L., Martín-García, B., Najafi, L., Bellani, S., Moreels, I., Prato,  
1409 M., Bonaccorso, F., Di Carlo, A., 2019. Two-Dimensional Material Interface Engineering for  
1410 Efficient Perovskite Large-Area Modules. *ACS Energy Lett.* 1862–1871.  
1411 doi:10.1021/acsenerylett.9b01151
- 1412 Ahn, K.S., Yoo, S.J., Kang, M.S., Lee, J.W., Sung, Y.E., 2007. Tandem dye-sensitized solar cell-  
1413 powered electrochromic devices for the photovoltaic-powered smart window. *J. Power Sources*  
1414 168, 533–536. doi:10.1016/j.jpowsour.2006.12.114
- 1415 Ahuja, G., Madireddi, N., Mahanwar, P.A., 2017. Scalable super-hydrophilic nanocomposite latex  
1416 with self-cleaning action. *Prog. Org. Coatings* 110, 10–15. doi:10.1016/j.porgcoat.2016.12.008
- 1417 Akbari, H., Naydenova, I., Ahmed, H., McCormack, S., Martin, S., 2017. Development and testing of  
1418 low spatial frequency holographic concentrator elements for collection of solar energy. *Sol.*  
1419 *Energy* 155, 103–109. doi:10.1016/j.solener.2017.04.067
- 1420 Al-hasan, A.Y., Ghoneim, A.A., 2005. A new correlation between photovoltaic panel ' s efficiency  
1421 and amount of sand dust accumulated on their surface 6451. doi:10.1080/14786450500291834
- 1422 Alim, M.A., Tao, Z., Hassan, M.K., Rahman, A., Wang, B., Zhang, C., Samali, B., 2019. Is it time to  
1423 embrace building integrated Photovoltaics? A review with particular focus on Australia. *Sol.*  
1424 *Energy* 188, 1118–1133. doi:10.1016/j.solener.2019.07.002
- 1425 Allouhi, A., Saadani, R., Kousksou, T., Saidur, R., Jamil, A., Rahmoune, M., 2016. Grid-connected  
1426 PV systems installed on institutional buildings: Technology comparison, energy analysis and  
1427 economic performance. *Energy Build.* 130, 188–201. doi:10.1016/j.enbuild.2016.08.054
- 1428 Alnaser, N.W., 2018. First smart 8.64 kW BIPV in a building in Awali Town at Kingdom of Bahrain.  
1429 *Renew. Sustain. Energy Rev.* 82, 205–214. doi:10.1016/j.rser.2017.09.041
- 1430 Alnaser, N.W., Flanagan, R., 2007. The need of sustainable buildings construction in the Kingdom of

- 1431 Bahrain. *Build. Environ.* 42, 495–506. doi:10.1016/j.buildenv.2005.08.032
- 1432 Alrashidi, H., Ghosh, A., Issa, W., Sellami, N., Mallick, T.K., Sundaram, S., 2020a. Thermal  
1433 performance of semitransparent CdTe BIPV window at temperate climate. *Sol. Energy* 195,  
1434 536–543. doi:10.1016/j.solener.2019.11.084
- 1435 Alrashidi, H., Ghosh, A., Issa, W., Sellami, N., Mallick, T.K., Sundaram, S., 2019. Evaluation of solar  
1436 factor using spectral analysis for CdTe photovoltaic glazing. *Mater. Lett.* 237, 332–335.  
1437 doi:10.1016/j.matlet.2018.11.128
- 1438 Alrashidi, H., Issa, W., Sellami, N., Ghosh, A., Mallick, T.K., Sundaram, S., 2020b. Performance  
1439 assessment of cadmium telluride-based semi-transparent glazing for power saving in façade  
1440 buildings. *Energy Build.* 215, 109585. doi:10.1016/j.enbuild.2019.109585
- 1441 Amanlou, Y., Hashjin, T.T., Ghobadian, B., Najafi, G., Mamat, R., 2016. A comprehensive review of  
1442 Uniform Solar Illumination at Low Concentration Photovoltaic (LCPV) Systems. *Renew.*  
1443 *Sustain. Energy Rev.* 60, 1430–1441. doi:10.1016/j.rser.2016.03.032
- 1444 Anctil, A., Lee, E., Lunt, R.R., 2019. Net environmental and cost benefit of transparent organic solar  
1445 cells in building-integrated applications. *Appl. Energy* 261, 114429.  
1446 doi:10.1016/j.apenergy.2019.114429
- 1447 Andargie, M.S., Touchie, M., O'Brien, W., 2019. A review of factors affecting occupant comfort in  
1448 multi-unit residential buildings. *Build. Environ.* 160, 106182.  
1449 doi:10.1016/j.buildenv.2019.106182
- 1450 Andenæs, E., Jelle, B.P., Ramlo, K., Kolås, T., Selj, J., Foss, S.E., 2018. The influence of snow and  
1451 ice coverage on the energy generation from photovoltaic solar cells. *Sol. Energy* 159, 318–328.  
1452 doi:10.1016/j.solener.2017.10.078
- 1453 Andrews, R.W., Pollard, A., Pearce, J.M., 2013. The effects of snowfall on solar photovoltaic  
1454 performance. *Sol. Energy* 92, 84–97. doi:10.1016/j.solener.2013.02.014
- 1455 Appels, R., Lefevre, B., Herteleer, B., Goverde, H., Beerten, A., Paesen, R., De Medts, K., Driesen, J.,  
1456 Poortmans, J., 2013. Effect of Soiling on Photovoltaic Modules in Norway. *Sol. Energy* 96,  
1457 283–291. doi:https://doi.org/10.1016/j.solener.2013.07.017
- 1458 Aristizábal, A.J., Gordillo, G., 2008. Performance monitoring results of the first grid-connected BIPV  
1459 system in Colombia. *Renew. Energy* 33, 2475–2484. doi:10.1016/j.renene.2008.01.018
- 1460 Asghar, M.I., Zhang, J., Wang, H., Lund, P.D., 2017. Device stability of perovskite solar cells – A  
1461 review. *Renew. Sustain. Energy Rev.* 77, 131–146. doi:10.1016/j.rser.2017.04.003
- 1462 Aste, N., Del Pero, C., Leonforte, F., 2016. The first Italian BIPV project: Case study and long-term  
1463 performance analysis. *Sol. Energy* 134, 340–352. doi:10.1016/j.solener.2016.05.010
- 1464 Aste, N., Del Pero, C., Tagliabue, L.C., Leonforte, F., Testa, D., Fusco, R., 2015a. Performance  
1465 monitoring and building integration assessment of innovative LSC components. *5th Int. Conf.*  
1466 *Clean Electr. Power Renew. Energy Resour. Impact, ICCEP 2015* 129–133.  
1467 doi:10.1109/ICCEP.2015.7177612
- 1468 Aste, N., Tagliabue, L.C., Del Pero, C., Testa, D., Fusco, R., 2015b. Performance analysis of a large-  
1469 area luminescent solar concentrator module. *Renew. Energy* 76, 330–337.  
1470 doi:10.1016/j.renene.2014.11.026
- 1471 Aswathy, G., Rajesh, C.S., Sreejith, M.S., Vijayakumar, K.P., Sudha Kartha, C., 2018. Designing  
1472 photovoltaic concentrators using holographic lens recorded in nickel ion doped photopolymer  
1473 material. *Sol. Energy* 163, 70–77. doi:10.1016/j.solener.2018.01.017

- 1474 Azadian, F., Radzi, M.A.M., 2013. A general approach toward building integrated photovoltaic  
1475 systems and its implementation barriers: A review. *Renew. Sustain. Energy Rev.* 22, 527–538.  
1476 doi:10.1016/j.rser.2013.01.056
- 1477 Baetens, R., Jelle, B.P., Gustavsen, A., 2010. Phase change materials for building applications: A  
1478 state-of-the-art review. *Energy Build.* 42, 1361–1368. doi:10.1016/j.enbuild.2010.03.026
- 1479 Bai, S., Da, P., Li, C., Wang, Z., Yuan, Z., Fu, F., Kawecki, M., Liu, X., Sakai, N., Wang, J.T.W.,  
1480 Huettner, S., Buecheler, S., Fahlman, M., Gao, F., Snaith, H.J., 2019. Planar perovskite solar  
1481 cells with long-term stability using ionic liquid additives. *Nature* 571, 245–250.  
1482 doi:10.1038/s41586-019-1357-2
- 1483 Baig, H., Heasman, K.C., Mallick, T.K., 2012. Non-uniform illumination in concentrating solar cells.  
1484 *Renew. Sustain. Energy Rev.* 16, 5890–5909. doi:10.1016/j.rser.2012.06.020
- 1485 Baig, H., Kanda, H., Asiri, A.M., Nazeeruddin, M.K., Mallick, T., 2020. Increasing efficiency of  
1486 perovskite solar cells using low concentrating photovoltaic systems. *Sustain. Energy Fuels.*  
1487 doi:10.1039/C9SE00550A
- 1488 Baig, H., Mallick, T., 2018. Solar Squared : Transforming Glass Bricks into a BIPV product, in:  
1489 *Advanced Building Skins*. Bern, Switzerland.
- 1490 Baig, H., Sarmah, N., Chemisana, D., Rosell, J., Mallick, T.K., 2014. Enhancing performance of a  
1491 linear dielectric based concentrating photovoltaic system using a reflective film along the edge.  
1492 *Energy* 73, 177–191. doi:10.1016/j.energy.2014.06.008
- 1493 Baig, H., Sarmah, N., Heasman, K.C., Mallick, T.K., 2013. Numerical modelling and experimental  
1494 validation of a low concentrating photovoltaic system. *Sol. Energy Mater. Sol. Cells* 113, 201–  
1495 219. doi:10.1016/j.solmat.2013.01.035
- 1496 Baig, H., Sellami, N., Mallick, T.K., 2015. Trapping light escaping from the edges of the optical  
1497 element in a Concentrating Photovoltaic system. *Energy Convers. Manag.* 90, 238–246.  
1498 doi:10.1016/j.enconman.2014.11.026
- 1499 Bakos, G.C., Soursos, M., Tsagas, N.F., 2003. Technoeconomic assessment of a building-integrated  
1500 PV system for electrical energy saving in residential sector. *Energy Build.* 35, 757–762.  
1501 doi:10.1016/S0378-7788(02)00229-3
- 1502 Baljit, S.S.S., Chan, H.Y., Sopian, K., 2016. Review of building integrated applications of  
1503 photovoltaic and solar thermal systems. *J. Clean. Prod.* 137, 677–689.  
1504 doi:10.1016/j.jclepro.2016.07.150
- 1505 Ballif, C., Perret-Aebi, L.E., Lufkin, S., Rey, E., 2018. Integrated thinking for photovoltaics in  
1506 buildings. *Nat. Energy* 3, 438–442. doi:10.1038/s41560-018-0176-2
- 1507 Barman, S., Chowdhury, A., Mathur, S., Mathur, J., 2018. Assessment of the efficiency of window  
1508 integrated CdTe based semi-transparent photovoltaic module. *Sustain. Cities Soc.* 37, 250–262.  
1509 doi:10.1016/j.scs.2017.09.036
- 1510 Barrios, D., Vergaz, R., Sánchez-Pena, J.M., García-Cámara, B., Granqvist, C.G., Niklasson, G.A.,  
1511 2015. Simulation of the thickness dependence of the optical properties of suspended particle  
1512 devices. *Sol. Energy Mater. Sol. Cells* 143, 613–622. doi:10.1016/j.solmat.2015.05.044
- 1513 Battaglia, C., Cuevas, A., De Wolf, S., 2016. High-efficiency crystalline silicon solar cells: Status and  
1514 perspectives. *Energy Environ. Sci.* 9, 1552–1576. doi:10.1039/c5ee03380b
- 1515 Bauer, A., Menrad, K., 2019. Standing up for the Paris Agreement : Do global climate targets  
1516 influence individuals ' greenhouse gas emissions ? *Environ. Sci. Policy* 99, 72–79.

- 1517 doi:10.1016/j.envsci.2019.05.015
- 1518 Bell, J.M., Matthews, J.P., 2001. Temperature dependence of kinetic behaviour of sol-gel deposited  
1519 electrochromics. *Sol. Energy Mater. Sol. Cells* 68, 249–263. doi:10.1016/S0927-  
1520 0248(00)00360-3
- 1521 Belussi, L., Barozzi, B., Bellazzi, A., Danza, L., Devitofrancesco, A., Fanciulli, C., Ghellere, M.,  
1522 Guazzi, G., Meroni, I., Salamone, F., Scamoni, F., Scrosati, C., 2019. A review of performance  
1523 of zero energy buildings and energy efficiency solutions. *J. Build. Eng.* 25, 100772.  
1524 doi:10.1016/j.jobe.2019.100772
- 1525 Benemann, J., Chehab, O., Schaar-Gabriel, E., 2001. Building-integrated PV modules. *Sol. Energy*  
1526 *Mater. Sol. Cells* 67, 345–354. doi:10.1016/S0927-0248(00)00302-0
- 1527 Bergren, M.R., Makarov, N.S., Ramasamy, K., Jackson, A., Guglielmetti, R., McDaniel, H., 2018.  
1528 High-Performance CuInS<sub>2</sub> Quantum Dot Laminated Glass Luminescent Solar Concentrators for  
1529 Windows. *ACS Energy Lett.* 3, 520–525. doi:10.1021/acsenergylett.7b01346
- 1530 Berny, S., Blouin, N., Distler, A., Egelhaaf, H.J., Krompiec, M., Lohr, A., Lozman, O.R., Morse,  
1531 G.E., Nanson, L., Pron, A., Sauermaun, T., Seidler, N., Tierney, S., Tiwana, P., Wagner, M.,  
1532 Wilson, H., 2015. Solar trees: First large-scale demonstration of fully solution coated,  
1533 semitransparent, flexible organic photovoltaic modules. *Adv. Sci.* 3, 1–7.  
1534 doi:10.1002/advs.201500342
- 1535 Bhandari, S., Roy, A., Ghosh, A., Mallick, T.K., Sundaram, S., 2019. Performance of WO<sub>3</sub> -  
1536 Incorporated Carbon Electrodes for Ambient Mesoscopic Perovskite Solar Cells . *ACS Omega*  
1537 5, 422–429. doi:10.1021/acsomega.9b02934
- 1538 Bhatti, A.R., Salam, Z., Aziz, M.J.B.A., Yee, K.P., Ashique, R.H., 2016. Electric vehicles charging  
1539 using photovoltaic: Status and technological review. *Renew. Sustain. Energy Rev.* 54, 34–47.  
1540 doi:10.1016/j.rser.2015.09.091
- 1541 Bi, D., Yi, C., Luo, J., Décoppet, J.-D., Zhang, F., Zakeeruddin, S.M., Li, X., Hagfeldt, A., Grätzel,  
1542 M., 2016. Polymer-templated nucleation and crystal growth of perovskite films for solar cells  
1543 with efficiency greater than 21%. *Nat. Energy* 1, 16142. doi:10.1038/nenergy.2016.142
- 1544 Birnie, D.P., 2009. Solar-to-vehicle (S2V) systems for powering commuters of the future. *J. Power*  
1545 *Sources* 186, 539–542. doi:10.1016/j.jpowsour.2008.09.118
- 1546 Biswas, D., Szocs, C., Chacko, R., Wansink, B., 2016. Shining Light on Atmospheric: How Ambient  
1547 Light Influences Food Choices. *J. Mark. Res.* 54, 111–123. doi:10.1509/jmr.14.0115
- 1548 Biyik, E., Araz, M., Hepbasli, A., Shahrestani, M., Yao, R., Shao, L., Essah, E., Oliveira, A.C., del  
1549 Caño, T., Rico, E., Lechón, J.L., Andrade, L., Mendes, A., Atlı, Y.B., 2017. A key review of  
1550 building integrated photovoltaic (BIPV) systems. *Eng. Sci. Technol. an Int. J.* 20, 833–858.  
1551 doi:10.1016/j.jestch.2017.01.009
- 1552 Bock, J., Robinson, J., 2008. An efficient power management approach for self-cleaning solar panels  
1553 with integrated electrodynamic screens. *Proc. ESA Annu. Meet. Electrostat.*  
1554 doi:http://www.electrostatics.org/images/esa\_2008\_o2.pdf
- 1555 Bodart, M., De Herde, A., 2002. Global energy savings in offices buildings by the use of daylighting.  
1556 *Energy Build.* 34, 421–429. doi:10.1016/S0378-7788(01)00117-7
- 1557 Bogacka, M., Pikoń, K., Landrat, M., 2017. Environmental impact of PV cell waste scenario. *Waste*  
1558 *Manag.* 70, 198–203. doi:10.1016/j.wasman.2017.09.007
- 1559 Borrebæk, P.O.A., Jelle, B.P., Zhang, Z., 2020. Avoiding snow and ice accretion on building

- 1560 integrated photovoltaics – challenges, strategies, and opportunities. *Sol. Energy Mater. Sol.*  
1561 *Cells* 206. doi:10.1016/j.solmat.2019.110306
- 1562 Brench, B.L., 1979. Snow-covering effects on the power output of solar photovoltaic arrays.  
1563 doi:doi:10.2172/5232456.
- 1564 Brinkworth, B.J., Cross, B.M., Marshall, R.H., Yang, H., 1997. Thermal regulation of photovoltaic  
1565 cladding. *Sol. Energy* 61, 169–178. doi:10.1016/S0038-092X(97)00044-3
- 1566 Bristow, N., Kettle, J., 2018. Outdoor organic photovoltaic module characteristics: Benchmarking  
1567 against other PV technologies for performance, calculation of Ross coefficient and outdoor  
1568 stability monitoring. *Sol. Energy Mater. Sol. Cells* 175, 52–59.  
1569 doi:10.1016/j.solmat.2017.10.008
- 1570 Bristow, N., Kettle, J., 2016. Outdoor performance of organic photovoltaics : Diurnal analysis ,  
1571 dependence on temperature , irradiance , and degradation Outdoor performance of organic  
1572 photovoltaics : Diurnal analysis , dependence on temperature , irradiance , and degradation  
1573 013111. doi:10.1063/1.4906915
- 1574 Brooks, A.E., Lonij, V.P.A., Cronin, A.D., Kostuk, R.K., Russo, J.M., Zhang, D., Vorndran, S., 2012.  
1575 One year of field studies of holographic planar concentrators at the Tucson Electric Power Solar  
1576 Test Yard. *World Renew. Energy Forum, WREF 2012, Incl. World Renew. Energy Congr. XII*  
1577 *Color. Renew. Energy Soc. Annu. Conf. 2*, 812–818.
- 1578 Browne, M.C., Norton, B., McCormack, S.J., 2016. Heat retention of a photovoltaic/thermal collector  
1579 with PCM. *Sol. Energy* 133, 533–548. doi:10.1016/j.solener.2016.04.024
- 1580 Browne, M.C., Norton, B., McCormack, S.J., 2015. Phase change materials for photovoltaic thermal  
1581 management. *Renew. Sustain. Energy Rev.* 47, 762–782. doi:10.1016/j.rser.2015.03.050
- 1582 Bücher, K., 1997. Site dependence of the energy collection of PV modules. *Sol. Energy Mater. Sol.*  
1583 *Cells* 47, 85–94. doi:10.1016/S0927-0248(97)00028-7
- 1584 Bush, K.A., Bailie, C.D., Chen, Y., Bowering, A.R., Wang, W., Ma, W., Leijtens, T., Moghadam, F.,  
1585 McGehee, M.D., 2016. Thermal and environmental stability of semi-transparent perovskite solar  
1586 cells for tandems by a solution-processed nanoparticle buffer layer and sputtered ITO electrode.  
1587 *Conf. Rec. IEEE Photovolt. Spec. Conf. 2016-Novem*, 246–248.  
1588 doi:10.1109/PVSC.2016.7749588
- 1589 Byrnes, L., Brown, C., Foster, J., Wagner, L.D., 2013. Australian renewable energy policy: Barriers  
1590 and challenges. *Renew. Energy* 60, 711–721. doi:10.1016/j.renene.2013.06.024
- 1591 Cai, L., Liang, L., Wu, J., Ding, B., Gao, L., Fan, B., 2017. Large area perovskite solar cell module. *J.*  
1592 *Semicond.* 38, 2–5. doi:10.1088/1674-4926/38/1/014006
- 1593 Calle, C.I., Buhler, C.R., McFall, J.L., Snyder, S.J., 2009. Particle removal by electrostatic and  
1594 dielectrophoretic forces for dust control during lunar exploration missions. *J. Electrostat.* 67, 89–  
1595 92. doi:10.1016/j.elstat.2009.02.012
- 1596 Cañete, C., Carretero, J., Sidrach-de-Cardona, M., 2014. Energy performance of different photovoltaic  
1597 module technologies under outdoor conditions. *Energy* 65, 295–302.  
1598 doi:10.1016/j.energy.2013.12.013
- 1599 Cannavale, A., Cossari, P., Eperon, G.E., Colella, S., Fiorito, F., Gigli, G., Snaith, H.J., Listorti, A.,  
1600 2016. Forthcoming perspectives of photoelectrochromic devices: A critical review. *Energy*  
1601 *Environ. Sci.* 9, 2682–2719. doi:10.1039/c6ee01514j
- 1602 Cannavale, A., H?rantner, M., Eperon, G.E., Snaith, H.J., Fiorito, F., Ayr, U., Martellotta, F., 2017a.



- 1603 Building integration of semitransparent perovskite-based solar cells: Energy performance and  
1604 visual comfort assessment. *Appl. Energy* 194, 94–107. doi:10.1016/j.apenergy.2017.03.011
- 1605 Cannavale, A., Ierardi, L., Hörantner, M., Eperon, G.E., Snaith, H.J., Ayr, U., Martellotta, F., 2017b.  
1606 Improving energy and visual performance in offices using building integrated perovskite-based  
1607 solar cells: A case study in Southern Italy. *Appl. Energy* 205, 834–846.  
1608 doi:10.1016/j.apenergy.2017.08.112
- 1609 Cao, X., Dai, X., Liu, J., 2016. Building energy-consumption status worldwide and the state-of-the-art  
1610 technologies for zero-energy buildings during the past decade. *Energy Build.* 128, 198–213.  
1611 doi:10.1016/j.enbuild.2016.06.089
- 1612 Chanchangi, Yusuf N, Ghosh, A., Sundaram, S., Mallick, T.K., 2020. An analytical indoor  
1613 experimental study on the effect of soiling on PV, focusing on dust properties and PV surface  
1614 material. *Sol. Energy* 203, 46–68. doi:10.1016/j.solener.2020.03.089
- 1615 Chanchangi, Yusuf N., Ghosh, A., Sundaram, S., Mallick, T.K., 2020. Dust and PV Performance in  
1616 Nigeria: A review. *Renew. Sustain. Energy Rev.* 121, 109704. doi:10.1016/j.rser.2020.109704
- 1617 Chandra Mouli, G.R., Bauer, P., Zeman, M., 2016. System design for a solar powered electric vehicle  
1618 charging station for workplaces. *Appl. Energy* 168, 434–443.  
1619 doi:10.1016/j.apenergy.2016.01.110
- 1620 Chandra Mouli, G.R., Schijffelen, J., Van Den Heuvel, M., Kardolus, M., Bauer, P., 2019. A 10 kW  
1621 Solar-Powered Bidirectional EV Charger Compatible with Chademo and COMBO. *IEEE Trans.*  
1622 *Power Electron.* 34, 1082–1098. doi:10.1109/TPEL.2018.2829211
- 1623 Chandra, S., Doran, J., McCormack, S.J., Kennedy, M., Chatten, A.J., 2012. Enhanced quantum dot  
1624 emission for luminescent solar concentrators using plasmonic interaction. *Sol. Energy Mater.*  
1625 *Sol. Cells* 98, 385–390. doi:10.1016/j.solmat.2011.11.030
- 1626 Chandra, S., McCormack, S.J., Kennedy, M., Doran, J., 2015. Quantum dot solar concentrator:  
1627 Optical transportation and doping concentration optimization. *Sol. Energy* 115, 552–561.  
1628 doi:10.1016/j.solener.2015.01.048
- 1629 Chandrasekar, M., Rajkumar, S., Valavan, D., 2015. A review on the thermal regulation techniques  
1630 for non integrated flat PV modules mounted on building top. *Energy Build.* 86, 692–697.  
1631 doi:10.1016/j.enbuild.2014.10.071
- 1632 Chatzipanagi, A., Frontini, F., Virtuani, A., 2016. BIPV-temp: A demonstrative Building Integrated  
1633 Photovoltaic installation. *Appl. Energy* 173, 1–12. doi:10.1016/j.apenergy.2016.03.097
- 1634 Chau, J.L.H., Chen, R.T., Hwang, G.L., Tsai, P.Y., Lin, C.C., 2010. Transparent solar cell window  
1635 module. *Sol. Energy Mater. Sol. Cells* 94, 588–591. doi:10.1016/j.solmat.2009.12.003
- 1636 Chemisana, D., 2011. Building integrated concentrating photovoltaics: A review. *Renew. Sustain.*  
1637 *Energy Rev.* 15, 603–611. doi:10.1016/j.rser.2010.07.017
- 1638 Chemisana, D., Collados, M.V., Quintanilla, M., Atencia, J., 2013. Holographic lenses for building  
1639 integrated concentrating photovoltaics. *Appl. Energy* 110, 227–235.  
1640 doi:10.1016/j.apenergy.2013.04.049
- 1641 Chemisana, D., Moreno, A., Polo, M., Aranda, C., Riverola, A., Ortega, E., Lamnatou, C., Domènech,  
1642 A., Blanco, G., Cot, A., 2019. Performance and stability of semitransparent OPVs for building  
1643 integration: A benchmarking analysis. *Renew. Energy* 137, 177–188.  
1644 doi:10.1016/j.renene.2018.03.073
- 1645 Chen, K.S., Salinas, J.F., Yip, H.L., Huo, L., Hou, J., Jen, A.K.Y., 2012. Semi-transparent polymer

- 1646 solar cells with 6% PCE, 25% average visible transmittance and a color rendering index close to  
 1647 100 for power generating window applications. *Energy Environ. Sci.* 5, 9551–9557.  
 1648 doi:10.1039/c2ee22623e
- 1649 Chong, K.K., Lau, S.L., Yew, T.K., Tan, P.C.L., 2013. Design and development in optics of  
 1650 concentrator photovoltaic system. *Renew. Sustain. Energy Rev.* 19, 598–612.  
 1651 doi:10.1016/j.rser.2012.11.005
- 1652 Chow, T.T., 2010. A review on photovoltaic/thermal hybrid solar technology. *Appl. Energy* 87, 365–  
 1653 379. doi:10.1016/j.apenergy.2009.06.037
- 1654 Chow, T.T., Chan, A.L.S., Fong, K.F., Lin, Z., He, W., Ji, J., 2009. Annual performance of building-  
 1655 integrated photovoltaic/water-heating system for warm climate application. *Appl. Energy* 86,  
 1656 689–696. doi:10.1016/j.apenergy.2008.09.014
- 1657 Chow, T.T., Fong, K.F., He, W., Lin, Z., Chan, A.L.S., 2007. Performance evaluation of a PV  
 1658 ventilated window applying to office building of Hong Kong. *Energy Build.* 39, 643–650.  
 1659 doi:10.1016/j.enbuild.2006.09.014
- 1660 Chowdhury, M.S., Rahman, K.S., Chowdhury, T., Nuthammachot, N., Techato, K., Akhtaruzzaman,  
 1661 M., Tiong, S.K., Sopian, K., Amin, N., 2020. An overview of solar photovoltaic panels' end-of-  
 1662 life material recycling. *Energy Strateg. Rev.* 27, 100431. doi:10.1016/j.esr.2019.100431
- 1663 Clark, R., Zucker, N., Urpelainen, J., 2020. The future of coal-fired power generation in Southeast  
 1664 Asia. *Renew. Sustain. Energy Rev.* 121, 109650. doi:10.1016/j.rser.2019.109650
- 1665 Codani, P., Portez, P.-L. Le, Claverie, P., Petit, M., Perez, Y., 2016. Coupling local renewable energy  
 1666 production with electric vehicle charging: a survey of the French case. *Int. J. Automat. Technol.*  
 1667 *Manag.* 16, 55–69. doi:https://dx.doi.org/10.1504/IJATM.2016.076443
- 1668 Collados, M.V., Chemisana, D., Atencia, J., 2016. Holographic solar energy systems: The role of  
 1669 optical elements. *Renew. Sustain. Energy Rev.* 59, 130–140. doi:10.1016/j.rser.2015.12.260
- 1670 Cornaro, C., Renzi, L., Pierro, M., Di Carlo, A., Guglielmotti, A., 2018. Thermal and electrical  
 1671 characterization of a semi-transparent dye-sensitized photovoltaic module under real operating  
 1672 conditions. *Energies* 11. doi:10.3390/en11010155
- 1673 Cronemberger, J., Corpas, M.A., Cer??n, I., Caama??o-Mart??n, E., S??nchez, S.V., 2014. BIPV  
 1674 technology application: Highlighting advances, tendencies and solutions through Solar  
 1675 Decathlon Europe houses. *Energy Build.* 83, 44–56. doi:10.1016/j.enbuild.2014.03.079
- 1676 Cucchiella, F., D'Adamo, I., Gastaldi, M., Koh, S.C.L., 2012. Renewable energy options for  
 1677 buildings: Performance evaluations of integrated photovoltaic systems. *Energy Build.* 55, 208–  
 1678 217. doi:10.1016/j.enbuild.2012.08.029
- 1679 Cuce, E., Riffat, S.B., Young, C.H., 2015a. Thermal insulation, power generation, lighting and energy  
 1680 saving performance of heat insulation solar glass as a curtain wall application in Taiwan: A  
 1681 comparative experimental study. *Energy Convers. Manag.* 96, 31–38.  
 1682 doi:10.1016/j.enconman.2015.02.062
- 1683 Cuce, E., Young, C.-H., Riffat, S.B., 2015b. Thermal performance investigation of heat insulation  
 1684 solar glass: A comparative experimental study. *Energy Build.* 86, 595–600.  
 1685 doi:10.1016/j.enbuild.2014.10.063
- 1686 Ćurpek, J., Ćekon, M., 2020. Climate response of a BiPV façade system enhanced with latent PCM-  
 1687 based thermal energy storage. *Renew. Energy* 152, 368–384. doi:10.1016/j.renene.2020.01.070
- 1688 Curpek, J., Cekon, M., Hraska, J., 2019. PCM Integrated in BiPV Ventilated Façade Concepts:

- 1689 Experimental Test Cell Platform and Initial Full-Scale Measurements. IOP Conf. Ser. Earth  
1690 Environ. Sci. 290. doi:10.1088/1755-1315/290/1/012072
- 1691 Darling, S.B., You, F., 2013. The case for organic photovoltaics. RSC Adv. 3, 17633–17648.  
1692 doi:10.1039/c3ra42989j
- 1693 Das, H.S., Rahman, M.M., Li, S., Tan, C.W., 2020. Electric vehicles standards, charging  
1694 infrastructure, and impact on grid integration: A technological review. Renew. Sustain. Energy  
1695 Rev. 120. doi:10.1016/j.rser.2019.109618
- 1696 Das, S.K., Verma, D., Nema, S., Nema, R.K., 2017. Shading mitigation techniques: State-of-the-art in  
1697 photovoltaic applications. Renew. Sustain. Energy Rev. 78, 369–390.  
1698 doi:10.1016/j.rser.2017.04.093
- 1699 Davidsson, H., Perers, B., Karlsson, B., 2012. System analysis of a multifunctional PV/T hybrid solar  
1700 window. Sol. Energy 86, 903–910. doi:10.1016/j.solener.2011.12.020
- 1701 Day, J., Senthilarasu, S., Mallick, T.K., 2019. Enhanced efficiency for building integrated  
1702 concentrator photovoltaic modules based on rare earth doped optics. Sol. Energy Mater. Sol.  
1703 Cells 199, 83–90. doi:10.1016/j.solmat.2019.04.013
- 1704 Deb, S.K., Lee, S.H., Edwin Tracy, C., Roland Pitts, J., Gregg, B.A., Branz, H.M., 2001. Stand-alone  
1705 photovoltaic-powered electrochromic smart window. Electrochim. Acta 46, 2125–2130.  
1706 doi:10.1016/S0013-4686(01)00390-5
- 1707 Debbarma, M., Sudhakar, K., Baredar, P., 2016. Comparison of BIPV and BIPVT: A review. Resour.  
1708 Technol. 3, 263–271. doi:10.1016/j.refit.2016.11.013
- 1709 Debije, M., 2015. Better luminescent solar panels in prospect “ A Spotlight on deep-brain stimulation.  
1710 Nature 519, 298.
- 1711 Delgado-Sanchez, J.-M., Sanchez-Cortezon, E., Lopez-Lopez, C., Aninat, R., Alba, M.D., 2017.  
1712 Failure mode and effect analysis of a large scale thin-film CIGS photovoltaic module. Eng. Fail.  
1713 Anal. 76, 55–60. doi:10.1016/j.engfailanal.2017.02.004
- 1714 Della Gaspera, E., Peng, Y., Hou, Q., Spiccia, L., Bach, U., Jasieniak, J.J., Cheng, Y.B., 2015. Ultra-  
1715 thin high efficiency semitransparent perovskite solar cells. Nano Energy 13, 249–257.  
1716 doi:10.1016/j.nanoen.2015.02.028
- 1717 Dhere, N.G., 2011. Scale-up issues of CIGS thin film PV modules. Sol. Energy Mater. Sol. Cells 95,  
1718 277–280. doi:10.1016/j.solmat.2010.02.019
- 1719 Dixit, M.K., Yan, W., 2012. BIPV prototype for the solar insolation calculation. 2012 Proc. 29th Int.  
1720 Symp. Autom. Robot. Constr. ISARC 2012 2–5. doi:10.4017/gt.2012.11.02.539.716
- 1721 Dobson, K.D., Visoly-Fisher, I., Hodes, G., Cahen, D., 2000. Stability of CdTe/CdS thin-film solar  
1722 cells. Sol. Energy Mater. Sol. Cells 62, 295–325. doi:10.1016/S0927-0248(00)00014-3
- 1723 Duan, L., Yi, H., 2019. Sustainable Energy & Fuels Semitransparent organic solar cells based on P ff  
1724 BT4T-2OD with a thick active layer and near neutral colour perception for window applications  
1725 † 0–7. doi:10.1039/c9se00413k
- 1726 Duan, L., Yi, H., Wang, Z., Zhang, Y., Haque, F., Sang, B., Deng, R., Uddin, A., 2019.  
1727 Semitransparent organic solar cells based on PffBT4T-2OD with a thick active layer and near  
1728 neutral colour perception for window applications. Sustain. Energy Fuels 0–7.  
1729 doi:10.1039/C9SE00413K
- 1730 Dupré, O., Vaillon, R., Green, M.A., 2015. Physics of the temperature coefficients of solar cells. Sol.

- 1731 Energy Mater. Sol. Cells 140, 92–100. doi:10.1016/j.solmat.2015.03.025
- 1732 Eder, G., Peharz, G., Trattinig, R., Bonomo, P., Saretta, E., Frontini, F., Polo López, C.S., Rose  
1733 Wilson, H., Eisenlohr, J., Martin Chivelet, N., Karlsson, S., Jakica, N., Zanelli Politecnico di  
1734 Milano, A., 2019. Coloured BIPV-Market, Research and Development 60.
- 1735 Eiffert, P., 2003. Guidelines for the Economic Evaluation of Building Integrated Photovoltaic Power  
1736 Systems 1–52. doi:https://www.nrel.gov/docs/fy03osti/31977.pdf
- 1737 Eke, R., Betts, T.R., Gottschalg, R., 2017. Spectral irradiance effects on the outdoor performance of  
1738 photovoltaic modules. *Renew. Sustain. Energy Rev.* 69, 429–434.  
1739 doi:10.1016/j.rser.2016.10.062
- 1740 Elavarasan, R.M., Ghosh, A., Mallick, T.K., Krishnamurthy, A., Saravanan, M., 2019. Investigations  
1741 on performance enhancement measures of the bidirectional converter in PV–wind  
1742 interconnected microgrid system. *Energies* 12. doi:10.3390/en12142672
- 1743 Eltawil, M.A., Zhao, Z., 2010. Grid-connected photovoltaic power systems: Technical and potential  
1744 problems-A review. *Renew. Sustain. Energy Rev.* 14, 112–129. doi:10.1016/j.rser.2009.07.015
- 1745 Elumalai, N.K., Uddin, A., 2016. Open circuit voltage of organic solar cells: An in-depth review.  
1746 *Energy Environ. Sci.* 9, 391–410. doi:10.1039/c5ee02871j
- 1747 Enríquez, J., Mathew, X., 2003. Influence of the thickness on structural, optical and electrical  
1748 properties of chemical bath deposited CdS thin films. *Sol. Energy Mater. Sol. Cells* 76, 313–322.  
1749 doi:10.1016/S0927-0248(02)00283-0
- 1750 Esfandyari, A., Norton, B., Conlon, M., McCormack, S.J., 2019. Performance of a campus  
1751 photovoltaic electric vehicle charging station in a temperate climate. *Sol. Energy* 177, 762–771.  
1752 doi:10.1016/j.solener.2018.12.005
- 1753 Espinosa, N., García-Valverde, R., Urbina, A., Krebs, F.C., 2011. A life cycle analysis of polymer  
1754 solar cell modules prepared using roll-to-roll methods under ambient conditions. *Sol. Energy  
1755 Mater. Sol. Cells* 95, 1293–1302. doi:10.1016/j.solmat.2010.08.020
- 1756 Evola, G., Margani, G., 2016. Renovation of apartment blocks with BIPV: Energy and economic  
1757 evaluation in temperate climate. *Energy Build.* 130, 794–810. doi:10.1016/j.enbuild.2016.08.085
- 1758 Fang, Y., Hyde, T.J., Arya, F., Hewitt, N., Eames, P.C., Norton, B., Miller, S., 2014. Indium alloy-  
1759 sealed vacuum glazing development and context. *Renew. Sustain. Energy Rev.* 37, 480–501.  
1760 doi:10.1016/j.rser.2014.05.029
- 1761 Farhana, K., Kadirgama, K., Rahman, M.M., Ramasamy, D., Noor, M.M., Najafi, G., Samykano, M.,  
1762 Mahamude, A.S.F., 2019. Improvement in the performance of solar collectors with nanofluids  
1763 — A state-of-the-art review. *Nano-Structures and Nano-Objects* 18.  
1764 doi:10.1016/j.nanoso.2019.100276
- 1765 Fathi, M., Abderrezek, M., Djahli, F., 2017. Experimentations on luminescent glazing for solar  
1766 electricity generation in buildings. *Opt. - Int. J. Light Electron Opt.* 148, 14–27.  
1767 doi:10.1016/j.ijleo.2017.08.127
- 1768 Fattori, F., Anglani, N., Muliere, G., 2014. Combining photovoltaic energy with electric vehicles,  
1769 smart charging and vehicle-to-grid. *Sol. Energy* 110, 438–451.  
1770 doi:10.1016/j.solener.2014.09.034
- 1771 Ferrara, C., Wilson, H.R., Sprenger, W., 2017. The Performance of Photovoltaic (PV) Systems, 8 -  
1772 Building-integrated photovoltaics (BIPV).

- 1773 Feurer, T., Reinhard, P., Avancini, E., Bissig, B., Löckinger, J., Fuchs, P., Carron, R., Weiss, T.P.,  
 1774 Perrenoud, J., Stutterheim, S., Buecheler, S., Tiwari, A.N., 2017. Progress in thin film CIGS  
 1775 photovoltaics – Research and development, manufacturing, and applications. Prog.  
 1776 Photovoltaics Res. Appl. 25, 645–667. doi:10.1002/pip.2811
- 1777 Figgis, B., Ennaoui, A., Ahzi, S., Rémond, Y., 2017. Review of PV soiling particle mechanics in  
 1778 desert environments. Renew. Sustain. Energy Rev. 76, 872–881. doi:10.1016/j.rser.2017.03.100
- 1779 Fillion, R.M., Riahi, A.R., Edrisy, A., 2014. A review of icing prevention in photovoltaic devices by  
 1780 surface engineering. Renew. Sustain. Energy Rev. 32, 797–809. doi:10.1016/j.rser.2014.01.015
- 1781 Fossa, M., Ménézo, C., Leonardi, E., 2008. Experimental natural convection on vertical surfaces for  
 1782 building integrated photovoltaic (BIPV) applications. Exp. Therm. Fluid Sci. 32, 980–990.  
 1783 doi:10.1016/j.expthermflusci.2007.11.004
- 1784 Foster, S., Muhammad-Sukki, F., Ramirez-Iniguez, R., Freier, D., Deciga-Gusi, J., Abu-Bakar, S.H.,  
 1785 Bani, N.A., Munir, A.B., Abubakar Mas'Ud, A., Ardila-Rey, J.A., 2020. Annual Energy Output  
 1786 Simulation of an Optical Concentrator Based PV System for Energy Security. IOP Conf. Ser.  
 1787 Mater. Sci. Eng. 736. doi:10.1088/1757-899X/736/3/032018
- 1788 Friman Peretz, M., Geoola, F., Yehia, I., Ozer, S., Levi, A., Magadley, E., Brikman, R., Rosenfeld, L.,  
 1789 Levy, A., Kacira, M., Teitel, M., 2019. Testing organic photovoltaic modules for application as  
 1790 greenhouse cover or shading element. Biosyst. Eng. 184, 24–36.  
 1791 doi:10.1016/j.biosystemseng.2019.05.003
- 1792 Fthenakis, V.M., 2004. Life cycle impact analysis of cadmium in CdTe PV production, Renewable  
 1793 and Sustainable Energy Reviews. doi:10.1016/j.rser.2003.12.001
- 1794 Fu, R., James, T.L., Woodhouse, M., 2015. Economic measurements of polysilicon for the  
 1795 photovoltaic industry: Market competition and manufacturing competitiveness. IEEE J.  
 1796 Photovoltaics 5, 515–524. doi:10.1109/JPHOTOV.2014.2388076
- 1797 Fung, T.Y.Y., Yang, H., 2008. Study on thermal performance of semi-transparent building-integrated  
 1798 photovoltaic glazings. Energy Build. 40, 341–350. doi:10.1016/j.enbuild.2007.03.002
- 1799 Future, Ma.R., 2018. Concentrated Photovoltaic (CPV) Market Research Report – Forecast to 2023.  
 1800 doi:https://www.marketresearchfuture.com/reports/concentrated-photovoltaic-market-5946
- 1801 Gao, H., Koch, C., Wu, Y., 2019. Building information modelling based building energy modelling:  
 1802 A review. Appl. Energy 238, 320–343. doi:10.1016/j.apenergy.2019.01.032
- 1803 Gao, W., Liu, P., Crandall, R.S., Lee, S.-H., Benson, D.K., Branz, H.M., 2000. Approaches for large-  
 1804 area a-SiC:H photovoltaic-powered electrochromic window coatings. J. Non. Cryst. Solids 266–  
 1805 269, 1140–1144. doi:10.1016/S0022-3093(99)00918-7
- 1806 García Kerdan, I., Raslan, R., Ruyssevelt, P., Morillón Gálvez, D., 2016. An exergoeconomic-based  
 1807 parametric study to examine the effects of active and passive energy retrofit strategies for  
 1808 buildings. Energy Build. 133, 155–171. doi:10.1016/j.enbuild.2016.09.029
- 1809 Garg, H.P., Adhikari, R.S., 1999. System Performance Studies on a Photovoltaic/thermal (PV/T) air  
 1810 heating collector. Renew. Energy 16, 725–730.
- 1811 Gasimli, O., ul Haq, I., Gamage, S.K.N., Shihadeh, F., Rajapakshe, P.S.K., Shafiq, M., 2019. Energy,  
 1812 Trade, Urbanization and Environmental Degradation Nexus in Sri Lanka: Bounds Testing  
 1813 Approach. Energies 12, 1–16. doi:10.3390/en12091655
- 1814 Ghadiri, M., Sardarabadi, M., Pasandideh-Fard, M., Moghadam, A.J., 2015. Experimental  
 1815 investigation of a PVT system performance using nano ferrofluids. Energy Convers. Manag.

- 1816 103, 468–476. doi:10.1016/j.enconman.2015.06.077
- 1817 Ghani, F., Duke, M., Carson, J.K., 2012. Effect of flow distribution on the photovoltaic performance  
1818 of a building integrated photovoltaic/thermal (BIPV/T) collector. *Sol. Energy* 86, 1518–1530.  
1819 doi:10.1016/j.solener.2012.02.013
- 1820 Ghazi, S., Ip, K., Sayigh, A., 2013. Preliminary study of environmental solid particles on solar flat  
1821 surfaces in the UK. *Energy Procedia* 42, 765–774. doi:10.1016/j.egypro.2013.11.080
- 1822 Ghazi, S., Sayigh, A., Ip, K., 2014. Dust effect on flat surfaces - A review paper. *Renew. Sustain.*  
1823 *Energy Rev.* 33, 742–751. doi:10.1016/j.rser.2014.02.016
- 1824 Ghosh, A., 2020a. Soiling Losses : A Barrier for India ' s Energy Security Dependency from  
1825 Photovoltaic Power. *Challenges* 11, 1–9. doi:10.3390/challe11010009
- 1826 Ghosh, A., 2020b. Possibilities and Challenges for the Inclusion of the Electric Vehicle ( EV ) to  
1827 Reduce the Carbon Footprint in the Transport Sector : A Review. *Energies* 13, 2602.
- 1828 Ghosh, A., Bhandari, S., Sundaram, S., Mallick, T.K., 2020. Carbon counter electrode mesoscopic  
1829 ambient processed & characterised perovskite for adaptive BIPV fenestration. *Renew.*  
1830 *Energy* 145, 2151–2158. doi:10.1016/j.renene.2019.07.119
- 1831 Ghosh, A., Mallick, T.K., 2018. Evaluation of colour properties due to switching behaviour of a  
1832 PDLC glazing for adaptive building integration. *Renew. Energy* 120, 126–133.  
1833 doi:10.1016/j.renene.2017.12.094
- 1834 Ghosh, A., Mallick, T.K., 2017. Evaluation of optical properties and protection factors of a PDLC  
1835 switchable glazing for low energy building integration. *Sol. Energy Mater. Sol. Cells* 0–1.  
1836 doi:10.1016/j.solmat.2017.10.026
- 1837 Ghosh, Abhijit, Nirala, A.K., Yadav, H.L., 2018. Optical design and characterization of holographic  
1838 solar concentrators for photovoltaic applications. *Optik (Stuttg)*. 168, 625–649.  
1839 doi:10.1016/j.ijleo.2018.04.060
- 1840 Ghosh, Abhijit, Nirala, A.K., Yadav, H.L., 2015. Dependence of wavelength selectivity of  
1841 holographic PV concentrator on processing parameters. *Optik (Stuttg)*. 126, 622–625.  
1842 doi:10.1016/j.ijleo.2015.01.014
- 1843 Ghosh, A., Norton, B., 2019. Optimization of PV powered SPD switchable glazing to minimise  
1844 probability of loss of power supply. *Renew. Energy* 131, 993–1001.  
1845 doi:10.1016/j.renene.2018.07.115
- 1846 Ghosh, A., Norton, B., 2018. Advances in switchable and highly insulating autonomous (self-  
1847 powered) glazing systems for adaptive low energy buildings. *Renew. Energy* 126, 1003–1031.  
1848 doi:10.1016/j.renene.2018.04.038
- 1849 Ghosh, A., Norton, B., 2017a. Interior colour rendering of daylight transmitted through a suspended  
1850 particle device switchable glazing. *Sol. Energy Mater. Sol. Cells* 163, 218–223.  
1851 doi:10.1016/j.solmat.2017.01.041
- 1852 Ghosh, A., Norton, B., 2017b. Durability of switching behaviour after outdoor exposure for a  
1853 suspended particle device switchable glazing. *Sol. Energy Mater. Sol. Cells* 163, 178–184.  
1854 doi:10.1016/j.solmat.2017.01.036
- 1855 Ghosh, A., Norton, B., Duffy, A., 2017a. Effect of sky conditions on light transmission through a  
1856 suspended particle device switchable glazing. *Sol. Energy Mater. Sol. Cells* 160, 134–140.  
1857 doi:10.1016/j.solmat.2016.09.049

- 1858 Ghosh, A., Norton, B., Duffy, A., 2017b. Effect of atmospheric transmittance on performance of  
1859 adaptive SPD-vacuum switchable glazing. *Sol. Energy Mater. Sol. Cells* 161, 424–431.  
1860 doi:10.1016/j.solmat.2016.12.022
- 1861 Ghosh, A., Norton, B., Duffy, A., 2017c. Effect of sky clearness index on transmission of evacuated  
1862 (vacuum) glazing. *Renew. Energy* 105, 160–166. doi:10.1016/j.renene.2016.12.056
- 1863 Ghosh, A., Norton, B., Duffy, A., 2016a. Behaviour of a SPD switchable glazing in an outdoor test  
1864 cell with heat removal under varying weather conditions. *Appl. Energy* 180, 695–706.  
1865 doi:10.1016/j.apenergy.2016.08.029
- 1866 Ghosh, A., Norton, B., Duffy, A., 2016b. First outdoor characterisation of a PV powered suspended  
1867 particle device switchable glazing. *Sol. Energy Mater. Sol. Cells* 157, 1–9.  
1868 doi:10.1016/j.solmat.2016.05.013
- 1869 Ghosh, A., Norton, B., Duffy, A., 2016c. Daylighting performance and glare calculation of a  
1870 suspended particle device switchable glazing. *Sol. Energy* 132, 114–128.  
1871 doi:10.1016/j.solener.2016.02.051
- 1872 Ghosh, A., Norton, B., Duffy, A., 2016d. Measured thermal & daylight performance of an evacuated  
1873 glazing using an outdoor test cell. *Appl. Energy* 177, 196–203.  
1874 doi:10.1016/j.apenergy.2016.05.118
- 1875 Ghosh, A., Norton, B., Duffy, A., 2016e. Measured thermal performance of a combined suspended  
1876 particle switchable device evacuated glazing. *Appl. Energy* 169, 469–480.  
1877 doi:10.1016/j.apenergy.2016.02.031
- 1878 Ghosh, Aritra, Norton, B., Duffy, A., 2015. Measured overall heat transfer coefficient of a suspended  
1879 particle device switchable glazing. *Appl. Energy* 159, 362–369.  
1880 doi:10.1016/j.apenergy.2015.09.019
- 1881 Ghosh, Aritra, Norton, B., Mallick, T.K., 2018a. Influence of atmospheric clearness on PDLC  
1882 switchable glazing transmission. *Energy Build.* 172, 257–264.  
1883 doi:10.1016/j.enbuild.2018.05.008
- 1884 Ghosh, Aritra, Norton, B., Mallick, T.K., 2018b. Daylight characteristics of a polymer dispersed  
1885 liquid crystal switchable glazing. *Sol. Energy Mater. Sol. Cells* 174, 572–576.  
1886 doi:10.1016/j.solmat.2017.09.047
- 1887 Ghosh, A., Sarmah, N., Sundaram, S., Mallick, T.K., 2019a. Numerical studies of thermal comfort for  
1888 semi-transparent building integrated photovoltaic ( BIPV ) -vacuum glazing system. *Sol. Energy*  
1889 190, 608–616. doi:10.1016/j.solener.2019.08.049
- 1890 Ghosh, Aritra, Selvaraj, P., Sundaram, S., Mallick, T.K., 2018c. The colour rendering index and  
1891 correlated colour temperature of dye-sensitized solar cell for adaptive glazing application. *Sol.*  
1892 *Energy* 163, 537–544. doi:10.1016/j.solener.2018.02.021
- 1893 Ghosh, A., Sundaram, S., Mallick, T.K., 2019b. Colour properties and glazing factors evaluation of  
1894 multicrystalline based semi-transparent Photovoltaic-vacuum glazing for BIPV application.  
1895 *Renew. Energy* 131, 730–736. doi:10.1016/j.renene.2018.07.088
- 1896 Ghosh, Aritra, Sundaram, S., Mallick, T.K., 2018d. Investigation of thermal and electrical  
1897 performances of a combined semi-transparent PV-vacuum glazing. *Appl. Energy* 228, 1591–  
1898 1600. doi:10.1016/j.apenergy.2018.07.040
- 1899 Ghotge, R., Snow, Y., Farahani, S., Lukszo, Z., van Wijk, A., 2020. Optimized scheduling of EV  
1900 charging in solar parking lots for local peak reduction under EV demand uncertainty. *Energies*  
1901 13. doi:10.3390/en13051275

- 1902 Gil-Lopez, T., Gimenez-Molina, C., 2013a. Influence of double glazing with a circulating water  
1903 chamber on the thermal energy savings in buildings. *Energy Build.* 56, 56–65.  
1904 doi:10.1016/j.enbuild.2012.10.008
- 1905 Gil-Lopez, T., Gimenez-Molina, C., 2013b. Environmental, economic and energy analysis of double  
1906 glazing with a circulating water chamber in residential buildings. *Appl. Energy* 101, 572–581.  
1907 doi:10.1016/j.apenergy.2012.06.055
- 1908 Glunz, S.W., Preu, R., Biro, D., 2012. Crystalline silicon solar cells. State-of-the-art and future  
1909 developments, *Comprehensive Renewable Energy*. Elsevier Ltd. doi:10.1016/B978-0-08-  
1910 087872-0.00117-7
- 1911 Gong, J., Darling, S.B., You, F., 2015. Perovskite photovoltaics: Life-cycle assessment of energy and  
1912 environmental impacts. *Energy Environ. Sci.* 8, 1953–1968. doi:10.1039/c5ee00615e
- 1913 Gong, J., Liang, J., Sumathy, K., 2012. Review on dye-sensitized solar cells (DSSCs): Fundamental  
1914 concepts and novel materials. *Renew. Sustain. Energy Rev.* 16, 5848–5860.  
1915 doi:10.1016/j.rser.2012.04.044
- 1916 Gong, J., Sumathy, K., Qiao, Q., Zhou, Z., 2017. Review on dye-sensitized solar cells (DSSCs):  
1917 Advanced techniques and research trends. *Renew. Sustain. Energy Rev.* 68, 234–246.  
1918 doi:10.1016/j.rser.2016.09.097
- 1919 Goossens, D., Offer, Z.Y., Zangvil, A., 1993. Wind tunnel experiments and field investigations of  
1920 eolian dust deposition on photovoltaic solar collectors. *Sol. Energy* 50, 75–84.  
1921 doi:10.1016/0038-092X(93)90009-D
- 1922 Gorgolis, G., Karamanis, D., 2016. Solar energy materials for glazing technologies. *Sol. Energy*  
1923 *Mater. Sol. Cells* 144, 559–578. doi:10.1016/j.solmat.2015.09.040
- 1924 Gossen, K., Ehrmann, A., 2019. Optik Influence of FTO glass cleaning on DSSC performance 183,  
1925 253–256. doi:10.1016/j.ijleo.2019.02.041
- 1926 Graabak, I., Wu, Q., Warland, L., Liu, Z., 2016. Optimal planning of the Nordic transmission system  
1927 with 100% electric vehicle penetration of passenger cars by 2050. *Energy* 107, 648–660.  
1928 doi:10.1016/j.energy.2016.04.060
- 1929 Granqvist, C.G., Bayrak Pehlivan, I., Niklasson, G.A., 2017. Electrochromics on a roll: Web-coating  
1930 and lamination for smart windows. *Surf. Coatings Technol.* 6–11.  
1931 doi:10.1016/j.surfcoat.2017.08.006
- 1932 Grätzel, M., 2003. Dye-sensitized solar cells. *J. Photochem. Photobiol. C Photochem. Rev.* 4, 145–  
1933 153. doi:10.1016/S1389-5567(03)00026-1
- 1934 Green, M.A., Hishikawa, Y., Dunlop, E.D., Levi, D.H., Hohl-Ebinger, J., Yoshita, M., Ho-Baillie,  
1935 A.W.Y., 2019. Solar cell efficiency tables (Version 53). *Prog. Photovoltaics Res. Appl.* 27, 3–  
1936 12. doi:10.1002/pip.3102
- 1937 Greijer, H., Karlson, L., Lindquist, S.E., Hagfeldt, A., 2001. Environmental aspects of electricity  
1938 generation from a nanocrystalline dye sensitized solar cell system. *Renew. energy* 23, 27–39.  
1939 doi:10.1016/S0960-1481(00)00111-7
- 1940 Guess, M., 2018. Five solar roof shingles that aren't from Tesla. *ars Tech.*  
1941 doi:https://arstechnica.com/science/2018/10/five-solar-roof-shingles-that-arent-from-tesla/
- 1942 Gullbrekken, L., Kvande, T., Time, B., 2015. Roof-integrated PV in Nordic climate - Building  
1943 physical challenges. *Energy Procedia* 78, 1962–1967. doi:10.1016/j.egypro.2015.11.382



- 1944 Gunde, M.K., Krašovec, U.O., Platzer, W.J., 2005. Color rendering properties of interior lighting  
1945 influenced by a switchable window. *J. Opt. Soc. Am. A* 22, 416. doi:10.1364/JOSAA.22.000416
- 1946 Gupta, A., Cemesova, A., Hopfe, C.J., Rezgui, Y., Sweet, T., 2014. A conceptual framework to  
1947 support solar PV simulation using an open-BIM data exchange standard. *Autom. Constr.* 37,  
1948 166–181. doi:10.1016/j.autcon.2013.10.005
- 1949 Hachana, O., Tina, G.M., Hemsas, K.E., 2016. PV array fault Diagnostic Technique for BIPV systems.  
1950 *Energy Build.* 126, 263–274. doi:10.1016/j.enbuild.2016.05.031
- 1951 Haegel, N.M., Atwater, H., Barnes, T., Breyer, C., Burrell, A., Chiang, Y.-M., De Wolf, S., Dimmler,  
1952 B., Feldman, D., Glunz, S., Goldschmidt, J.C., Hochschild, D., Inzunza, R., Kaizuka, I.,  
1953 Kroposki, B., Kurtz, S., Leu, S., Margolis, R., Matsubara, K., Metz, A., Metzger, W.K.,  
1954 Morjaria, M., Niki, S., Nowak, S., Peters, I.M., Philipps, S., Reindl, T., Richter, A., Rose, D.,  
1955 Sakurai, K., Schlatmann, R., Shikano, M., Sinke, W., Sinton, R., Stanbery, B.J., Topic, M.,  
1956 Tumas, W., Ueda, Y., van de Lagemaat, J., Verlinden, P., Vetter, M., Warren, E., Werner, M.,  
1957 Yamaguchi, M., Bett, A.W., 2019. Terawatt-scale photovoltaics: Transform global energy.  
1958 *Science* (80-. ). 364, 836–838. doi:10.1126/science.aaw1845
- 1959 Hagemann, I., 1996. PV in buildings- the influence of PV on the design and planning process of a  
1960 building, in: *World Renewable Energy Congress*. Aachen, Germany, pp. 467–470.
- 1961 Hammond, G.P., Harajli, H.A., Jones, C.I., Winnett, A.B., 2012. Whole systems appraisal of a UK  
1962 Building Integrated Photovoltaic (BIPV) system: Energy, environmental, and economic  
1963 evaluations. *Energy Policy* 40, 219–230. doi:10.1016/j.enpol.2011.09.048
- 1964 Han, J., Lu, L., Yang, H., 2009. Thermal behavior of a novel type see-through glazing system with  
1965 integrated PV cells. *Build. Environ.* 44, 2129–2136. doi:10.1016/j.buildenv.2009.03.003
- 1966 Hanaei, H., Assadi, M.K., Saidur, R., 2016. Highly efficient antireflective and self-cleaning coatings  
1967 that incorporate carbon nanotubes (CNTs) into solar cells: A review. *Renew. Sustain. Energy*  
1968 *Rev.* 59, 620–635. doi:10.1016/j.rser.2016.01.017
- 1969 Hasan, A., McCormack, S.J., Huang, M.J., Norton, B., 2014. Energy and cost saving of a  
1970 photovoltaic-phase change materials (PV-PCM) System through temperature regulation and  
1971 performance enhancement of photovoltaics. *Energies* 7, 1318–1331. doi:10.3390/en7031318
- 1972 Hasan, A., McCormack, S.J., Huang, M.J., Norton, B., 2010. Evaluation of phase change materials for  
1973 thermal regulation enhancement of building integrated photovoltaics. *Sol. Energy* 84, 1601–  
1974 1612. doi:10.1016/j.solener.2010.06.010
- 1975 Hasan, A., McCormack, S.J., Huang, M.J., Sarwar, J., Norton, B., 2015. Increased photovoltaic  
1976 performance through temperature regulation by phase change materials: Materials comparison in  
1977 different climates. *Sol. Energy* 115, 264–276. doi:10.1016/j.solener.2015.02.003
- 1978 Hasan, A., Sarwar, J., Alnoman, H., Abdelbaqi, S., 2017. Yearly energy performance of a  
1979 photovoltaic-phase change material (PV-PCM) system in hot climate. *Sol. Energy* 146, 417–  
1980 429. doi:10.1016/j.solener.2017.01.070
- 1981 Hasan, R., Mekhilef, S., Seyedmahmoudian, M., Horan, B., 2017. Grid-connected isolated PV  
1982 microinverters: A review. *Renew. Sustain. Energy Rev.* 67, 1065–1080.  
1983 doi:10.1016/j.rser.2016.09.082
- 1984 Hasanuzzaman, M., Malek, A.B.M.A., Islam, M.M., Pandey, A.K., Rahim, N.A., 2016. Global  
1985 advancement of cooling technologies for PV systems: A review. *Sol. Energy* 137, 25–45.  
1986 doi:10.1016/j.solener.2016.07.010
- 1987 He, W., Zhang, Y.X., Sun, W., Hou, J.X., Jiang, Q.Y., Ji, J., 2011. Experimental and numerical

- 1988 investigation on the performance of amorphous silicon photovoltaics window in East China.  
1989 Build. Environ. 46, 363–369. doi:10.1016/j.buildenv.2010.07.030
- 1990 Hegazy, A.A., 2001. Effect of dust accumulation on solar transmittance through glass covers of plate-  
1991 type collectors. Renew. energy 22, 525–540. doi:10.1016/S0960-1481(00)00093-8
- 1992 Hegazy, A.A., 2000. Comparative study of the performances of four photovoltaic/thermal solar air  
1993 collectors. Energy Convers. Manag. 41, 861–881. doi:10.1016/S0196-8904(99)00136-3
- 1994 Heinstejn, P., Ballif, C., Perret-Aebi, L.E., 2013. Building integrated photovoltaics (BIPV): Review,  
1995 potentials, barriers and myths. Green 3, 125–156. doi:10.1515/green-2013-0020
- 1996 Hejazi, V., Sobolev, K., Nosonovsky, M., 2013. From superhydrophobicity to icephobicity: Forces  
1997 and interaction analysis. Sci. Rep. 3. doi:10.1038/srep02194
- 1998 Hemaida, A., Ghosh, A., Sundaram, S., Mallick, T.K., 2020. Evaluation of thermal performance for a  
1999 smart switchable adaptive polymer dispersed liquid crystal ( PDLC ) glazing. Sol. Energy 195,  
2000 185–193. doi:10.1016/j.solener.2019.11.024
- 2001 Hermann, A.M., 1982. Luminescent solar concentrators-A review. Sol. Energy 29, 323–329.  
2002 doi:10.1016/0038-092X(82)90247-X
- 2003 Hernández-Andrés, J., Lee, R.L., Romero, J., 1999. Calculating correlated color temperatures across  
2004 the entire gamut of daylight and skylight chromaticities. Appl. Opt. 38, 5703–9.  
2005 doi:10.1364/AO.38.005703
- 2006 Howard, I.A., Abzieher, T., Hossain, I.M., Eggers, H., Schackmar, F., Ternes, S., Richards, B.S.,  
2007 Lemmer, U., Paetzold, U.W., 2019. Coated and Printed Perovskites for Photovoltaic  
2008 Applications. Adv. Mater. 1806702. doi:10.1002/adma.201806702
- 2009 Hu, M., Qiu, Y., 2019. A comparison of building energy codes and policies in the USA, Germany,  
2010 and China: progress toward the net-zero building goal in three countries. Clean Technol.  
2011 Environ. Policy 21, 291–305. doi:10.1007/s10098-018-1636-x
- 2012 Hu, Y., Si, S., Mei, A., Rong, Y., Liu, H., Li, X., Han, H., 2017. Stable Large-Area (10 × 10 cm<sup>2</sup>)  
2013 Printable Mesoscopic Perovskite Module Exceeding 10% Efficiency . Sol. RRL 1, 1600019.  
2014 doi:10.1002/solr.201600019
- 2015 Huang, B.J., Yang, P.E., Lin, Y.P., Lin, B.Y., Chen, H.J., Lai, R.C., Cheng, J.S., 2011. Solar cell  
2016 junction temperature measurement of PV module. Sol. Energy 85, 388–392.  
2017 doi:10.1016/j.solener.2010.11.006
- 2018 Huang, J., Chen, X., Yang, H., Zhang, W., 2018. Numerical investigation of a novel vacuum  
2019 photovoltaic curtain wall and integrated optimization of photovoltaic envelope systems. Appl.  
2020 Energy 229, 1048–1060. doi:10.1016/j.apenergy.2018.08.095
- 2021 Huang, L.M., Hu, C.W., Liu, H.C., Hsu, C.Y., Chen, C.H., Ho, K.C., 2012a. Photovoltaic  
2022 electrochromic device for solar cell module and self-powered smart glass applications. Sol.  
2023 Energy Mater. Sol. Cells 99, 154–159. doi:10.1016/j.solmat.2011.03.036
- 2024 Huang, L.M., Kung, C.P., Hu, C.W., Peng, C.Y., Liu, H.C., 2012b. Tunable photovoltaic  
2025 electrochromic device and module. Sol. Energy Mater. Sol. Cells 107, 390–395.  
2026 doi:10.1016/j.solmat.2012.07.021
- 2027 Huang, M.J., Eames, P.C., Norton, B., 2006. Phase change materials for limiting temperature rise in  
2028 building integrated photovoltaics. Sol. Energy 80, 1121–1130.  
2029 doi:10.1016/j.solener.2005.10.006

- 2030 Huang, M.J., Eames, P.C., Norton, B., 2004. Thermal regulation of building-integrated photovoltaics  
 2031 using phase change materials. *Int. J. Heat Mass Transf.* 47, 2715–2733.  
 2032 doi:10.1016/j.ijheatmasstransfer.2003.11.015
- 2033 Huang, M.J., Eames, P.C., Norton, B., Hewitt, N.J., 2011. Natural convection in an internally finned  
 2034 phase change material heat sink for the thermal management of photovoltaics. *Sol. Energy*  
 2035 *Mater. Sol. Cells* 95, 1598–1603. doi:10.1016/j.solmat.2011.01.008
- 2036 Huang, Y.C., Chan, C.C., Wang, S.J., Lee, S.K., 2014. Development of building integrated  
 2037 photovoltaic (BIPV) system with PV ceramic tile and its application for building façade. *Energy*  
 2038 *Procedia* 61, 1874–1878. doi:10.1016/j.egypro.2014.12.232
- 2039 Huang, Z., Cai, C., Kuai, L., Li, T., Huttula, M., Cao, W., 2018. Leaf-structure patterning for  
 2040 antireflective and self-cleaning surfaces on Si-based solar cells. *Sol. Energy* 159, 733–741.  
 2041 doi:10.1016/j.solener.2017.11.020
- 2042 Hull, J., Lauer, J., Broadbent, D., 1987. Holographic solar concentrators. *Energy* 12, 209–215.  
 2043 doi:10.1016/0360-5442(87)90079-X
- 2044 Igualada, L., Corchero, C., Cruz-Zambrano, M., Heredia, F.J., 2014. Optimal energy management for  
 2045 a residential microgrid including a vehicle-to-grid system. *IEEE Trans. Smart Grid* 5, 2163–  
 2046 2172. doi:10.1109/TSG.2014.2318836
- 2047 Ilse, K., Micheli, L., Figgis, B.W., Lange, K., Daßler, D., Hanifi, H., Wolfertstetter, F., Naumann, V.,  
 2048 Hagendorf, C., Gottschalg, R., Bagdahn, J., 2019. Techno-Economic Assessment of Soiling  
 2049 Losses and Mitigation Strategies for Solar Power Generation. *Joule* 2303–2321.  
 2050 doi:10.1016/j.joule.2019.08.019
- 2051 IPCC, 2014. Contribution of working group III (Chapter 9 buildings), *Climate Change 2014:*  
 2052 *Mitigation of Climate Change*. Cambridge Press, London and New York.
- 2053 Islam, M.S., Mithulananthan, N., 2018. PV based EV charging at universities using supplied historical  
 2054 PV output ramp. *Renew. Energy* 118, 306–327. doi:10.1016/j.renene.2017.11.009
- 2055 ITRPV, 2015. International Technology Roadmap for Photovoltaic ( ITRPV ) 2014 Results. *Itrpv* 1–  
 2056 38. doi:http://www.vdma.org/documents/105945/0/ITRPV%202014/7d7e1a20-fa96-447b-bd5d-  
 2057 de1ad3849c1a
- 2058 Jaaz, A.H., Hasan, H.A., Sopian, K., Haji Ruslan, M.H. Bin, Zaidi, S.H., 2017. Design and  
 2059 development of compound parabolic concentrating for photovoltaic solar collector: Review.  
 2060 *Renew. Sustain. Energy Rev.* 76, 1108–1121. doi:10.1016/j.rser.2017.03.127
- 2061 Jacobson, M.Z., Delucchi, M.A., Bauer, Z.A.F., Goodman, S.C., Chapman, W.E., Cameron, M.A.,  
 2062 Bozonnat, C., Chobadi, L., Clonts, H.A., Enevoldsen, P., Erwin, J.R., Fobi, S.N., Goldstrom,  
 2063 O.K., Hennessy, E.M., Liu, J., Lo, J., Meyer, C.B., Morris, S.B., Moy, K.R., O’Neill, P.L.,  
 2064 Petkov, I., Redfern, S., Schucker, R., Sontag, M.A., Wang, J., Weiner, E., Yachanin, A.S., 2017.  
 2065 100% Clean and Renewable Wind, Water, and Sunlight All-Sector Energy Roadmaps for 139  
 2066 Countries of the World. *Joule* 1, 108–121. doi:10.1016/j.joule.2017.07.005
- 2067 Jäger-Waldau, A., Kougias, I., Taylor, N., Thiel, C., 2020. How photovoltaics can contribute to GHG  
 2068 emission reductions of 55% in the EU by 2030. *Renew. Sustain. Energy Rev.* 126.  
 2069 doi:10.1016/j.rser.2020.109836
- 2070 Jakica, N., 2018. State-of-the-art review of solar design tools and methods for assessing daylighting  
 2071 and solar potential for building-integrated photovoltaics. *Renew. Sustain. Energy Rev.* 81, 1296–  
 2072 1328. doi:10.1016/j.rser.2017.05.080
- 2073 Jang, G.G., Smith, D.B., Polizos, G., Collins, L., Keum, J.K., Lee, D.F., 2019. *Nanoscale Advances*

- 2074 Transparent superhydrophilic and superhydrophobic nanoparticle textured coatings :  
2075 comparative study of anti-soiling performance †‡ 1249–1260. doi:10.1039/c8na00349a
- 2076 Jayathissa, P., Jansen, M., Heeren, N., Nagy, Z., Schlueter, A., 2016. Life cycle assessment of  
2077 dynamic building integrated photovoltaics. *Sol. Energy Mater. Sol. Cells* 156, 75–82.  
2078 doi:10.1016/j.solmat.2016.04.017
- 2079 Jaymin, G., 2018. Zero energy buildings: Decarbonising India by tapping the sun.  
2080 doi:https://www.pv-tech.org/guest-blog/zero-energy-buildings-decarbonising-india-by-tapping-  
2081 the-sun
- 2082 Jelle, B.P., 2016. Building integrated photovoltaics: A concise description of the current state of the  
2083 art and possible research pathways. *Energies* 9, 1–30. doi:10.3390/en9010021
- 2084 Jelle, B.P., 2013. The challenge of removing snow downfall on photovoltaic solar cell roofs in order  
2085 to maximize solar energy efficiency - Research opportunities for the future. *Energy Build.* 67,  
2086 334–351. doi:10.1016/j.enbuild.2013.08.010
- 2087 Jelle, B.P., Breivik, C., Drolsum R??kenes, H., 2012. Building integrated photovoltaic products: A  
2088 state-of-the-art review and future research opportunities. *Sol. Energy Mater. Sol. Cells* 100, 69–  
2089 96. doi:10.1016/j.solmat.2011.12.016
- 2090 Jelle, B.P., Kaln??s, S.E., Gao, T., 2015. Low-emissivity materials for building applications: A state-  
2091 of-the-art review and future research perspectives. *Energy Build.* 96, 329–356.  
2092 doi:10.1016/j.enbuild.2015.03.024
- 2093 Jia, Y., Alva, G., Fang, G., 2019. Development and applications of photovoltaic–thermal systems: A  
2094 review. *Renew. Sustain. Energy Rev.* 102, 249–265. doi:10.1016/j.rser.2018.12.030
- 2095 Jiang, J.A., Wang, J.C., Kuo, K.C., Su, Y.L., Shieh, J.C., Chou, J.J., 2012. Analysis of the junction  
2096 temperature and thermal characteristics of photovoltaic modules under various operation  
2097 conditions. *Energy* 44, 292–301. doi:10.1016/j.energy.2012.06.029
- 2098 John, A., Conklin, A., 2017. Building integrated photovoltaic devices as smart sensor for intelligent  
2099 building energy management systems. US 9772260B2.
- 2100 Jordan, D.C., Kurtz, S.R., 2013. Photovoltaic degradation rates - An Analytical Review. *Prog.*  
2101 *Photovoltaics Res. Appl.* 21, 12–29. doi:10.1002/pip.1182
- 2102 Joshi, S.S., Dhoble, A.S., 2018. Photovoltaic -Thermal systems (PVT): Technology review and future  
2103 trends. *Renew. Sustain. Energy Rev.* 92, 848–882. doi:10.1016/j.rser.2018.04.067
- 2104 K.S., S., V., L.V., K.S., R., 2016. ZnO–propylene glycol–water nanofluids with improved properties  
2105 for potential applications in renewable energy and thermal management, *Colloids and Surfaces*  
2106 *A: Physicochemical and Engineering Aspects.* Elsevier B.V. doi:10.1016/j.colsurfa.2016.06.007
- 2107 Kadar, P., Varga, A., 2013. Photovoltaic EV charge station, in: *Proceedings of IEEE 11th*  
2108 *International Symposium on Applied Machine Intelligence and Informatics (SAMi).* Herlany,  
2109 Slovakia, pp. 57–60.
- 2110 Kahl, A., Dujardin, J., Lehning, M., 2019. The bright side of PV production in snow-covered  
2111 mountains. *Proc. Natl. Acad. Sci.* 116, 1162–1167. doi:10.1073/pnas.1720808116
- 2112 Kaldellis, J.K., Fragos, P., 2011. Ash deposition impact on the energy performance of photovoltaic  
2113 generators. *J. Clean. Prod.* 19, 311–317. doi:10.1016/j.jclepro.2010.11.008
- 2114 Kalnæs, S.E., Jelle, B.P., 2015. Phase change materials and products for building applications: A  
2115 state-of-the-art review and future research opportunities. *Energy Build.* 94, 150–176.

- 2116 doi:10.1016/j.enbuild.2015.02.023
- 2117 Kalogirou, S.A., Tripanagnostopoulos, Y., 2006. Hybrid PV/T solar systems for domestic hot water  
2118 and electricity production. *Energy Convers. Manag.* 47, 3368–3382.  
2119 doi:10.1016/j.enconman.2006.01.012
- 2120 Kamthania, D., Nayak, S., Tiwari, G.N., 2011. Performance evaluation of a hybrid photovoltaic  
2121 thermal double pass facade for space heating. *Energy Build.* 43, 2274–2281.  
2122 doi:10.1016/j.enbuild.2011.05.007
- 2123 Kang, M.G., Park, N.G., Park, Y.J., Ryu, K.S., Chang, S.H., 2003. Manufacturing method for  
2124 transparent electric windows using dye-sensitized TiO<sub>2</sub> solar cells. *Sol. Energy Mater. Sol. Cells*  
2125 75, 475–479. doi:10.1016/S0927-0248(02)00202-7
- 2126 Kant, K., Pitchumani, R., Shukla, A., Sharma, A., 2019. Analysis and design of air ventilated building  
2127 integrated photovoltaic (BIPV) system incorporating phase change materials. *Energy Convers.*  
2128 *Manag.* 196, 149–164. doi:10.1016/j.enconman.2019.05.073
- 2129 Karplus, V.J., Zhang, S., Almond, D., 2018. Quantifying coal power plant responses to tighter SO<sub>2</sub>  
2130 emissions standards in China. *Proc. Natl. Acad. Sci. U. S. A.* 115, 7004–7009.  
2131 doi:10.1073/pnas.1800605115
- 2132 Karthick, A., Kalidasa Murugavel, K., Ghosh, A., Sudhakar, K., Ramanan, P., 2020. Investigation of a  
2133 binary eutectic mixture of phase change material for building integrated photovoltaic (BIPV)  
2134 system. *Sol. Energy Mater. Sol. Cells* 207, 110360. doi:10.1016/j.solmat.2019.110360
- 2135 Karthick, A., Kalidasa Murugavel, K., Kalaivani, L., 2018. Performance analysis of semitransparent  
2136 photovoltaic module for skylights. *Energy* 162, 798–812. doi:10.1016/j.energy.2018.08.043
- 2137 Karthick, Alagar, Ramanan, P., Ghosh, A., Stalin, B., Kumar, R.V., Baranilingesan, I., 2020.  
2138 Performance enhancement of copper indium diselenide photovoltaic module using inorganic  
2139 phase change material. *Asia -Pacific J. Chem. Eng.* 1–11. doi:10.1002/apj.2480
- 2140 Kavan, L., Yum, J.H., Grätzel, M., 2011. Graphene nanoplatelets outperforming platinum as the  
2141 electrocatalyst in co-bipyridine-mediated dye-sensitized solar cells. *Nano Lett.* 11, 5501–5506.  
2142 doi:10.1021/nl203329c
- 2143 Kazem, H.A., Khatib, T., 2013. Techno-economical assessment of grid connected photovoltaic power  
2144 systems productivity in Sohar, Oman. *Sustain. Energy Technol. Assessments* 3, 61–65.  
2145 doi:10.1016/j.seta.2013.06.002
- 2146 Kazmerski, L.L., White, F.R., Morgan, G.K., 1976. thin-film CuInSe<sub>2</sub>/CdS heterojunction solar cells.  
2147 *Appl. Phys. Lett.* 29, 268–270.
- 2148 Kim, A., Lee, C., Kim, H., Kim, J., 2015. Simple approach to superhydrophobic nanostructured al for  
2149 practical antifrosting application based on enhanced self-propelled jumping droplets. *ACS Appl.*  
2150 *Mater. Interfaces* 7, 7206–7213. doi:10.1021/acsami.5b00292
- 2151 Kim, J.B., Jeong, W., Clayton, M.J., Haberl, J.S., Yan, W., 2015. Developing a physical BIM library  
2152 for building thermal energy simulation. *Autom. Constr.* 50, 16–28.  
2153 doi:10.1016/j.autcon.2014.10.011
- 2154 Kineavy, F., Duffy, M., 2014. Modelling and design of electric vehicle charging systems that include  
2155 on-site renewable energy sources. 2014 IEEE 5th Int. Symp. Power Electron. Distrib. Gener.  
2156 *Syst. PEDG* 2014 1–8. doi:10.1109/PEDG.2014.6878651
- 2157 Kippelen, B., Brédas, J.L., 2009. Organic photovoltaics. *Energy Environ. Sci.* 2, 251–261.  
2158 doi:10.1039/b812502n

- 2159 Kjaer, S.B., Pedersen, J.K., Blaabjerg, F., 2005. A review of single-phase grid-connected inverters for  
2160 photovoltaic modules. *IEEE Trans. Ind. Appl.* 41, 1292–1306. doi:10.1109/TIA.2005.853371
- 2161 Koinegg, J., Brudermann, T., Posch, A., Mrotzek, M., 2013. “It would be a shame if we did not take  
2162 advantage of the spirit of the times □”: An analysis of prospects and barriers of Building  
2163 integrated photovoltaics. *Gaia* 22, 39–45. doi:10.14512/gaia.22.1.11
- 2164 Krauter, S., Araújo, R.G., Schroer, S., Hanitsch, R., Salhi, M.J., Triebel, C., Lemoine, R., 1999.  
2165 Combined photovoltaic and solar thermal systems for facade integration and building insulation.  
2166 *Sol. Energy* 67, 239–248. doi:10.1016/S0038-092X(00)00071-2
- 2167 Ku, Z., Rong, Y., Xu, M., Liu, T., Han, H., 2013. Full printable processed mesoscopic CH<sub>3</sub> NH<sub>3</sub> PbI  
2168 3 /TiO<sub>2</sub> heterojunction solar cells with carbon counter electrode. *Sci. Rep.* 3.  
2169 doi:10.1038/srep03132
- 2170 Kuhn, L., Reggiani, U., Sandrolini, L., Gorji, N.E., 2016. Physical device modeling of CdTe ultrathin  
2171 film solar cells. *Sol. Energy* 132, 165–172. doi:10.1016/j.solener.2016.02.046
- 2172 Kulinich, S.A., Farhadi, S., Nose, K., Du, X.W., 2011. Superhydrophobic surfaces: Are they really  
2173 ice-repellent? *Langmuir* 27, 25–29. doi:10.1021/la104277q
- 2174 Kumar, N.M., Sudhakar, K., Samykano, M., 2019. Performance comparison of BAPV and BIPV  
2175 systems with c-Si, CIS and CdTe photovoltaic technologies under tropical weather conditions.  
2176 *Case Stud. Therm. Eng.* 13, 100374. doi:10.1016/j.csite.2018.100374
- 2177 Kumar, S., Hong, H., Choi, W., Akhtar, I., Rehman, M.A., Seo, Y., 2019. Acrylate-assisted fractal  
2178 nanostructured polymer dispersed liquid crystal droplet based vibrant colored smart-windows.  
2179 *RSC Adv.* 9, 12645–12655. doi:10.1039/C9RA00729F
- 2180 Kuo, H.J., Hsieh, S.H., Guo, R.C., Chan, C.C., 2016. A verification study for energy analysis of BIPV  
2181 buildings with BIM. *Energy Build.* 130, 676–691. doi:10.1016/j.enbuild.2016.08.048
- 2182 Kuribayashi, K., Matsumoto, H., Uda, H., Komatsu, Y., Nakano, A., Ikegami, S., 1983. Preparation of  
2183 low resistance contact electrode in screen printed CdS/CdTe solar cell. *Jpn. J. Appl. Phys.* 22,  
2184 1828–1831. doi:10.1143/JJAP.22.1828
- 2185 Kurtz, S.R., Leilaoui, A.M., King, R.R., Peters, I.M., Heben, M.J., Metzger, W.K., Haegel, N.M.,  
2186 2020. Revisiting the Terawatt Challenge. *MRS Bull.* 45, 159–164. doi:10.1557/mrs.2020.73
- 2187 Kwon, H.K., Lee, K.T., Hur, K., Moon, S.H., Quasim, M.M., Wilkinson, T.D., Han, J.Y., Ko, H.,  
2188 Han, I.K., Park, B., Min, B.K., Ju, B.K., Morris, S.M., Friend, R.H., Ko, D.H., 2015. Optically  
2189 switchable smart windows with integrated photovoltaic devices. *Adv. Energy Mater.* 5, 1–6.  
2190 doi:10.1002/aenm.201401347
- 2191 Lam, J.C., Li, D.H.W., 1999. An analysis of daylighting and solar heat for cooling-dominated office  
2192 buildings. *Sol. Energy* 65, 251–262. doi:10.1016/S0038-092X(98)00136-4
- 2193 Lamnatou, C., Chemisana, D., 2017. Photovoltaic/thermal (PVT) systems: A review with emphasis on  
2194 environmental issues. *Renew. Energy* 105, 270–287. doi:10.1016/j.renene.2016.12.009
- 2195 Lee, H.M., Yoon, J.H., 2018. Power performance analysis of a transparent DSSC BIPV window based  
2196 on 2 year measurement data in a full-scale mock-up. *Appl. Energy* 225, 1013–1021.  
2197 doi:10.1016/j.apenergy.2018.04.086
- 2198 Lee, T.D., Ebong, A.U., 2017. A review of thin film solar cell technologies and challenges. *Renew.*  
2199 *Sustain. Energy Rev.* 70, 1286–1297. doi:10.1016/j.rser.2016.12.028
- 2200 Leon, J.I., Vinnikov, D., 2015. Grid-Connected Photovoltaic Systems: An Overview of Recent

- 2201 Research and Emerging PV Converter Technology. *IEEE Ind. Electron. Mag.* 9, 47–61.  
2202 doi:10.1109/MIE.2014.2376976
- 2203 Li, G., Xuan, Q., Akram, M.W., Golizadeh Akhlaghi, Y., Liu, H., Shittu, S., 2020. Building integrated  
2204 solar concentrating systems: A review. *Appl. Energy* 260, 114288.  
2205 doi:10.1016/j.apenergy.2019.114288
- 2206 Li, G., Xuan, Q., Pei, G., Su, Y., Lu, Y., Ji, J., 2018. Life-cycle assessment of a low-concentration PV  
2207 module for building south wall integration in China. *Appl. Energy* 215, 174–185.  
2208 doi:10.1016/j.apenergy.2018.02.005
- 2209 Li, J., Afsari, K., Li, N., Peng, J., Wu, Z., Cui, H., 2020. A review for presenting building information  
2210 modeling education and research in China. *J. Clean. Prod.* 259, 120885.  
2211 doi:10.1016/j.jclepro.2020.120885
- 2212 Li, X., Lopes, L., Williamson, S., 2009. On the suitability of plug-in hybrid electric vehicles (PHEV)  
2213 charging infrastructure based on wind and solar energy, in: *Proceedings of the IEEE Power &  
2214 Energy Society General Meeting*. Calgary, Canada, pp. 1–8. doi:10.1109/PES.2009.5275171
- 2215 Liao, W., Xu, S., 2015. Energy performance comparison among see-through amorphous-silicon PV  
2216 (photovoltaic) glazings and traditional glazings under different architectural conditions in China.  
2217 *Energy* 83, 267–275. doi:10.1016/j.energy.2015.02.023
- 2218 Liserre, M., Dell’Aquila, A., Blaabjerg, F., 2004. Genetic algorithm-based design of the active  
2219 damping for an LCL-filter three-phase active rectifier. *IEEE Trans. Power Electron.* 19, 76–86.  
2220 doi:10.1109/TPEL.2003.820540
- 2221 Liu, G., Rasul, M.G., Amanullah, M.T.O., Khan, M.M.K., 2012. Techno-economic simulation and  
2222 optimization of residential grid-connected PV system for the Queensland climate. *Renew.  
2223 Energy* 45, 146–155. doi:10.1016/j.renene.2012.02.029
- 2224 Liu, Y., Xu, Q.F., Lyons, A.M., 2019. Durable, optically transparent, superhydrophobic polymer  
2225 films. *Appl. Surf. Sci.* 470, 187–195. doi:10.1016/j.apsusc.2018.11.113
- 2226 Lo Piano, S., Saltelli, A., van der Sluijs, J.P., 2019. Silver as a constraint for a large-scale  
2227 development of solar photovoltaics? Scenario-making to the year 2050 supported by expert  
2228 engagement and global sensitivity analysis. *Front. Energy Res.* 7, 1–13.  
2229 doi:10.3389/fenrg.2019.00056
- 2230 Loh, P.C., Li, D., Chai, Y.K., Blaabjerg, F., 2013. Hybrid AC-DC microgrids with energy storages  
2231 and progressive energy flow tuning. *IEEE Trans. Power Electron.* 28, 1533–1543.  
2232 doi:10.1109/TPEL.2012.2210445
- 2233 Lopez-Garcia, J., Pozza, A., Sample, T., 2016. Long-term soiling of silicon PV modules in a moderate  
2234 subtropical climate. *Sol. Energy* 130, 174–183. doi:10.1016/j.solener.2016.02.025
- 2235 Lu, L., Yang, H.X., 2010. Environmental payback time analysis of a roof-mounted building-  
2236 integrated photovoltaic (BIPV) system in Hong Kong. *Appl. Energy* 87, 3625–3631.  
2237 doi:10.1016/j.apenergy.2010.06.011
- 2238 Lu, M., Lai, J.H.K., 2019. Building energy: A review on consumptions, policies, rating schemes and  
2239 standards. *Energy Procedia* 158, 3633–3638. doi:10.1016/j.egypro.2019.01.899
- 2240 Lucera, L., Machui, F., Schmidt, H.D., Ahmad, T., Kubis, P., Strohm, S., Hepp, J., Vetter, A.,  
2241 Egelhaaf, H.J., Brabec, C.J., 2017. Printed semi-transparent large area organic photovoltaic  
2242 modules with power conversion efficiencies of close to 5 %. *Org. Electron. physics, Mater.  
2243 Appl.* 45, 209–214. doi:10.1016/j.orgel.2017.03.013

- 2244 Ludin, N.A., Mustafa, N.I., Hanafiah, M.M., Ibrahim, M.A., Asri Mat Teridi, M., Sepeai, S., Zaharim,  
2245 A., Sopian, K., 2018. Prospects of life cycle assessment of renewable energy from solar  
2246 photovoltaic technologies: A review. *Renew. Sustain. Energy Rev.* 96, 11–28.  
2247 doi:10.1016/j.rser.2018.07.048
- 2248 Lufkin, S., 2019. Towards dynamic active façades. *Nat. Energy* 4, 635–636. doi:10.1038/s41560-019-  
2249 0443-x
- 2250 Luo, C., Posen, I.D., Hoornweg, D., MacLean, H.L., 2020. Modelling future patterns of urbanization,  
2251 residential energy use and greenhouse gas emissions in Dar es Salaam with the Shared Socio-  
2252 Economic Pathways. *J. Clean. Prod.* 254, 119998. doi:10.1016/j.jclepro.2020.119998
- 2253 Luo, W., Khoo, Y.S., Kumar, A., Low, J.S.C., Li, Y., Tan, Y.S., Wang, Y., Aberle, A.G.,  
2254 Ramakrishna, S., 2018. A comparative life-cycle assessment of photovoltaic electricity  
2255 generation in Singapore by multicrystalline silicon technologies. *Sol. Energy Mater. Sol. Cells*  
2256 174, 157–162. doi:10.1016/j.solmat.2017.08.040
- 2257 Ma, R.H., Chen, Y.C., 2012. BIPV-powered smart windows utilizing photovoltaic and electrochromic  
2258 devices. *Sensors* 12, 359–372. doi:10.3390/s120100359
- 2259 Ma, T., Yang, H., Lu, L., 2014. A feasibility study of a stand-alone hybrid solar-wind-battery system  
2260 for a remote island. *Appl. Energy* 121, 149–158. doi:10.1016/j.apenergy.2014.01.090
- 2261 Mahmoudzadeh Andwari, A., Pesiridis, A., Rajoo, S., Martinez-Botas, R., Esfahanian, V., 2017. A  
2262 review of Battery Electric Vehicle technology and readiness levels. *Renew. Sustain. Energy*  
2263 *Rev.* 78, 414–430. doi:10.1016/j.rser.2017.03.138
- 2264 Mallick, T.K., Eames, P.C., 2007. Design and fabrication of low concentrating second generation  
2265 PRIDE concentrator. *Sol. Energy Mater. Sol. Cells* 91, 597–608.  
2266 doi:10.1016/j.solmat.2006.11.016
- 2267 Mallick, T.K., Eames, P.C., Hyde, T.J., Norton, B., 2004. The design and experimental  
2268 characterisation of an asymmetric compound parabolic photovoltaic concentrator for building  
2269 facade integration in the UK. *Sol. Energy* 77, 319–327. doi:10.1016/j.solener.2004.05.015
- 2270 Marcos, J., Marroyo, L., Lorenzo, E., Alvira, D., Izco, E., 2011. Power output fluctuations in large  
2271 scale pv plants: One year observations with one second resolution and a derived analytic model.  
2272 *Prog. Photovoltaics Res. Appl.* 19, 218–227. doi:10.1002/pip.1016
- 2273 Marín-Sáez, J., Chemisana, D., Atencia, J., Collados, M.V., 2019. Outdoor performance evaluation of  
2274 a holographic solar concentrator optimized for building integration. *Appl. Energy* 250, 1073–  
2275 1084. doi:10.1016/j.apenergy.2019.05.075
- 2276 Martins, A.C., Chapuis, V., Sculati-Meillaud, F., Virtuani, A., Ballif, C., 2018a. Light and durable:  
2277 Composite structures for building-integrated photovoltaic modules. *Prog. Photovoltaics Res.*  
2278 *Appl.* 26, 718–729. doi:10.1002/pip.3009
- 2279 Martins, A.C., Chapuis, V., Virtuani, A., Li, H.Y., Perret-Aebi, L.E., Ballif, C., 2018b. Thermo-  
2280 mechanical stability of lightweight glass-free photovoltaic modules based on a composite  
2281 substrate. *Sol. Energy Mater. Sol. Cells* 187, 82–90. doi:10.1016/j.solmat.2018.07.015
- 2282 Mathew, S., Yella, A., Gao, P., Humphry-Baker, R., Curchod, B.F.E., Ashari-Astani, N., Tavernelli,  
2283 I., Rothlisberger, U., Nazeeruddin, M.K., Grätzel, M., 2014. Dye-sensitized solar cells with 13%  
2284 efficiency achieved through the molecular engineering of porphyrin sensitizers. *Nat. Chem.* 6,  
2285 242–247. doi:10.1038/nchem.1861
- 2286 Matsui, T., Sai, H., Bidiville, A., Hsu, H.J., Matsubara, K., 2018. Progress and limitations of thin-film  
2287 silicon solar cells. *Sol. Energy* 170, 486–498. doi:10.1016/j.solener.2018.05.077



- 2288 Matthews, J.P., Bell, J.M., Skryabin, I.L., 2001. Simulation of electrochromic switching voltages at  
2289 elevated temperatures. *Electrochim. Acta* 46, 1957–1961. doi:10.1016/S0013-4686(01)00386-3
- 2290 Mehmood, U., Al-Sulaiman, F.A., Yilbas, B.S., Salhi, B., Ahmed, S.H.A., Hossain, M.K., 2016.  
2291 Superhydrophobic surfaces with antireflection properties for solar applications: A critical  
2292 review. *Sol. Energy Mater. Sol. Cells* 157, 604–623. doi:10.1016/j.solmat.2016.07.038
- 2293 Meinardi, F., Bruni, F., Brovelli, S., 2017. Luminescent solar concentrators for building-integrated  
2294 photovoltaics. *Nat. Rev. Mater.* 2, 1–9. doi:10.1038/natrevmats.2017.72
- 2295 Menoufi, K., Chemisana, D., Rosell, J.I., 2013. Life Cycle Assessment of a Building Integrated  
2296 Concentrated Photovoltaic scheme. *Appl. Energy* 111, 505–514.  
2297 doi:10.1016/j.apenergy.2013.05.037
- 2298 Mertin, S., Hody-Le Caër, V., Joly, M., Mack, I., Oelhafen, P., Scartezzini, J.L., Schüler, A., 2014.  
2299 Reactively sputtered coatings on architectural glazing for coloured active solar thermal façades.  
2300 *Energy Build.* 68, 764–770. doi:10.1016/j.enbuild.2012.12.030
- 2301 Mertin, S., Hody-Le Caër, V., Joly, M., Scartezzini, J.L., Schüler, A., 2011. COLOURED  
2302 COATINGS FOR GLAZING OF ACTIVE SOLAR THERMAL FAÇADES BY REACTIVE  
2303 MAGNETRON SPUTTERING, in: CISBAT. Lausanne.
- 2304 Mesquita, I., Andrade, L., Mendes, A., 2019. Temperature Impact on Perovskite Solar Cells Under  
2305 Operation. *ChemSusChem* 12, 2186–2194. doi:10.1002/cssc.201802899
- 2306 Micheli, L., Caballero, J.A., Fernandez, E.F., Smestad, G.P., Nofuentes, G., Mallick, T.K.,  
2307 Almonacid, F., 2019. Correlating photovoltaic soiling losses to waveband and single-value  
2308 transmittance measurements. *Energy* 180, 376–386. doi:10.1016/j.energy.2019.05.097
- 2309 Micheli, L., Deceglie, M.G., Muller, M., 2018a. Interpolation Techniques. *IEEE J. Photovoltaics PP*,  
2310 1–6. doi:10.1109/JPHOTOV.2018.2872548
- 2311 Micheli, L., Fernandez, E.F., Smestad, G.P., Alrashidi, H., Sarmah, N., Sellami, N., Hassan, I.A.I.,  
2312 Kasry, A., Nofuentes, G., Sood, N., Pesala, B., Senthilarasu, S., Almonacid, F., Reddy, K.S.,  
2313 Muller, M., Mallick, T.K., 2018b. A unified global investigation on the spectral effects of soiling  
2314 losses of PV glass substrates: preliminary results 2858–2863. doi:10.1109/pvsc.2017.8366317
- 2315 Micheli, L., Muller, M., 2017. An investigation of the key parameters for predicting PV soiling losses.  
2316 *Prog. Photovoltaics Res. Appl.* 25, 291–307. doi:10.1002/pip.2860
- 2317 Milan Pradanovic and Timothy Green, 2003. Control and filter design of three phase inverter for high  
2318 power quality grid connection. *IEEE Trans. Power Electron.* 18, 1–8.
- 2319 Miller, W., Liu, L.A., Amin, Z., Gray, M., 2018. Involving occupants in net-zero-energy solar  
2320 housing retrofits: An Australian sub-tropical case study. *Sol. Energy* 159, 390–404.  
2321 doi:10.1016/j.solener.2017.10.008
- 2322 Miyazaki, T., Akisawa, A., Kashiwagi, T., 2005. Energy savings of office buildings by the use of  
2323 semi-transparent solar cells for windows. *Renew. Energy* 30, 281–304.  
2324 doi:10.1016/j.renene.2004.05.010
- 2325 Mizuno, K., Ishii, J., Kishida, H., Hayamizu, Y., Yasuda, S., Futaba, D.N., Yumura, M., Hata, K.,  
2326 2009. A black body absorber from vertically aligned single-walled carbon nanotubes. *Proc. Natl.*  
2327 *Acad. Sci. U. S. A.* 106, 6044–6047. doi:10.1073/pnas.0900155106
- 2328 Mondol, J.D., Yohanis, Y.G., Norton, B., 2006. Optimal sizing of array and inverter for grid-  
2329 connected photovoltaic systems. *Sol. Energy* 80, 1517–1539. doi:10.1016/j.solener.2006.01.006

- 2330 Muhammad-Sukki, F., Abu-Bakar, S.H., Ramirez-Iniguez, R., McMeekin, S.G., Stewart, B.G.,  
2331 Sarmah, N., Mallick, T.K., Munir, A.B., Mohd Yasin, S.H., Abdul Rahim, R., 2014. Mirror  
2332 symmetrical dielectric totally internally reflecting concentrator for building integrated  
2333 photovoltaic systems. *Appl. Energy* 113, 32–40. doi:10.1016/j.apenergy.2013.07.010
- 2334 Müller, H.F.O., 1994. Application of holographic optical elements in buildings for various purposes  
2335 like daylighting, solar shading and photovoltaic power generation. *Renew. Energy* 5, 935–941.  
2336 doi:10.1016/0960-1481(94)90114-7
- 2337 Mulligan, C.J., Wilson, M., Bryant, G., Vaughan, B., Zhou, X., Belcher, W.J., Dastoor, P.C., 2014. A  
2338 projection of commercial-scale organic photovoltaic module costs. *Sol. Energy Mater. Sol. Cells*  
2339 120, 9–17. doi:10.1016/j.solmat.2013.07.041
- 2340 Muñoz-García, M.A., Marin, O., Alonso-García, M.C., Chenlo, F., 2012. Characterization of thin film  
2341 PV modules under standard test conditions: Results of indoor and outdoor measurements and the  
2342 effects of sunlight exposure. *Sol. Energy* 86, 3049–3056. doi:10.1016/j.solener.2012.07.015
- 2343 Murray, J., Ma, D., Munday, J.N., 2017. Electrically controllable light trapping for self-powered  
2344 switchable solar windows. *ACS Photonics* 4, 1–7. doi:10.1021/acsp Photonics.6b00518
- 2345 Mustafa, N.I., Ludin, N.A., Mohamed, N.M., Ibrahim, M.A., Teridi, M.A.M., Sepeai, S., Zaharim, A.,  
2346 Sopian, K., 2019. Environmental performance of window-integrated systems using dye-  
2347 sensitised solar module technology in Malaysia. *Sol. Energy* 187, 379–392.  
2348 doi:10.1016/j.solener.2019.05.059
- 2349 Nayak, P.K., Mahesh, S., Snaith, H.J., Cahen, D., 2019. Photovoltaic solar cell technologies:  
2350 analysing the state of the art. *Nat. Rev. Mater.* 4.
- 2351 Naydenova, I., Akbari, H., Dalton, C., so Mohamed Ilyas, M.Y., Tee Wei, C.P., Toal, V., Marti, S.,  
2352 2013. Photopolymer Holographic Optical Elements for Application in Solar Energy  
2353 Concentrators. *Hologr. - Basic Princ. Contemp. Appl.* doi:10.5772/55109
- 2354 Ng, P.K., Mithraratne, N., 2014a. Lifetime performance of semi-transparent building-integrated  
2355 photovoltaic (BIPV) glazing systems in the tropics. *Renew. Sustain. Energy Rev.* 31, 736–745.  
2356 doi:10.1016/j.rser.2013.12.044
- 2357 Ng, P.K., Mithraratne, N., 2014b. Lifetime performance of semi-transparent building-integrated  
2358 photovoltaic (BIPV) glazing systems in the tropics. *Renew. Sustain. Energy Rev.* 31, 736–745.  
2359 doi:10.1016/j.rser.2013.12.044
- 2360 Ng, P.K., Mithraratne, N., Kua, H.W., 2013. Energy analysis of semi-transparent BIPV in Singapore  
2361 buildings. *Energy Build.* 66, 274–281. doi:10.1016/j.enbuild.2013.07.029
- 2362 Niu, T., Lu, J., Tang, M.C., Barrit, D., Smilgies, D.M., Yang, Z., Li, J., Fan, Y., Luo, T., McCulloch,  
2363 I., Amassian, A., Liu, S., Zhao, K., 2018. High performance ambient-air-stable FAPbI<sub>3</sub>  
2364 perovskite solar cells with molecule-passivated Ruddlesden-Popper/3D heterostructured film.  
2365 *Energy Environ. Sci.* 11, 3358–3366. doi:10.1039/c8ee02542h
- 2366 Norton, B., Eames, P.C., Mallick, T.K., Huang, M.J., McCormack, S.J., Mondol, J.D., Yohanis, Y.G.,  
2367 2011. Enhancing the performance of building integrated photovoltaics. *Sol. Energy* 85, 1629–  
2368 1664. doi:10.1016/j.solener.2009.10.004
- 2369 Nosonovsky, M., Hejazi, V., 2012. Why superhydrophobic surfaces are not always icephobic. *ACS*  
2370 *Nano* 6, 8488–8491. doi:10.1021/nn302138r
- 2371 Nundy, S., Ghosh, A., Mallick, T.K., 2020. Hydrophilic and Superhydrophilic Self-Cleaning Coatings  
2372 by Morphologically Varying ZnO Microstructures for Photovoltaic and Glazing Applications.  
2373 *ACS Omega* 5, 1033–1039. doi:10.1021/acsomega.9b02758

- 2374 Nunes, P., Farias, T., Brito, M.C., 2015. Day charging electric vehicles with excess solar electricity  
2375 for a sustainable energy system. *Energy* 80, 263–274. doi:10.1016/j.energy.2014.11.069
- 2376 O'Regan, B., Gratzel, M., 1991. A low-cost, high efficiency solar cell based on dye-sensitized  
2377 colloidal TiO<sub>2</sub> films. *Nature* 353, 737–740.
- 2378 Ogbomo, O.O., Amalu, E.H., Ekere, N.N., Olagbegi, P.O., 2017. A review of photovoltaic module  
2379 technologies for increased performance in tropical climate. *Renew. Sustain. Energy Rev.* 75,  
2380 1225–1238. doi:10.1016/j.rser.2016.11.109
- 2381 Oliver, M., Jackson, T., 2000. The evolution of economic and environmental cost for crystalline  
2382 silicon photovoltaics. *Energy Policy* 28, 1011–1021. doi:10.1016/S0301-4215(00)00088-4
- 2383 Osseweijer, F.J.W., van den Hurk, L.B.P., Teunissen, E.J.H.M., van Sark, W.G.J.H.M., 2018. A  
2384 comparative review of building integrated photovoltaics ecosystems in selected European  
2385 countries. *Renew. Sustain. Energy Rev.* 90, 1027–1040. doi:10.1016/j.rser.2018.03.001
- 2386 Özkul, F.B., Kayabasi, E., Çelik, E., Kurt, H., Arcaklioğlu, E., 2018. Investigating the effects of  
2387 cooling options on photovoltaic panel efficiency: State of the art and future plan. *PVCon 2018 -*  
2388 *Int. Conf. Photovolt. Sci. Technol.* doi:10.1109/PVCon.2018.8523948
- 2389 Pagliaro, M., Ciriminna, R., Palmisano, G., 2010. BIPV: Merging the photovoltaic with the  
2390 construction industry. *Prog. Photovoltaics Res. Appl.* 18, 61–72. doi:10.1002/pip.920
- 2391 Panayiotou, G.P., Kalogirou, S.A., Tassou, S.A., 2016. Evaluation of the application of Phase Change  
2392 Materials (PCM) on the envelope of a typical dwelling in the Mediterranean region. *Renew.*  
2393 *Energy* 97, 24–32. doi:10.1016/j.renene.2016.05.043
- 2394 Parida, B., Iniyar, S., Goic, R., 2011. A review of solar photovoltaic technologies. *Renew. Sustain.*  
2395 *Energy Rev.* 15, 1625–1636. doi:10.1016/j.rser.2010.11.032
- 2396 Parisi, A., Pernice, R., And??, A., Cino, A.C., Franzitta, V., Busacca, A.C., 2017. Electro-optical  
2397 characterization of ruthenium-based dye sensitized solar cells: A study of light soaking, ageing  
2398 and temperature effects. *Optik (Stuttg.)* 135, 227–237. doi:10.1016/j.ijleo.2017.01.100
- 2399 Parisi, M.L., Maranghi, S., Basosi, R., 2014. The evolution of the dye sensitized solar cells from  
2400 Grätzel prototype to up-scaled solar applications: A life cycle assessment approach. *Renew.*  
2401 *Sustain. Energy Rev.* 39, 124–138. doi:10.1016/j.rser.2014.07.079
- 2402 Parisi, M.L., Sinicropi, A., Basosi, R., 2011. Life cycle assessment of gratzel-type cell production for  
2403 non conventional photovoltaics from novel organic dyes. *Int. J. Heat Technol.* 29, 161–169.
- 2404 Park, J., Kim, T., Leigh, S.B., 2014. Application of a phase-change material to improve the electrical  
2405 performance of vertical-building-added photovoltaics considering the annual weather conditions.  
2406 *Sol. Energy* 105, 561–574. doi:10.1016/j.solener.2014.04.020
- 2407 Park, K.E., Kang, G.H., Kim, H.I., Yu, G.J., Kim, J.T., 2010. Analysis of thermal and electrical  
2408 performance of semi-transparent photovoltaic (PV) module. *Energy* 35, 2681–2687.  
2409 doi:10.1016/j.energy.2009.07.019
- 2410 Paul, D., Mandal, S.N., Mukherjee, D., Bhadra Chaudhuri, S.R., 2010. Optimization of significant  
2411 insolation distribution parameters - A new approach towards BIPV system design. *Renew.*  
2412 *Energy* 35, 2182–2191. doi:10.1016/j.renene.2010.02.026
- 2413 Peng, C., Huang, Y., Wu, Z., 2011. Building-integrated photovoltaics (BIPV) in architectural design  
2414 in China. *Energy Build.* 43, 3592–3598. doi:10.1016/j.enbuild.2011.09.032
- 2415 Peng, J., Curcija, D.C., Lu, L., Selkowitz, S.E., Yang, H., Zhang, W., 2016. Numerical investigation

- 2416 of the energy saving potential of a semi-transparent photovoltaic double-skin facade in a cool-  
2417 summer Mediterranean climate. *Appl. Energy* 165, 345–356.  
2418 doi:10.1016/j.apenergy.2015.12.074
- 2419 Peng, J., Curcija, D.C., Thanachareonkit, A., Lee, E.S., Goudey, H., Selkowitz, S.E., 2019. Study on  
2420 the overall energy performance of a novel c-Si based semitransparent solar photovoltaic  
2421 window. *Appl. Energy* 242, 854–872. doi:10.1016/j.apenergy.2019.03.107
- 2422 Peng, J., Lu, L., 2013. Investigation on the development potential of rooftop PV system in Hong Kong  
2423 and its environmental benefits. *Renew. Sustain. Energy Rev.* 27, 149–162.  
2424 doi:10.1016/j.rser.2013.06.030
- 2425 Peng, J., Lu, L., Yang, H., 2013a. Review on life cycle assessment of energy payback and greenhouse  
2426 gas emission of solar photovoltaic systems. *Renew. Sustain. Energy Rev.* 19, 255–274.  
2427 doi:10.1016/j.rser.2012.11.035
- 2428 Peng, J., Lu, L., Yang, H., Han, J., 2013b. Investigation on the annual thermal performance of a  
2429 photovoltaic wall mounted on a multi-layer façade. *Appl. Energy* 112, 646–656.  
2430 doi:10.1016/j.apenergy.2012.12.026
- 2431 Perovich, D.K., 2007. Light reflection and transmission by a temperate snow cover. *J. Glaciol.* 53,  
2432 201–210. doi:10.3189/172756507782202919
- 2433 Petersen, J., 2011. Global autos: Don't believe the hype—analyzing the costs & potential of fuel-  
2434 efficient technology. Bernstein Global Wealth Management.  
2435 doi:https://trove.nla.gov.au/work/232398274
- 2436 Phiraphat, S., Prommas, R., Puangsombut, W., 2017. Experimental study of natural convection in PV  
2437 roof solar collector. *Int. Commun. Heat Mass Transf.* 89, 31–38.  
2438 doi:10.1016/j.icheatmasstransfer.2017.09.022
- 2439 Pielichowska, K., Pielichowski, K., 2014. Phase change materials for thermal energy storage. *Prog.*  
2440 *Mater. Sci.* 65, 67–123. doi:10.1016/j.pmatsci.2014.03.005
- 2441 Polo, J., Alonso-Abella, M., Ruiz-Arias, J.A., Balenzategui, J.L., 2017. Worldwide analysis of  
2442 spectral factors for seven photovoltaic technologies. *Sol. Energy* 142, 194–203.  
2443 doi:10.1016/j.solener.2016.12.024
- 2444 Power, T., 2019. 2.67 MW Solar Plant – Carport, Cochin International Airport Ltd. [WWW  
2445 Document]. URL <https://www.tatapowersolar.com/project/2-67-mw-solar-plant-carport-cochin-international-airport-ltd/>
- 2447 Powers, L., Newmiller, J., Townsend, T., 2010. Measuring and modeling the effect of snow on  
2448 photovoltaic system performance. 2010 35th IEEE Photovolt. Spec. Conf. 000973–000978.  
2449 doi:10.1109/PVSC.2010.5614572
- 2450 Prakash, J., 1994. Transient analysis of a photovoltaic-thermal solar collector for co-generation of  
2451 electricity and hot air/water. *Energy Convers. Manag.* 35, 967–972. doi:10.1016/0196-  
2452 8904(94)90027-2
- 2453 Prathap, S., Sunny, S., Nair, A.S., 2016. Colour Temperature Tuning to Improve Efficacy of White  
2454 Light. *Procedia Technol.* 24, 1186–1193. doi:10.1016/j.protcy.2016.05.076
- 2455 Qiu, C., Yang, H., Zhang, W., 2019. Investigation on the energy performance of a novel BIPV system  
2456 integrated with vacuum glazing. *Build. Simul.* 12, 29–39. doi:https://doi.org/10.1007/s12273-  
2457 018-0464-6
- 2458 Rafiee, M., Chandra, S., Ahmed, H., McCormack, S.J., 2019. An overview of various configurations

- 2459 of Luminescent Solar Concentrators for photovoltaic applications. *Opt. Mater. (Amst)*. 91, 212–  
2460 227. doi:10.1016/j.optmat.2019.01.007
- 2461 Raga, S.R., Fabregat-Santiago, F., 2013. Temperature effects in dye-sensitized solar cells. *Phys.*  
2462 *Chem. Chem. Phys.* 15, 2328–2336. doi:10.1039/c2cp43220j
- 2463 Raghoebarsing, A., Reinders, A., 2018. Status of building integrated Photovoltaics (BIPV) in Latin  
2464 America and the case of Suriname, in: 35th EUPVSEC. doi:10.6013/jbrewsocjapan1915.62.477
- 2465 Ramanujam, J., Bishop, D.M., Todorov, T.K., Gunawan, O., Rath, J., Nekovei, R., Artegiani, E.,  
2466 Romeo, A., 2020. Flexible CIGS, CdTe and a-Si:H based thin film solar cells: A review. *Prog.*  
2467 *Mater. Sci.* 110, 1–20. doi:10.1016/j.pmatsci.2019.100619
- 2468 Ramli, M.A.M., Prasetyono, E., Wicaksana, R.W., Windarko, N.A., Sedraoui, K., Al-Turki, Y.A.,  
2469 2016. On the investigation of photovoltaic output power reduction due to dust accumulation and  
2470 weather conditions. *Renew. Energy* 99, 836–844. doi:10.1016/j.renene.2016.07.063
- 2471 Rand, B.P., Genoe, J., Heremans, P., Poortmans, J., 2007. Solar Cells Utilizing Small Molecular  
2472 Weight Organic Semiconductors. *Prog. Photovolt Res. Appl.* 15, 659–676. doi:10.1002/pip
- 2473 Ransome, S., 2009. Are kWh/kWp values really the best way to differentiate between PV  
2474 technologies?, in: *Proc. 24th EUPVSEC, Hamburg*.
- 2475 Rattankumar, V., Gopinath, N., 2012. Solar powered car using Brushless DC hub motor with  
2476 advanced PIC microcontroller, in: *Proceedings of International Conference on Emerging Trends*  
2477 *in Electrical Engineering and Energy Management. ICETEEEM*. pp. 422–23.
- 2478 Raugai, M., Isasa, M., Palmer, P.F., 2012. Potential Cd emissions from end-of-life CdTe PV. *Int. J.*  
2479 *Life Cycle Assess.* 17, 192–198. doi:10.1007/s11367-011-0348-9
- 2480 Ravyts, S., Vecchia, M.D., Van Den Broeck, G., Driesen, J., 2019. Review on building-integrated  
2481 photovoltaics electrical system requirements and module-integrated converter recommendations.  
2482 *Energies* 12. doi:10.3390/en12081532
- 2483 Rawat, R., Kaushik, S.C., Sastry, O.S., Bora, B., Singh, Y.K., 2018. Long-term Performance Analysis  
2484 of CdTe PV module in real operating conditions. *Mater. Today Proc.* 5, 23210–23217.  
2485 doi:10.1016/j.matpr.2018.11.052
- 2486 Reddy, P., Gupta, M.V.N.S., Nundy, S., Karthick, A., 2020. Status of BIPV and BAPV System for  
2487 Less Energy-Hungry Building in India — A Review. *Appl. Sci.* 10, 2337.
- 2488 Reddy, S.R., Ebadian, M.A., Lin, C.X., 2015. A review of PV-T systems: Thermal management and  
2489 efficiency with single phase cooling. *Int. J. Heat Mass Transf.* 91, 861–871.  
2490 doi:10.1016/j.ijheatmasstransfer.2015.07.134
- 2491 Reese, M.O., Glynn, S., Kempe, M.D., McGott, D.L., Dabney, M.S., Barnes, T.M., Booth, S.,  
2492 Feldman, D., Haegel, N.M., 2018. Increasing markets and decreasing package weight for high-  
2493 specific-power photovoltaics. *Nat. Energy* 3, 1002–1012. doi:10.1038/s41560-018-0258-1
- 2494 Reich, N.H., Sark, W. Van, Alsema, E. a, Kan, S.Y., Silvester, S., Heide, A. Van Der, Lof, R.W.,  
2495 Schropp, R., 2005. Weak light performance and spectral response of different solar cell types.  
2496 *20th Eur. Photovolt. Sol. Energy Conf.* 4–7.
- 2497 Reinfeld, R., Shamrakov, D., Jorgensen, C., 1994. Photostable solar concentrators based on  
2498 fluorescent glass films. *Sol. Energy Mater. Sol. Cells* 33, 417–427. doi:10.1016/0927-  
2499 0248(94)90002-7
- 2500 Rejeb, O., Sardarabadi, M., Ménéz, C., Passandideh-Fard, M., Dhaou, M.H., Jemni, A., 2016.

- 2501 Numerical and model validation of uncovered nanofluid sheet and tube type photovoltaic  
2502 thermal solar system. *Energy Convers. Manag.* 110, 367–377.  
2503 doi:10.1016/j.enconman.2015.11.063
- 2504 Ren, X., Li, J., Hu, M., Pei, G., Jiao, D., Zhao, X., Ji, J., 2019. Feasibility of an innovative amorphous  
2505 silicon photovoltaic/thermal system for medium temperature applications. *Appl. Energy* 252,  
2506 113427. doi:10.1016/j.apenergy.2019.113427
- 2507 Report, M., 2020. Global Thin Film Solar Cell Market - Premium Insight, Competitive News Feed  
2508 Analysis, Company Usability Profiles, Market Sizing & Forecasts to 2025.  
2509 doi:https://www.reportlinker.com/p05871666/Global-Thin-Film-Solar-Cell-Market-Premium-  
2510 Insight-Competitive-News-Feed-Analysis-Company-Usability-Profiles-Market-Sizing-  
2511 Forecasts-to.html?utm\_source=GNW
- 2512 Report, M.R., 2018. Organic Solar Cell Market Size, Share & Industry Analysis, By Material (Small  
2513 molecules, Polymers), By Application (Consumer Electronics, BIPV & Architecture, Wearable  
2514 Devices, Military & Defense, Automotive, Others) and Regional Forecast, 2019-2026.  
2515 doi:https://www.fortunebusinessinsights.com/industry-reports/organic-solar-cell-market-101555
- 2516 Research, B., 2018. Perovskite Solar Cells: Materials, Fabrication, and Global Markets.  
2517 doi:https://www.bccresearch.com/market-research/energy-and-resources/perovskite-solar-cells-  
2518 materials-fabrication-and-global-markets-report.html
- 2519 Research, E.M., 2020. Global Solar Cells and Modules Market 2020 by Manufacturers, Regions,  
2520 Type and Application, Forecast to 2025. doi:https://www.eonmarketresearch.com/global-solar-  
2521 cells-and-modules-market-2020-63332
- 2522 Research, Z.M., 2018. BIPV Glass Market: Global Industry Analysis, Size, Share, Growth, Trends,  
2523 and Forecasts 2016–2024. doi:https://www.zionmarketresearch.com/report/bipv-glass-market
- 2524 Rezaei, S.D., Shannigrahi, S., Ramakrishna, S., 2017. A review of conventional, advanced, and smart  
2525 glazing technologies and materials for improving indoor environment. *Sol. Energy Mater. Sol.*  
2526 *Cells* 159, 26–51. doi:10.1016/j.solmat.2016.08.026
- 2527 Richardson, D.B., 2013. Electric vehicles and the electric grid: A review of modeling approaches,  
2528 Impacts, and renewable energy integration. *Renew. Sustain. Energy Rev.* 19, 247–254.  
2529 doi:10.1016/j.rser.2012.11.042
- 2530 Riverola, A., Mellor, A., Alonso Alvarez, D., Ferre Llin, L., Guarracino, I., Markides, C.N., Paul,  
2531 D.J., Chemisana, D., Ekins-Daukes, N., 2018. Mid-infrared emissivity of crystalline silicon solar  
2532 cells. *Sol. Energy Mater. Sol. Cells* 174, 607–615. doi:10.1016/j.solmat.2017.10.002
- 2533 Rodriguez, J.L., Li, S., Chou, H.C., Rahatgi, A., Thomas, E.W., Kamra, S., Bhat, a K., 1995. Effects  
2534 of Cu on CdTe / CdS Heterojunction Solar Cells with Au / Cu Contacts. *J. Electrochem. Soc.*  
2535 142, 254–259.
- 2536 Roslizar, A., Dottermusch, S., Vüllers, F., Kavalenka, M.N., Guttman, M., Schneider, M., Paetzold,  
2537 U.W., Hölscher, H., Richards, B.S., Klampaftis, E., 2019. Self-cleaning performance of  
2538 superhydrophobic hot-embossed fluoropolymer films for photovoltaic modules. *Sol. Energy*  
2539 *Mater. Sol. Cells* 189, 188–196. doi:10.1016/j.solmat.2018.09.017
- 2540 Roy, A., Ghosh, A., Bhandari, S., Selvaraj, P., Sundaram, S., Mallick, T.K., 2019. Color Comfort  
2541 Evaluation of Dye-Sensitized Solar Cell (DSSC) Based Building-Integrated Photovoltaic (BIPV)  
2542 Glazing after 2 Years of Ambient Exposure. *J. Phys. Chem. C* 123, 23834–23837.  
2543 doi:10.1021/acs.jpcc.9b05591
- 2544 Roy, P., Kumar Sinha, N., Tiwari, S., Khare, A., 2020. A review on perovskite solar cells: Evolution

- 2545 of architecture, fabrication techniques, commercialization issues and status. *Sol. Energy* 198,  
2546 665–688. doi:10.1016/j.solener.2020.01.080
- 2547 R  ther, R., Kleiss, G., Reiche, K., 2002. Spectral effects on amorphous silicon solar module fill  
2548 factors. *Sol. Energy Mater. Sol. Cells* 71, 375–385. doi:10.1016/S0927-0248(01)00095-2
- 2549 R  ther, R., Livingstone, J., 1995. Seasonal variations in amorphous silicon solar module outputs and  
2550 thin film characteristics. *Sol. Energy Mater. Sol. Cells* 36, 29–43. doi:10.1016/0927-  
2551 0248(94)00165-O
- 2552 Saga, T., 2010. Advances in crystalline silicon solar cell technology for industrial mass production 2,  
2553 96–102. doi:10.1038/asiamat.2010.82
- 2554 Said, S.A.M., Hassan, G., Walwil, H.M., Al-Aqeeli, N., 2018. The effect of environmental factors and  
2555 dust accumulation on photovoltaic modules and dust-accumulation mitigation strategies. *Renew.*  
2556 *Sustain. Energy Rev.* 82, 743–760. doi:10.1016/j.rser.2017.09.042
- 2557 Said, Z., Saidur, R., Rahim, N.A., Alim, M.A., 2014. Analyses of exergy efficiency and pumping  
2558 power for a conventional flat plate solar collector using SWCNTs based nanofluid. *Energy*  
2559 *Build.* 78, 1–9. doi:10.1016/j.enbuild.2014.03.061
- 2560 Saifullah, M., Gwak, J., Yun, J.H., 2016. Comprehensive review on material requirements, present  
2561 status, and future prospects for building-integrated semitransparent photovoltaics (BISTPV). *J.*  
2562 *Mater. Chem. A* 4, 8512–8540. doi:10.1039/C6TA01016D
- 2563 Sampson, L., Ettman, C.K., Galea, S., 2020. Urbanization, urbanicity, and depression. *Curr. Opin.*  
2564 *Psychiatry* 33, 233–244. doi:10.1097/ycp.0000000000000588
- 2565 S  nchez-palencia, P., Mart  n-chivelet, N., Chenlo, F., 2019. Modeling temperature and thermal  
2566 transmittance of building integrated photovoltaic modules 184, 153–161.  
2567 doi:10.1016/j.solener.2019.03.096
- 2568 Sanhudo, L., Ramos, N.M.M., Po  as Martins, J., Almeida, R.M.S.F., Barreira, E., Sim  es, M.L.,  
2569 Cardoso, V., 2018. Building information modeling for energy retrofitting – A review. *Renew.*  
2570 *Sustain. Energy Rev.* 89, 249–260. doi:10.1016/j.rser.2018.03.064
- 2571 Santa-Nokki, H., Kallioinen, J., Korppi-Tommola, J., 2007. A dye-sensitized solar cell driven  
2572 electrochromic device. *Photochem. Photobiol. Sci.* 6, 63–66. doi:10.1039/B611158K
- 2573 Santbergen, R., van Zolingen, R.J.C., 2008. The absorption factor of crystalline silicon PV cells: A  
2574 numerical and experimental study. *Sol. Energy Mater. Sol. Cells* 92, 432–444.  
2575 doi:10.1016/j.solmat.2007.10.005
- 2576 Saretta, E., Bonomo, P., Frontini, F., 2020. A calculation method for the BIPV potential of Swiss  
2577 fa  ades at LOD2.5 in urban areas: A case from Ticino region. *Sol. Energy* 195, 150–165.  
2578 doi:10.1016/j.solener.2019.11.062
- 2579 Saretta, E., Caputo, P., Frontini, F., 2019. A review study about energy renovation of building facades  
2580 with BIPV in urban environment. *Sustain. Cities Soc.* 44, 343–355.  
2581 doi:10.1016/j.scs.2018.10.002
- 2582 Sarmah, N., Richards, B.S., Mallick, T.K., 2014. Design, development and indoor performance  
2583 analysis of a low concentrating dielectric photovoltaic module. *Sol. Energy* 103, 390–401.  
2584 doi:10.1016/j.solener.2014.02.029
- 2585 Sato, R., Chiba, Y., Chikamatsu, M., Yoshida, Y., Taima, T., Kasu, M., Masuda, A., 2019.  
2586 Investigation of the power generation of organic photovoltaic modules connected to the power  
2587 grid for more than three years. *Jpn. J. Appl. Phys.* 58, 052001. doi:10.7567/1347-4065/ab0742

- 2588 Schill, C., Brachmann, S., Koehl, M., 2015. Impact of soiling on IV-curves and efficiency of PV-  
2589 modules. *Sol. Energy* 112, 259–262. doi:10.1016/j.solener.2014.12.003
- 2590 Scognamiglio, A., 2017. Building-Integrated Photovoltaics (BIPV) for Cost-Effective Energy-  
2591 Efficient Retrofitting, *Cost-Effective Energy Efficient Building Retrofitting: Materials,*  
2592 *Technologies, Optimization and Case Studies.* Elsevier Ltd. doi:10.1016/B978-0-08-101128-  
2593 7.00006-X
- 2594 Scognamiglio, A., Rostvik, H.N., 2013. Photovoltaics and zero energy buildings: a new opportunity  
2595 and challenge for design. *Prog. Photovoltaics* 21, 1319–1336.
- 2596 Sebastián, P.J., Olea, A., Campos, J., Toledo, J.A., Gamboa, S.A., 2004. Temperature dependence and  
2597 the oscillatory behavior of the opto-electronic properties of a dye-sensitized nanocrystalline  
2598 TiO<sub>2</sub> solar cell. *Sol. Energy Mater. Sol. Cells* 81, 349–361. doi:10.1016/j.solmat.2003.11.011
- 2599 Sellami, N., Mallick, T.K., 2013a. Optical efficiency study of PV Crossed Compound Parabolic  
2600 Concentrator. *Appl. Energy* 102, 868–876. doi:10.1016/j.apenergy.2012.08.052
- 2601 Sellami, N., Mallick, T.K., 2013b. Optical characterisation and optimisation of a static Window  
2602 Integrated Concentrating Photovoltaic system. *Sol. Energy* 91, 273–282.  
2603 doi:10.1016/j.solener.2013.02.012
- 2604 Selvaraj, P., Baig, H., Mallick, T.K., Siviter, J., Montecucco, A., Li, W., Paul, M., Sweet, T., Gao, M.,  
2605 Knox, A.R., Sundaram, S., 2018. Enhancing the efficiency of transparent dye-sensitized solar  
2606 cells using concentrated light. *Sol. Energy Mater. Sol. Cells* 175, 29–34.  
2607 doi:10.1016/j.solmat.2017.10.006
- 2608 Selvaraj, P., Ghosh, A., Mallick, T.K., Sundaram, S., 2019. Investigation of semi-transparent dye-  
2609 sensitized solar cells for fenestration integration. *Renew. Energy* 141, 516–525.  
2610 doi:10.1016/j.renene.2019.03.146
- 2611 Senthilarasu, S., Fernández, E.F., Almonacid, F., Mallick, T.K., 2015. Effects of spectral coupling on  
2612 perovskite solar cells under diverse climatic conditions. *Sol. Energy Mater. Sol. Cells* 133, 92–  
2613 98. doi:10.1016/j.solmat.2014.10.037
- 2614 Seo, J., Park, S., Chan Kim, Y., Jeon, N.J., Noh, J.H., Yoon, S.C., Seok, S. Il, 2014. Benefits of very  
2615 thin PCBM and LiF layers for solution-processed p–i–n perovskite solar cells. *Energy Environ.*  
2616 *Sci.* 7, 2642–2646. doi:10.1039/C4EE01216J
- 2617 Sethi, V.K., Pandey, M., Shukla, P., 2011. Use of Nanotechnology in Solar PV Cell. *Int. J. Chem.*  
2618 *Eng. Appl.* 2, 77–80. doi:10.7763/IJCEA.2011.V2.79
- 2619 Shamshirband, M., Salehi, J., Gazijahani, F.S., 2018. Decentralized trading of plug-in electric vehicle  
2620 aggregation agents for optimal energy management of smart renewable penetrated microgrids  
2621 with the aim of CO<sub>2</sub> emission reduction. *J. Clean. Prod.* 200, 622–640.  
2622 doi:10.1016/j.jclepro.2018.07.315
- 2623 Shanks, K., Senthilarasu, S., French-Constant, R.H., Mallick, T.K., 2015. White butterflies as solar  
2624 photovoltaic concentrators. *Sci. Rep.* 5, 12267. doi:10.1038/srep12267
- 2625 Sharma, R., Wyatt, C.A., Zhang, J., Calle, C.I., Mardesich, N., Mazumder, M.K., 2009. Experimental  
2626 evaluation and analysis of electrodynamic screen as dust mitigation technology for future Mars  
2627 missions. *IEEE Trans. Ind. Appl.* 45, 591–596. doi:10.1109/TIA.2009.2013542
- 2628 Sharma, S., Jain, K.K., Sharma, A., 2015. Solar Cells: In Research and Applications—A Review.  
2629 *Mater. Sci. Appl.* 06, 1145–1155. doi:10.4236/msa.2015.612113
- 2630 Sharma, V., Kumar, A., Sastry, O.S., Chandel, S.S., 2013. Performance assessment of different solar



- 2631 photovoltaic technologies under similar outdoor conditions. *Energy* 58, 511–518.  
2632 doi:10.1016/j.energy.2013.05.068
- 2633 Shende, R.C., Ramaprabhu, S., 2016. Thermo-optical properties of partially unzipped multiwalled  
2634 carbon nanotubes dispersed nanofluids for direct absorption solar thermal energy systems. *Sol.*  
2635 *Energy Mater. Sol. Cells* 157, 117–125. doi:10.1016/j.solmat.2016.05.037
- 2636 Shivashankar, S., Mekhilef, S., Mokhlis, H., Karimi, M., 2016. Mitigating methods of power  
2637 fluctuation of photovoltaic (PV) sources - A review. *Renew. Sustain. Energy Rev.* 59, 1170–  
2638 1184. doi:10.1016/j.rser.2016.01.059
- 2639 Shukla, A., Kant, K., Sharma, A., Biwole, P.H., 2017. Cooling methodologies of photovoltaic module  
2640 for enhancing electrical efficiency: A review. *Sol. Energy Mater. Sol. Cells* 160, 275–286.  
2641 doi:10.1016/j.solmat.2016.10.047
- 2642 Shukla, A.K., Sudhakar, K., Baredar, P., 2017a. Recent advancement in BIPV product technologies:  
2643 A review. *Energy Build.* 140, 188–195. doi:10.1016/j.enbuild.2017.02.015
- 2644 Shukla, A.K., Sudhakar, K., Baredar, P., 2016a. Exergetic assessment of BIPV module using  
2645 parametric and photonic energy methods: A review. *Energy Build.* 119, 62–73.  
2646 doi:10.1016/j.enbuild.2016.03.022
- 2647 Shukla, A.K., Sudhakar, K., Baredar, P., 2016b. A comprehensive review on design of building  
2648 integrated photovoltaic system. *Energy Build.* 128, 99–110. doi:10.1016/j.enbuild.2016.06.077
- 2649 Shukla, A.K., Sudhakar, K., Baredar, P., Mamat, R., 2018. BIPV based sustainable building in South  
2650 Asian countries. *Sol. Energy* 170, 1162–1170. doi:10.1016/j.solener.2018.06.026
- 2651 Shukla, A.K., Sudhakar, K., Baredar, P., Mamat, R., 2017b. BIPV in Southeast Asian countries –  
2652 opportunities and challenges. *Renew. Energy Focus* 21, 25–32. doi:10.1016/j.ref.2017.07.001
- 2653 Shyam, Tiwari, G.N., Al-Helal, I.M., 2015. Analytical expression of temperature dependent electrical  
2654 efficiency of N-PVT water collectors connected in series. *Sol. Energy* 114, 61–76.  
2655 doi:10.1016/j.solener.2015.01.026
- 2656 Sierra, D., Aristizábal, A.J., Hernández, J.A., Ospina, D., 2020. Life cycle analysis of a building  
2657 integrated photovoltaic system operating in Bogotá, Colombia. *Energy Reports* 6, 10–19.  
2658 doi:10.1016/j.egy.2019.10.012
- 2659 Singh, D., Timofeeva, E., Yu, W., Routbort, J., France, D., Smith, D., Lopez-Cepero, J.M., 2009. An  
2660 investigation of silicon carbide-water nanofluid for heat transfer applications. *J. Appl. Phys.* 105.  
2661 doi:10.1063/1.3082094
- 2662 Singh, P., Ravindra, N.M., 2012. Temperature dependence of solar cell performance—an analysis.  
2663 *Sol. Energy Mater. Sol. Cells* 101, 36–45. doi:10.1016/j.solmat.2012.02.019
- 2664 Sinke, W.C., 2019. Development of photovoltaic technologies for global impact. *Renew. Energy* 138,  
2665 911–914. doi:10.1016/j.renene.2019.02.030
- 2666 Smestad, G.P., Germer, T.A., Alrashidi, H., Fernández, E.F., Dey, S., Brahma, H., Sarmah, N.,  
2667 Ghosh, A., Sellami, N., 2020. Modelling photovoltaic soiling losses through optical  
2668 characterization. *Sci. Rep.* 1–13. doi:10.1038/s41598-019-56868-z
- 2669 Smith, C.J., Forster, P.M., Crook, R., 2014. Global analysis of photovoltaic energy output enhanced  
2670 by phase change material cooling. *Appl. Energy* 126, 21–28.  
2671 doi:10.1016/j.apenergy.2014.03.083
- 2672 Smith, W.J., 2010. Can EV (electric vehicles) address Ireland's CO2 emissions from transport?

- 2673 Energy 35, 4514–4521. doi:10.1016/j.energy.2010.07.029
- 2674 Smolders, K.C.H.J., de Kort, Y.A.W., 2014. Bright light and mental fatigue: Effects on alertness,  
2675 vitality, performance and physiological arousal. *J. Environ. Psychol.* 39, 77–91.  
2676 doi:10.1016/j.jenvp.2013.12.010
- 2677 Snaith, H.J., 2018. Present status and future prospects of perovskite photovoltaics. *Nat. Mater.* 17,  
2678 372–376. doi:10.1038/s41563-018-0071-z
- 2679 Solanki, S.C., Dubey, S., Tiwari, A., 2009. Indoor simulation and testing of photovoltaic thermal  
2680 (PV/T) air collectors. *Appl. Energy* 86, 2421–2428. doi:10.1016/j.apenergy.2009.03.013
- 2681 Soman, A., Antony, A., 2019. Colored solar cells with spectrally selective photonic crystal reflectors  
2682 for application in building integrated photovoltaics. *Sol. Energy* 181, 1–8.  
2683 doi:10.1016/j.solener.2019.01.058
- 2684 Son, D.-Y., Lee, J.-W., Choi, Y.J., Jang, I.-H., Lee, S., Yoo, P.J., Shin, H., Ahn, N., Choi, M., Kim,  
2685 D., Park, N.-G., 2016. Self-formed grain boundary healing layer for highly efficient CH<sub>3</sub> NH<sub>3</sub>  
2686 PbI<sub>3</sub> perovskite solar cells. *Nat. Energy* 1, 16081. doi:10.1038/nenergy.2016.81
- 2687 Son, J., Kundu, S., Verma, L.K., Sakhuja, M., Danner, A.J., Bhatia, C.S., Yang, H., 2012. A practical  
2688 superhydrophilic self cleaning and antireflective surface for outdoor photovoltaic applications.  
2689 *Sol. Energy Mater. Sol. Cells* 98, 46–51. doi:10.1016/j.solmat.2011.10.011
- 2690 Song, J., Lu, S., Wu, Y., Zhou, C., Li, X., Li, J., 2020. Migration and distribution characteristics of  
2691 organic and inorganic fractions in condensable particulate matter emitted from an ultralow  
2692 emission coal-fired power plant. *Chemosphere* 243, 125346.  
2693 doi:10.1016/j.chemosphere.2019.125346
- 2694 Sorgato, M.J., Schneider, K., Rütger, R., 2018. Technical and economic evaluation of thin-film CdTe  
2695 building-integrated photovoltaics (BIPV) replacing façade and rooftop materials in office  
2696 buildings in a warm and sunny climate. *Renew. Energy* 118, 84–98.  
2697 doi:10.1016/j.renene.2017.10.091
- 2698 Sozer, H., Elnimeiri, M., 2007. Critical Factors in Reducing the Cost of Building Integrated  
2699 Photovoltaic (BIPV) Systems. *Archit. Sci. Rev.* 50, 115–121. doi:10.3763/asre.2007.5017
- 2700 Spiliotis, K., Gonçalves, J.E., Van De Sande, W., Ravyts, S., Daenen, M., Saelens, D., Baert, K.,  
2701 Driesen, J., 2019. Modeling and validation of a DC/DC power converter for building energy  
2702 simulations: Application to BIPV systems. *Appl. Energy* 240, 646–665.  
2703 doi:10.1016/j.apenergy.2019.02.071
- 2704 Sreebha, A.B., Suresh, S., Sreekala, C.O., Mahadevan Pillai, V.P., 2018. Volume holographic gratings  
2705 in acrylamidebased photopolymer to provide selective light as an added input for improving the  
2706 performance of dye-sensitized solar cells. *Curr. Sci.* 114, 2267–2272.  
2707 doi:10.18520/cs/v114/i11/2267-2272
- 2708 Staebler, D.L., Wronski, C.R., 1977. Reversible conductivity changes in discharged-produced  
2709 amorphous Si. *Appl. Phys. Lett.* 31, 274–292.
- 2710 Stephen, E.N., Asirvatham, L.G., Kandasamy, R., Solomon, B., Kondru, G.S., 2019. Heat transfer  
2711 performance of a compact loop heat pipe with alumina and silver nanofluid: A comparative  
2712 study. *J. Therm. Anal. Calorim.* 136, 211–222. doi:10.1007/s10973-018-7739-0
- 2713 Stoichkov, V., Sweet, T.K.N., Jenkins, N., Kettle, J., 2019. Studying the outdoor performance of  
2714 organic building-integrated photovoltaics laminated to the cladding of a building prototype. *Sol.*  
2715 *Energy Mater. Sol. Cells* 191, 356–364. doi:10.1016/j.solmat.2018.11.040

- 2716 Stuckelberger, M., Biron, R., Wyrsh, N., Haug, F.-J., Ballif, C., 2017. Review: Progress in solar cells  
2717 from hydrogenated amorphous silicon. *Renew. Sustain. Energy Rev.* 76, 1–27.  
2718 doi:10.1016/j.rser.2016.11.190
- 2719 Su, Y.W., 2019. Residential electricity demand in Taiwan: the effects of urbanization and energy  
2720 poverty. *J. Asia Pacific Econ.* 0, 1–24. doi:10.1080/13547860.2019.1706870
- 2721 Sun, Q.X., Yang, N.N., Cai, X.B., Hu, G.K., 2012. Mechanism of dust removal by a standing wave  
2722 electric curtain. *Sci. China Physics, Mech. Astron.* 55, 1018–1025. doi:10.1007/s11433-012-  
2723 4722-9
- 2724 Sun, W., Ji, J., Luo, C., He, W., 2011. Performance of PV-Trombe wall in winter correlated with  
2725 south façade design. *Appl. Energy* 88, 224–231. doi:10.1016/j.apenergy.2010.06.002
- 2726 Sun, Y., Shanks, K., Baig, H., Zhang, W., Hao, X., Li, Y., He, B., Wilson, R., Liu, H., Sundaram, S.,  
2727 Zhang, J., Xie, L., Mallick, T., Wu, Y., 2018. Integrated CdTe PV glazing into windows: energy  
2728 and daylight performance for different architecture designs. *Appl. Energy* 231, 972–984.  
2729 doi:10.1016/j.apenergy.2018.09.133
- 2730 Taffesse, F., Verma, A., Singh, S., Tiwari, G.N., 2016. Periodic modeling of semi-transparent  
2731 photovoltaic thermal-trombe wall (SPVT-TW). *Sol. Energy* 135, 265–273.  
2732 doi:10.1016/j.solener.2016.05.044
- 2733 Tai, Q., You, P., Sang, H., Liu, Z., Hu, C., Chan, H.L.W., Yan, F., 2016. in ambient air irrespective of  
2734 the humidity. *Nat. Commun.* 6, 1–8. doi:10.1038/ncomms11105
- 2735 Takeoka, A., Kouzuma, S., Tanaka, H., Inoue, H., Murata, K., Morizane, M., Nakamura, N.,  
2736 Nishiwaki, H., Ohnishi, M., Nakano, S., Kuwano, Y., 1993. Development and application of  
2737 see-through a-Si solar cells. *Sol. Energy Mater. Sol. Cells* 29, 243–252. doi:10.1016/0927-  
2738 0248(93)90039-6
- 2739 Tanesab, J., Parlevliet, D., Whale, J., Urmee, T., 2018. Energy and economic losses caused by dust on  
2740 residential photovoltaic (PV) systems deployed in different climate areas. *Renew. Energy* 120,  
2741 401–412. doi:10.1016/j.renene.2017.12.076
- 2742 Taveres-Cachat, E., Grynning, S., Thomsen, J., Selkowitz, S., 2019. Responsive building envelope  
2743 concepts in zero emission neighborhoods and smart cities - A roadmap to implementation.  
2744 *Build. Environ.* 149, 446–457. doi:10.1016/j.buildenv.2018.12.045
- 2745 The Lancet, 2019. Net zero by 2050 in the UK. *Lancet* 393, 1911. doi:10.1016/S0140-  
2746 6736(19)31004-9
- 2747 Theelen, M., Foster, C., Steijvers, H., Barreau, N., Vroon, Z., Zeman, M., 2015. The impact of  
2748 atmospheric species on the degradation of CIGS solar cells. *Sol. Energy Mater. Sol. Cells* 141,  
2749 49–56. doi:10.1016/j.solmat.2015.05.019
- 2750 Tian, H., Yu, X., Zhang, J., Duan, W., Tian, F., Yu, T., 2012. The influence of environmental factors  
2751 on DSSCs for BIPV. *Int. J. Electrochem. Sci.* 7, 4686–4691.
- 2752 Tian, M., Su, Y., Zheng, H., Pei, G., Li, G., Riffat, S., 2018. A review on the recent research progress  
2753 in the compound parabolic concentrator (CPC) for solar energy applications. *Renew. Sustain.*  
2754 *Energy Rev.* 82, 1272–1296. doi:10.1016/j.rser.2017.09.050
- 2755 Tie, S.F., Tan, C.W., 2013. A review of energy sources and energy management system in electric  
2756 vehicles. *Renew. Sustain. Energy Rev.* 20, 82–102. doi:10.1016/j.rser.2012.11.077
- 2757 Tomar, V., Tiwari, G.N., Bhatti, T.S., 2017. Performance of different photovoltaic-thermal (PVT)  
2758 configurations integrated on prototype test cells: An experimental approach. *Energy Convers.*

- 2759 Manag. 154, 394–419. doi:10.1016/j.enconman.2017.11.033
- 2760 Tossa, A.K., Soro, Y.M., Thiaw, L., Azoumah, Y., Sicot, L., Yamegueu, D., Lishou, C., Coulibaly,  
2761 Y., Razongles, G., 2016. Energy performance of different silicon photovoltaic technologies  
2762 under hot and harsh climate. *Energy* 103, 261–270. doi:10.1016/j.energy.2016.02.133
- 2763 Toth, S., Muller, M., Miller, D.C., Moutinho, H., To, B., Micheli, L., Linger, J., Engrakul, C.,  
2764 Einhorn, A., Simpson, L., 2018. Soiling and cleaning: Initial observations from 5-year  
2765 photovoltaic glass coating durability study. *Sol. Energy Mater. Sol. Cells* 185, 375–384.  
2766 doi:10.1016/j.solmat.2018.05.039
- 2767 Tripanagnostopoulos, Y., Nousia, T., Souliotis, M., Yianoulis, P., 2002. Hybrid photovoltaic/thermal  
2768 solar systems. *Sol. Energy* 72, 217–234. doi:10.1016/S0038-092X(01)00096-2
- 2769 Tripathy, M., Joshi, H., Panda, S.K., 2017. Energy payback time and life-cycle cost analysis of  
2770 building integrated photovoltaic thermal system influenced by adverse effect of shadow. *Appl.*  
2771 *Energy* 208, 376–389. doi:10.1016/j.apenergy.2017.10.025
- 2772 Tripathy, M., Sadhu, P.K., Panda, S.K., 2016. A critical review on building integrated photovoltaic  
2773 products and their applications. *Renew. Sustain. Energy Rev.* 61, 451–465.  
2774 doi:10.1016/j.rser.2016.04.008
- 2775 Tsai, Chin-Yi, Tsai, Chin-Yao, 2019. See-through, light-through, and color modules for large-area  
2776 tandem amorphous/microcrystalline silicon thin-film solar modules: Technology development  
2777 and practical considerations for building-integrated photovoltaic applications. *Renew. Energy*  
2778 145, 2637–2646. doi:10.1016/j.renene.2019.08.029
- 2779 Tsengenes, G., Adamidis, G., 2011. Investigation of the behavior of a three phase grid-connected  
2780 photovoltaic system to control active and reactive power. *Electr. Power Syst. Res.* 81, 177–184.  
2781 doi:10.1016/j.epsr.2010.08.008
- 2782 Upadhyaya, H.M., Senthilarasu, S., Hsu, M.H., Kumar, D.K., 2013. Recent progress and the status of  
2783 dye-sensitised solar cell (DSSC) technology with state-of-the-art conversion efficiencies. *Sol.*  
2784 *Energy Mater. Sol. Cells* 119, 291–295. doi:10.1016/j.solmat.2013.08.031
- 2785 Valencia, J.S.B., Giraldo, F.E.L., Bonilla, J.F.V., 2013. Calibration method for Correlated Color  
2786 Temperature (CCT) measurement using RGB color sensors. *Symp. Signals, Images Artif. Vis.* -  
2787 2013, STSIVA 2013. doi:10.1109/STSIVA.2013.6644921
- 2788 Van Roy, J., Leemput, N., Geth, F., Salebien, R., Buscher, J., Driesen, J., 2014. Operational Electric  
2789 Vehicle Charging Strategies. *IEEE Trans. Sustain. Energy* 5, 264–272.
- 2790 van Sark, W., Nemet, G., Schaeffer, G.J., Alsema, E., 2010. Photovoltaic solar energy, Technological  
2791 Learning in the Energy Sector: Lessons for Policy, Industry and Science.  
2792 doi:10.4337/9781849806848.00017
- 2793 van Sark, W.G.J.H.M., 2013. Luminescent solar concentrators - A low cost photovoltaics alternative.  
2794 *Renew. Energy* 49, 207–210. doi:10.1016/j.renene.2012.01.030
- 2795 Van Vliet, O., Brouwer, A.S., Kuramochi, T., Van Den Broek, M., Faaij, A., 2011. Energy use, cost  
2796 and CO<sub>2</sub> emissions of electric cars. *J. Power Sources* 196, 2298–2310.  
2797 doi:10.1016/j.jpowsour.2010.09.119
- 2798 Vasiliev, M., Nur-E-Alam, M., Alameh, K., 2019. Recent developments in solar energy-harvesting  
2799 technologies for building integration and distributed energy generation. *Energies* 12.  
2800 doi:10.3390/en12061080
- 2801 Vats, K., Tiwari, G.N., 2012. Performance evaluation of a building integrated semitransparent

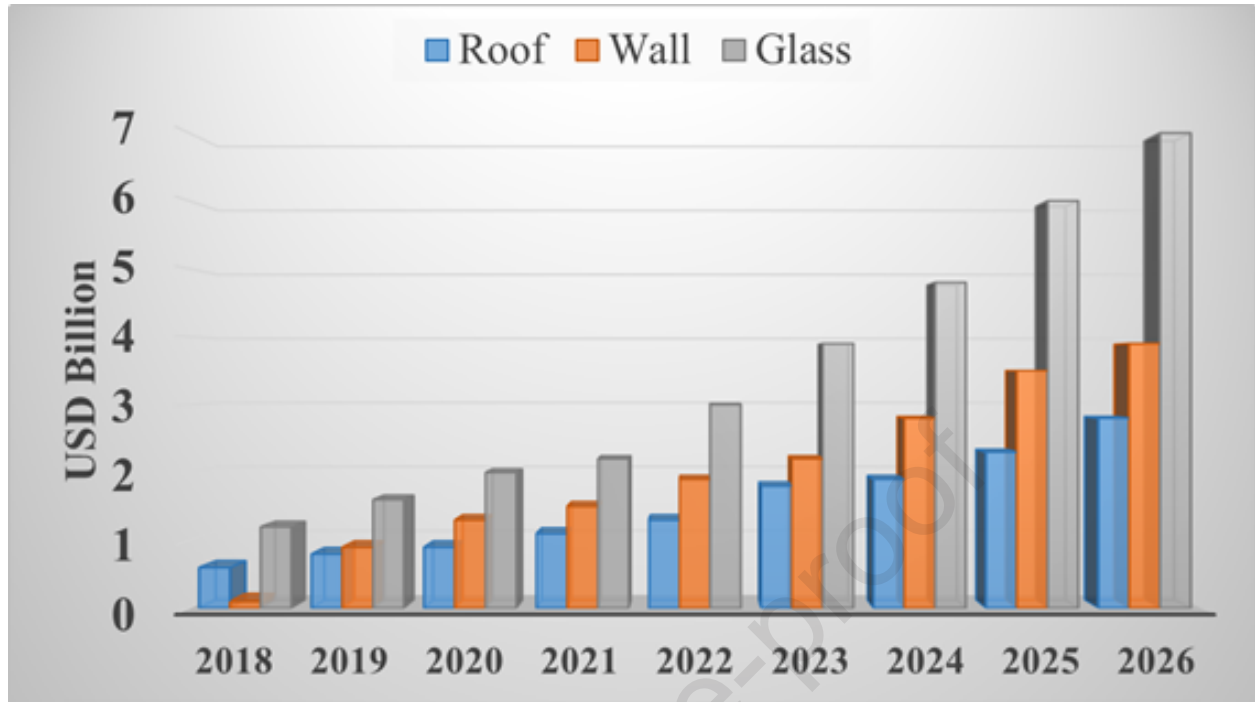
- 2802 photovoltaic thermal system for roof and faade. *Energy Build.* 45, 211–218.  
2803 doi:10.1016/j.enbuild.2011.11.008
- 2804 View, G.R., 2016. Dye Sensitized Solar Cell Market Size, Share & Trends Analysis Report By  
2805 Application (Portable Charging, BIPV/BAPV, Embedded Electronics, Outdoor Advertising,  
2806 Automotive (AIPV)), And Segment Forecasts, 2015 - 2022 98.  
2807 doi:https://www.grandviewresearch.com/industry-analysis/dye-sensitized-solar-cell-market
- 2808 Virtuani, A., Mullejans, H., Dunlop, E.D., 2011. Comparison of indoor and outdoor performance  
2809 measurements of recent commercially available solar modules. *Prog. Photovolt Res. Appl.* 15,  
2810 11–20. doi:10.1002/pip
- 2811 Virtuani, A., Strepparava, D., 2017. Modelling the performance of amorphous and crystalline silicon  
2812 in different typologies of building-integrated photovoltaic (BIPV) conditions. *Sol. Energy* 146,  
2813 113–118. doi:10.1016/j.solener.2017.02.035
- 2814 Visa, I., Burduhos, B., Neagoe, M., Moldovan, M., Duta, A., 2016. Comparative analysis of the  
2815 infield response of five types of photovoltaic modules. *Renew. Energy* 95, 178–190.  
2816 doi:10.1016/j.renene.2016.04.003
- 2817 Vossen, F.M., Aarts, M.P.J., Debije, M.G., 2016. Visual performance of red luminescent solar  
2818 concentrating windows in an office environment. *Energy Build.* 113, 123–132.  
2819 doi:10.1016/j.enbuild.2015.12.022
- 2820 Vüllers, F., Fritz, B., Roslizar, A., Striegel, A., Guttmann, M., Richards, B.S., Hölscher, H., Gomard,  
2821 G., Klampaftis, E., Kavalenka, M.N., 2018. Self-Cleaning Microcavity Array for Photovoltaic  
2822 Modules. *ACS Appl. Mater. Interfaces* 10, 2929–2936. doi:10.1021/acsami.7b15579
- 2823 Wang, L., Zhu, G., Wang, M., Yu, W., Zeng, J., Yu, X., Xie, H., Li, Q., 2019. Dual plasmonic  
2824 Au/TiN nanofluids for efficient solar photothermal conversion. *Sol. Energy* 184, 240–248.  
2825 doi:10.1016/j.solener.2019.04.013
- 2826 Wang, M., Peng, J., Li, N., Yang, H., Wang, C., Li, X., Lu, T., 2017. Comparison of energy  
2827 performance between PV double skin facades and PV insulating glass units. *Appl. Energy* 194,  
2828 148–160. doi:10.1016/j.apenergy.2017.03.019
- 2829 Wang, Y., Tian, W., Ren, J., Zhu, L., Wang, Q., 2006. Influence of a building's integrated-  
2830 photovoltaics on heating and cooling loads. *Appl. Energy* 83, 989–1003.  
2831 doi:10.1016/j.apenergy.2005.10.002
- 2832 Wang, Z., McMeekin, D.P., Sakai, N., van Reenen, S., Wojciechowski, K., Patel, J.B., Johnston,  
2833 M.B., Snaith, H.J., 2017. Efficient and Air-Stable Mixed-Cation Lead Mixed-Halide Perovskite  
2834 Solar Cells with n-Doped Organic Electron Extraction Layers. *Adv. Mater.* 29.  
2835 doi:10.1002/adma.201604186
- 2836 Weber, B., Quiñones, A., Almanza, R., Duran, M.D., 2014. Performance reduction of PV systems by  
2837 dust deposition. *Energy Procedia* 57, 99–108. doi:10.1016/j.egypro.2014.10.013
- 2838 Wei, D., Huang, H., Cui, P., Ji, J., Dou, S., Jia, E., Sajid, S., Cui, M., Chu, L., Li, Y., Jiang, B., Li, M.,  
2839 2019. Moisture-tolerant supermolecule for the stability enhancement of organic-inorganic  
2840 perovskite solar cells in ambient air. *Nanoscale* 11, 1228–1235. doi:10.1039/c8nr07638c
- 2841 Wheeler, L.M., Moore, D.T., Tenent, R.C., Blackburn, J.L., Ihly, R., Stanton, N.J., Miller, E.M.,  
2842 Neale, N.R., n.d. Switchable photovoltaic windows enabled by reversible photothermal complex  
2843 dissociation from methylammonium lead iodide. *Nat. Commun.* doi:10.1038/s41467-017-  
2844 01842-4
- 2845 Wheeler, L.M., Wheeler, V.M., 2019. Detailed Balance Analysis of Photovoltaic Windows.

- 2846 doi:10.1021/acseenergylett.9b01316
- 2847 Williams, A.M., Phaneuf, D.J., Barrett, M.A., Su, J.G., 2019. Short-term impact of PM 2.5 on  
2848 contemporaneous asthma medication use: Behavior and the value of pollution reductions. *Proc.*  
2849 *Natl. Acad. Sci. U. S. A.* 116, 5246–5253. doi:10.1073/pnas.1805647115
- 2850 Wilson, E., 2009. Theoretical and operational thermal performance of a “wet” crystalline silicon PV  
2851 module under Jamaican conditions. *Renew. Energy* 34, 1655–1660.  
2852 doi:10.1016/j.renene.2008.10.024
- 2853 Wojciechowski, K., Forgács, D., Rivera, T., 2019. Industrial Opportunities and Challenges for  
2854 Perovskite Photovoltaic Technology. *Sol. RRL* 3, 1900144. doi:10.1002/solr.201900144
- 2855 Woyte, A., Thong, V. Van, Belmans, R., Nijs, J., 2006. Voltage fluctuations on distribution level  
2856 introduced by photovoltaic systems. *IEEE Trans. Energy Convers.* 21, 202–209.  
2857 doi:10.1109/TEC.2005.845454
- 2858 Wu, Y.W., Wen, M.H.D., Young, L.M., Hsu, I.T., 2018. LCA-Based Economic Benefit Analysis for  
2859 Building Integrated Photovoltaic (BIPV) Façades: A Case Study in Taiwan. *Int. J. Green Energy*  
2860 15, 8–12. doi:10.1080/15435075.2016.1251924
- 2861 Xia, J., Li, F., Huang, C., Zhai, J., Jiang, L., 2006. Improved stability quasi-solid-state dye-sensitized  
2862 solar cell based on polyether framework gel electrolytes. *Sol. Energy Mater. Sol. Cells* 90, 944–  
2863 952. doi:10.1016/j.solmat.2005.05.021
- 2864 Xia, Y., Liang, X., Jiang, Y., Wang, S., Qi, Y., Liu, Y., Yu, L., 2019. High-Efficiency and Reliable  
2865 Smart Photovoltaic Windows Enabled by Multiresponsive Liquid Crystal Composite Films and  
2866 Semi-Transparent Perovskite Solar Cells 1900720, 1–8. doi:10.1002/aenm.201900720
- 2867 Xie, L., Yan, H., Zhang, S., Wei, C., 2020. Does urbanization increase residential energy use?  
2868 Evidence from the Chinese residential energy consumption survey 2012. *China Econ. Rev.* 59,  
2869 101374. doi:10.1016/j.chieco.2019.101374
- 2870 Xie, M., Wang, J., Kang, J., Zhang, L., Sun, X., Han, K., Luo, Q., Lin, J., Shi, L., Ma, C.Q., 2019.  
2871 Super-flexible perovskite solar cells with high power-per-weight on 17  $\mu\text{m}$  thick PET substrate  
2872 utilizing printed Ag nanowires bottom and top electrodes. *Flex. Print. Electron.* 4.  
2873 doi:10.1088/2058-8585/ab2f37
- 2874 Xiong, S., Yin, S., Wang, Y., Kong, Z., Lan, J., Zhang, R., Gong, M., Wu, B., Chu, J., Wang, X.,  
2875 2017. Organic/inorganic electrochromic nanocomposites with various interfacial interactions: A  
2876 review. *Mater. Sci. Eng. B Solid-State Mater. Adv. Technol.* 221, 41–53.  
2877 doi:10.1016/j.mseb.2017.03.017
- 2878 Xu, L., Luo, K., Ji, J., Yu, B., Li, Z., Huang, S., 2020. Study of a hybrid BIPV/T solar wall system.  
2879 *Energy* 193, 116578. doi:10.1016/j.energy.2019.116578
- 2880 Xu, R., Ni, K., Hu, Y., Si, J., Wen, H., Yu, D., 2017. Analysis of the optimum tilt angle for a soiled  
2881 PV panel. *Energy Convers. Manag.* 148, 100–109. doi:10.1016/j.enconman.2017.05.058
- 2882 Xuan, X., 2011. Application of building information modeling in building integrated photovoltaics.  
2883 *Adv. Mater. Res.* 171–172, 399–402. doi:10.4028/www.scientific.net/AMR.171-172.399
- 2884 Yadav, S., Panda, S.K., 2020. Thermal performance of BIPV system by considering periodic nature of  
2885 insolation and optimum tilt-angle of PV panel. *Renew. Energy* 150, 136–146.  
2886 doi:10.1016/j.renene.2019.12.133
- 2887 Yalçın, L., Öztürk, R., 2013. Performance comparison of c-Si, mc-Si and a-Si thin film PV by PV syst  
2888 simulation. *J. Optoelectron. Adv. Mater.* 15, 326–334. doi:10.1002/pip

- 2889 Yan, F., Noble, J., Peltola, J., Wicks, S., Balasubramanian, S., 2012. Semitransparent OPV modules  
2890 pass environmental chamber test requirements. *Sol. Energy Mater. Sol. Cells* 114, 214–218.  
2891 doi:10.1016/j.solmat.2012.09.031
- 2892 Yan, J., Yang, Y., Elia Campana, P., He, J., 2019. City-level analysis of subsidy-free solar  
2893 photovoltaic electricity price, profits and grid parity in China. *Nat. Energy* 4, 709–717.  
2894 doi:10.1038/s41560-019-0441-z
- 2895 Yang, H., Burnett, J., Ji, J., 2000. Simple approach to cooling load component calculation through PV  
2896 walls. *Energy Build.* 31, 285–290. doi:10.1016/S0378-7788(99)00041-9
- 2897 Yang, H., Zheng, G., Lou, C., An, D., Burnett, J., 2004. Grid-connected building-integrated  
2898 photovoltaics: A Hong Kong case study. *Sol. Energy* 76, 55–59.  
2899 doi:10.1016/j.solener.2003.09.007
- 2900 Yang, R.J., 2015. Overcoming technical barriers and risks in the application of building integrated  
2901 photovoltaics (BIPV): Hardware and software strategies. *Autom. Constr.* 51, 92–102.  
2902 doi:10.1016/j.autcon.2014.12.005
- 2903 Yang, R.J., Zou, P.X.W., 2016. Building integrated photovoltaics (BIPV): Costs, benefits, risks,  
2904 barriers and improvement strategy. *Int. J. Constr. Manag.* 16, 39–53.  
2905 doi:10.1080/15623599.2015.1117709
- 2906 Yang, T., Athienitis, A.K., 2014. A study of design options for a building integrated  
2907 photovoltaic/thermal (BIPV/T) system with glazed air collector and multiple inlets. *Sol. Energy*  
2908 104, 82–92. doi:10.1016/j.solener.2014.01.049
- 2909 Yang, X., Wang, H., Cai, B., Yu, Z., Sun, L., 2018. Progress in hole-transporting materials for  
2910 perovskite solar cells. *J. Energy Chem.* 27, 650–672. doi:10.1016/j.jechem.2017.12.017
- 2911 Yong, J.Y., Ramachandramurthy, V.K., Tan, K.M., Mithulananthan, N., 2015. A review on the state-  
2912 of-the-art technologies of electric vehicle, its impacts and prospects. *Renew. Sustain. Energy*  
2913 *Rev.* 49, 365–385. doi:10.1016/j.rser.2015.04.130
- 2914 Yoo, S.H., 2019. Optimization of a BIPV system to mitigate greenhouse gas and indoor environment.  
2915 *Sol. Energy* 188, 875–882. doi:10.1016/j.solener.2019.06.055
- 2916 Yoon, J.H., Shim, S.R., An, Y.S., Lee, K.H., 2013. An experimental study on the annual surface  
2917 temperature characteristics of amorphous silicon BIPV window. *Energy Build.* 62, 166–175.  
2918 doi:10.1016/j.enbuild.2013.01.020
- 2919 Yoon, J.H., Song, J., Lee, S.J., 2011. Practical application of building integrated photovoltaic (BIPV)  
2920 system using transparent amorphous silicon thin-film PV module. *Sol. Energy* 85, 723–733.  
2921 doi:10.1016/j.solener.2010.12.026
- 2922 Zarmai, M.T., Ekere, N.N., Oduoza, C.F., Amalu, E.H., 2015. A review of interconnection  
2923 technologies for improved crystalline silicon solar cell photovoltaic module assembly. *Appl.*  
2924 *Energy* 154, 173–182. doi:10.1016/j.apenergy.2015.04.120
- 2925 Zhang, D., 2011. One-axis tracking holographic planar concentrator systems. *J. Photonics Energy* 1,  
2926 015505. doi:10.1117/1.3590943
- 2927 Zhang, P., Lv, F.Y., 2015. A review of the recent advances in superhydrophobic surfaces and the  
2928 emerging energy-related applications. *Energy* 82, 1068–1087. doi:10.1016/j.energy.2015.01.061
- 2929 Zhang, T., Wang, M., Yang, H., 2018. A review of the energy performance and life-cycle assessment  
2930 of building-integrated photovoltaic (BIPV) systems. *Energies* 11. doi:10.3390/en11113157

- 2931 Zhang, W., Hao, B., Li, N., 2014. Experiment and Simulation Study on the Amorphous Silicon  
2932 Photovoltaic Walls. *Int. J. photoenergy* 2014, 1–14. doi:<https://doi.org/10.1155/2014/643637>
- 2933 Zhang, W., Lu, L., Chen, X., 2017. Performance evaluation of vacuum photovoltaic insulated glass  
2934 unit. *Energy Procedia* 105, 322–326. doi:10.1016/j.egypro.2017.03.321
- 2935 Zhong, H., Hu, Y., Wang, Y., Yang, H., 2017. TiO<sub>2</sub>/silane coupling agent composed of two layers  
2936 structure: A super-hydrophilic self-cleaning coating applied in PV panels. *Appl. Energy* 204,  
2937 932–938. doi:10.1016/j.apenergy.2017.04.057
- 2938 Zhou, L., Zuo, Y., Mallick, T.K., Sundaram, S., 2019. Enhanced Efficiency of Carbon-Based  
2939 Mesoscopic Perovskite Solar Cells through a Tungsten Oxide Nanoparticle Additive in the  
2940 Carbon Electrode. *Sci. Rep.* 9, 1–8. doi:10.1038/s41598-019-45374-x
- 2941 Zhou, Y., Cao, S., Hensen, J.L.M., Lund, P.D., 2019. Energy integration and interaction between  
2942 buildings and vehicles: A state-of-the-art review. *Renew. Sustain. Energy Rev.* 114, 109337.  
2943 doi:10.1016/j.rser.2019.109337
- 2944 Zhou, Y., Wen, R., Wang, H., Cai, H., 2020. Optimal battery electric vehicles range: A study  
2945 considering heterogeneous travel patterns, charging behaviors, and access to charging  
2946 infrastructure. *Energy* 197, 116945. doi:10.1016/j.energy.2020.116945
- 2947 Zhou, Z., Carbajales-Dale, M., 2018. Assessing the photovoltaic technology landscape: Efficiency  
2948 and energy return on investment (EROI). *Energy Environ. Sci.* 11, 603–608.  
2949 doi:10.1039/c7ee01806a
- 2950 Zidane, T.E.K., Adzman, M.R. Bin, Tajuddin, M.F.N., Mat Zali, S., Durusu, A., 2019. Optimal  
2951 configuration of photovoltaic power plant using grey wolf optimizer: A comparative analysis  
2952 considering CdTe and c-Si PV modules. *Sol. Energy* 188, 247–257.  
2953 doi:10.1016/j.solener.2019.06.002
- 2954 Zomer, C.D., Costa, M.R., Nobre, A., Rüther, R., 2013. Performance compromises of building-  
2955 integrated and building-applied photovoltaics (BIPV and BAPV) in Brazilian airports. *Energy*  
2956 *Build.* 66, 607–615. doi:10.1016/j.enbuild.2013.07.076
- 2957
- 2958
- 2959
- 2960





**Declaration of interests**

The authors declare that they have no known competing financial interests or personal relationships that could have appeared to influence the work reported in this paper.

The authors declare the following financial interests/personal relationships which may be considered as potential competing interests:

Journal Pre-proof